



# Microbial induced acid corrosion in sewer environments

DOCTORAL THESIS

to achieve the university degree of  
Doktor der Naturwissenschaften  
submitted to  
Graz University of Technology

by

Cyrill Grengg

December 2017

Supervisors:

Prof. Martin Dietzel  
Dr. Florian Mittermayr

Reviewer committee:

Prof. Martin Dietzel  
Prof. Alexandra Bertron

## Statutory declaration

*I declare that I have authored this thesis independently, that I have not used other than the declared sources/resources, and that I have explicitly marked all material which has been quoted either literally or by content from the used sources.*

*Graz, 27.11.2017*

---

# Acknowledgement

To begin with I would like to greatly thank my supervisors Florian Mittermayr and Martin Dietzel for their incredible support, positive encouragement and great collaboration during the entire last three years. A great thank you to my colleagues at the Institute of Applied Geosciences, it has been and still is a great pleasure to work with you. In this context special thanks to our laboratory members for their tolerance and robustness in respect to the often hygienically challenging analytics.

Furthermore, I want to thank Günther Koraimann from the Institute of Molecular Biosciences of University of Graz for the great collaboration and his input concerning all microbiological aspects.

This project has been financially supported by the Department of Water Resources Management and the Department of Energy, Residential Constructions and Technology of the Styrian Government. A great thank you to Peter Rappold and Heinz Lackner for their preparedness and interests in this project.

Last but not least the biggest thank you to my entire family and all my friends for supporting me in all aspects of my life. I would not be where I am without you all.

## Abstract

Microbial induced concrete corrosion (MICC) is one of the main chemical degradation mechanisms of sewage transportation networks worldwide with high economic, hygienic and environmental relevance. Under certain conditions it may reduce the service life of sewer systems down to less than 10 years. Although this type of concrete and metal degradation has been known since the beginning of the 20<sup>th</sup> century, many aspects regarding complex process mechanisms and environmental conditions responsible are still in debate. Also, to date no material exists withstanding the harsh conditions of MICC environments over its entire service life. Reasons therefore might be the interdisciplinary characteristics of MICC which comprise aspects ranging from microbiology, mineralogy, engineering and material sciences.

This thesis comprises a holistic approach to close remaining gaps in process understanding as well as to present advances in construction material development, based on different field study applications in Austrian sewer systems. Therefore, advanced mineralogical, hydro-geochemical and microbiological methods, together with monitoring programs were applied. Additionally, stable isotope systems of sulfur, oxygen and hydrogen were used to decipher specific underlying microbiological and physicochemical reaction mechanisms. Newly insights were summarized within a novel model for advanced MICC environments, describing a dynamic system of dissolution and re-precipitation of solids controlled by pH and diffusion.

Knowledge gained is consequently compared and intensively discussed in reference to the state of the art, resulting in recommendations for potentially sustainable alternative materials for aggressive sewer environments. In this context geopolymer materials are presented as a multi-functional material with great potential for the sewer infrastructure. Compared to conventional Portland cement-based concretes, geopolymers are acid resistant and are expected to provide a much longer lasting and stable barrier against MICC, while acting as an implicit pipe protection.

# Table of Content

Statutory declaration.....	2
Acknowledgement .....	3
Abstract.....	4
<b>Chapter 1 .....</b>	<b>.....</b>
<b>Microbial induced concrete corrosion in a global perspective .....</b>	<b>7</b>
1.1. General observations and hygienic aspects.....	7
1.2. Economic impact.....	7
1.3. Health considerations.....	8
1.4. Structural introduction and Outlook.....	9
1.5. Bibliography.....	11
<b>Chapter 2 .....</b>	<b>.....</b>
<b>Microbiologically induced concrete corrosion: A case study from a combined sewer network ..</b>	<b>12</b>
2.1. Abstract.....	12
2.2. Introduction.....	13
2.3. Study site.....	14
2.4. Materials and Methods .....	16
2.5. Results.....	19
2.6. Discussion.....	26
2.7. Summary and Conclusion.....	30
2.8. Acknowledgements.....	30
2.9. Bibliography.....	31
2.10. Appendix .....	34
<b>Chapter 3 .....</b>	<b>.....</b>
<b>The decisive role of acidophilic bacteria in concrete sewer networks: A new model for fast progressing microbial concrete corrosion .....</b>	<b>35</b>
3.1. Abstract.....	35
3.2. Introduction.....	35
3.3. Study site, Materials and Methods .....	37
3.4. Results.....	42
3.5. Discussion.....	45
3.6. Conclusion .....	49
3.7. Acknowledgement .....	49
3.8. Bibliography.....	49
3.9. Appendix 1.....	53

<b>Chapter 4 .....</b>	<b>55</b>
<b>How stable isotopes can be used to decipher reaction mechanisms within microbial induced concrete corrosion environments.....</b>	<b>55</b>
4.1. Abstract .....	55
4.2. Introduction.....	55
4.3. Field Site .....	57
4.4. Methods .....	57
4.5. Results and Discussion .....	59
4.6. Conclusion .....	62
4.7. Bibliography.....	63
4.8. Appendix.....	64
<b>Chapter 5 .....</b>	<b>66</b>
<b>Advances in construction materials for sewer systems affected by microbial induced concrete corrosion: A review.....</b>	<b>66</b>
5.1. Abstract .....	66
5.2. Introduction.....	67
5.3. Characteristics of wastewater environments inducing MICC .....	69
5.4. Effect of concrete characteristics on MICC .....	73
5.5. Geopolymer technology for wastewater applications .....	76
5.6. Antimicrobial agents .....	81
5.7. Conclusions and Outlook.....	84
5.8. Acknowledgment.....	85
5.9. Bibliography.....	85
<b>Chapter 6 .....</b>	<b>91</b>
<b>Outlook and Afterword.....</b>	<b>91</b>
6.1. Outlook .....	91
6.2. Curriculum Vitae.....	91
6.3. References.....	92

# Chapter 1

## Microbial induced concrete corrosion in a global perspective

### 1.1. General observations and hygienic aspects

The establishment of modern underground sewer networks as we know them today represents a major step in the development of sanitary standards of modern society. Thereby, not only the raising quantities of sewage produced due to growing populations and increasing urbanisation within the last two centuries could be efficiently controlled, but also hygienic aspects such as water-borne diseases could be averted. Additionally, the hazardous impact of potential wastewater contamination for the adjacent environments could be limited. Nevertheless, still today especially many developing countries are facing lacking or insufficient operating sewer networks, which can potentially lead to the spread of severe infectious diseases or the contamination of drinking water sources (Hvitved-Jacobsen et al., 2013). The World Health Organization (WHO) reported in 2005 that around 2.6 billion people are still lacking basic sanitation, while “only” around 1.1 billion are lacking access to drinking water. This clearly indicates the still growing demand for efficient, safe and cost-effective collection, transport and digestion of sewage worldwide. A recent comprehensive survey on the status of sewer systems (Berger et al., 2016) confirmed the need to maintain their long-term performance, e.g. Germany has 575 580 km, France 280 000 km of public sewerage system, with an 11% (or 31%) increase during the last 10 (or 20) years. In this context, the durability and workability of construction materials applied is a central concern. Insufficient material performances are mainly caused by chemically aggressive conditions, which establish due to chemical and microbial processes during sewage transportation. In this matter microbial induced corrosion of concrete and metals is one of the central processes leading to sewer network degradation globally, with both economic and health-related impact.

### 1.2. Economic impact

As described in section 1.1, the efficient, safe and cost-effective collection and transport of sewage is a key criteria maintaining expected sanitary standards of modern society (Hvitved-Jacobsen et al., 2013). Approximately 40% of concrete failure in sewer systems can be directly attributed to microbial induced concrete corrosion (MICC) (Kaempfer and Berndt, 1999). Accordingly, MICC is recognized as one of the main degradation processes of subsurface infrastructure worldwide with high economic relevance (Grenng et al., 2016; Jiang et al., 2015). Due to increased aggressive conditions,

MICC may reduce the repair free service-life of sewer infrastructure from 100 years in the past, down to less than 10 years in severe cases (Grenng et al., 2017, 2015; Jensen, 2009). Typical damage pattern from field observations are displayed in Figure 1.



Figure 1: Typical damage pattern of MICC from different Austrian sewer manholes.

Remediation and repair of the latter corroded systems, are challenging and costly. Annual rehabilitation costs were estimated to reach values of €456 million in Germany (Kaempfer and Berndt, 1998), £84.8 million in the UK and 1 billion in France, while the US need to spent around \$390 billion within the next 20 years, in order to keep the existing wastewater infrastructure on life support (Gutiérrez-Padilla et al., 2010). Additionally, globally progressing separations of combined sewer networks into sanitary and storm sewer networks, due to technical and environmental considerations, will contribute towards intensifying the MICC problematic within the future, thereby increasing the need for sustainable and sufficient solutions.

### 1.3. Health considerations

Beside economic aspects the production of hazardous and odorous gases, such as hydrogen sulfide ( $H_2S$ ), carbon dioxide ( $CO_2$ ) but also methane ( $CH_4$ ) and other volatile organic compounds (VOCs), associated with MICC, are a subject of major concerns. These gases produced represent a significant health risk for community workers, sewer operators, as well as for private residents of affected communities (Gutierrez et al., 2014; World Health Organization, 2000). Especially  $H_2S$  is



known for its combined odor and health threatening potential. Critical H<sub>2</sub>S concentrations for human exposure are presented in Table 1.

Table 1: Relationship between critical hydrogen sulfide concentrations and associated effects for humans (World Health Organisation, 2000).

H <sub>2</sub> S concentration [ppm]	Effect
0.001-0.15	Odor threshold
10-20	Threshold for eye irritation
50-100	Serious eye damage
150-250	Loss of olfactory sense
320-530	Pulmonary edema with risk of death
530-1000	Strong central nervous system stimulation, hyperpnoea and respiratory arrest
1000-2000	Immediate collapse with paralysis of respiration

#### 1.4. Structural introduction and Outlook

The following chapters 2 to 5 will summarize different aspects of MICC ranging from (i) field studies conducted within heavily corroded systems (ii) to new aspects regarding process understanding, (iii) the applications of stable isotope systems in the latter environments and finally, (iv) possible advances in the development of stable construction materials. Since the single chapters represent already published manuscripts the structure is mainly kept the same, except for editorial aspects and short introductory passages in order to guarantee a reading flow.

Chapter 2 corresponds to “Microbiologically induced concrete corrosion: A case study from a combined sewer network”, by Grengg et al., 2015, published in Cement and Concrete research. Although MICC is known since decades (see 1.1) not many actual field studies exist describing detailed process mechanisms and degradation features as seen in actual systems affected. This paper describes the interaction between environmental parameters, microbiological aspects and materials incorporated leading to strong concrete degradation within an Austrian sewer system, by using a combined approach of hydro-geochemical, microbiological and mineralogical analytics.

Chapter 3 represents “The decisive role of acidophilic bacteria in concrete sewer networks: A new model for advanced microbial concrete corrosion”, by Grengg et al., 2017, also published in Cement and Concrete Research. Thereby a new model for advanced MICC environments is described

by using an interdisciplinary approach including microbial, mineralogical and hydro-geochemical analytics. Special focus was laid on the specific role of acidophilic bacteria on corrosion propagation and associated mineral dissolution and neo-formation. In depth knowledge gained comprise valuable information regarding the causes for the extremely high corrosion rates observed, as well as regarding aspects of microbial-cementitious material interactions.

Chapter 4 is based on a paper, entiteled “Stable isotope signatures within microbial induced concrete corrosion: A field study”, by Grengg et al., 2015, published in *Procedia Earth and Planetary Sciences* and presented at the 11<sup>th</sup> Applied Isotope Geochemistry Conference (2015) in Orleans. Therefore, already published aspects were extended with newly, more recently gained data. This paper critically assessed information that can be drawn from the application of stable sulfur, oxygen and hydrogen isotope systems within MICC environments. Therefore, stable sulfur, oxygen and hydrogen isotope ratios within a heavily deteriorated sewer system, strongly affected by MICC were quantified. Based on the results obtained, in depth knowledge regarding the impact of fluctuating environmental conditions on the formation of secondary sulfate salts could be gained. Additionally, the microbial controlled sulfur cycle from an isotope geochemical perspective and resulting observations on system dynamics and process implementations were discussed.

Chapter 5 corresponds to “Advances in construction materials for sewer systems affected by microbial induced concrete corrosion: A review”, by Grengg et al., 2017, which is currently under review. It comprised a critical assessment of advances in the field of microbial induced concrete corrosion in sewer systems from an interdisciplinary (hydro-geochemical, mineralogical and microbiological) perspective. Special focus was laid on the microorganisms-cementitious materials interaction responsible for material degradation, together with the presentation of recent advances in sustainable materials development for the latter systems. Additionally, a perspective for future research on MICC environments, with special focus on sustainable material development, such as the addition of antibacteriostatic agents in combination with innovative geopolymer technology was discussed.

Chapter 6 summarizes further research areas of interests together with continuative projects on aspects such as sustainable construction material development. Additionally, a summary of all relevant publications of the author of this thesis will be presented.

## 1.5. Bibliography

- Berger, C. et al. Zustand der Kanalisation in Deutschland: Ergebnisse der DWA-Umfrage 2015. Sonderdruck Korrespondenz Abwasser, Abfall (2016). doi:10.3242/kae2011/01.001
- Grengg, C., Kiliswa, M., Mittermayr, F. & Alexander, M. Microbially-induced Concrete Corrosion- A worldwide problem. in *Microorganisms-Cementitious Materials Interactions* 1–19 (2016).
- Grengg, C., Mittermayr, F., Baldermann, a., Böttcher, M.E., Leis, a., Koraimann, G., Grunert, P., Dietzel, M., 2015. Microbiologically induced concrete corrosion: A case study from a combined sewer network. *Cem. Concr. Res.* 77, 16–25. doi:10.1016/j.cemconres.2015.06.011
- Grengg, C., Mittermayr, F., Baldermann, A., Böttcher, M.E., Leis, A., Koraimann, G., Dietzel, M., 2015a. Stable Isotope Signatures within Microbial Induced Concrete Corrosion: A Field Study. *Procedia Earth Planet. Sci.* 13, 68–71. doi:10.1016/j.proeps.2015.07.016
- Grengg, C., Mittermayr, F., Koraimann, G., Konrad, F., Szabó, M., Demeny, A., Dietzel, M., 2017. The decisive role of acidophilic bacteria in concrete sewer networks: A new model for fast progressing microbial concrete corrosion. *Cem. Concr. Res.* doi:10.1016/j.cemconres.2017.08.020
- Grengg, C., Mittermayr, F., Ukrainczyk, N., Koraimann, G., Kienesberger, S., Dietzel, M., 2017. Advances in construction materials for sewer systems affected by microbial induced concrete corrosion: A review. Under Review.
- Gutierrez, O., Sudarjanto, G., Ren, G., Ganigué, R., Jiang, G., Yuan, Z., 2014. Assessment of pH shock as a method for controlling sulfide and methane formation in pressure main sewer systems. *Water Res.* 48, 569–78. doi:10.1016/j.watres.2013.10.021
- Gutiérrez-Padilla, M.G.D., Bielefeldt, A., Ovtchinnikov, S., Hernandez, M., Silverstein, J., 2010. Biogenic sulfuric acid attack on different types of commercially produced concrete sewer pipes. *Cem. Concr. Res.* 40, 293–301. doi:10.1016/j.cemconres.2009.10.002
- Hvitved-Jacobsen, T., Vollertsen, J., Nielsen, A.H., 2013. *Sewer Processes - Microbial and Chemical Process Engineering of Sewer Networks*, 2nd ed. CRC Press, London.
- Jensen, H.S., 2009. PhD thesis; Hydrogen sulfide induced concrete corrosion of sewer networks. Aalborg University.
- Jiang, G., Sun, X., Keller, J., Bond, P.L., 2015. Identification of controlling factors for the initiation of corrosion of fresh concrete sewers. *Water Res.* doi:10.1016/j.watres.2015.04.015
- Kaempfer W and M. Berndt. Estimation of Service Life of Concrete Pipes in Sewer. 8th Conf. Durab. Build. Mater. Components 1, 36–45. (1999).
- World Health Organisation, 2000. Hydrogen Sulfide, in: *Air Quality Guidelines for Europe*. Copenhagen, p. 7.

## Chapter 2

### Microbiologically induced concrete corrosion: A case study from a combined sewer network

Grengg, C.<sup>1</sup>, Mittermayr, F.<sup>2</sup>, Baldermann, A.<sup>1</sup>, Böttcher, M. E.<sup>3</sup>, Leis, A.<sup>4</sup>, Koraimann, G.<sup>5</sup>, Grunert, P.<sup>6,7</sup> & Dietzel, M.<sup>1</sup>

<sup>1</sup> *Institute of Applied Geosciences, Graz University of Technology, Rechbauerstraße 12, 8010, Graz, Austria*

<sup>2</sup> *Institute of Technology and Testing of Construction Materials, Graz University of Technology, Inffeldgasse 24, 8010, Graz, Austria*

<sup>3</sup> *Leibniz Institute for Baltic Sea Research (IOW), Seestraße 15, D-18119 Warnemünde, Germany*

<sup>4</sup> *RESOURCES – Institute for Water, Energy and Sustainability, Joanneum Research, Elisabethstraße 18/2, 8010, Graz, Austria*

<sup>5</sup> *Institute of Molecular Biosciences, Graz Karl-Franzens University, Humboldtstraße 50, 8010, Graz, Austria*

<sup>6</sup> *Institute of Earthsciences, Graz Karl-Franzens University, Heinrichstraße 26, 8010, Graz, Austria*

<sup>7</sup> *Department of Earth and Planetary Sciences, Rutgers University, 610 Taylor Road, Piscataway, NJ 08854-8066, United States of America*

Keywords: Bacteria; X-Ray Diffraction; Durability; Sulfate Attack; Degradation

#### 2.1. Abstract

In this study, a strongly deteriorated concrete-based sewer system was investigated by using a multi proxy approach based on gaseous, hydro-geochemical, microbiological, mineralogical and mechanical analyses. Therefore, gas, liquid, and solid samples were taken throughout the entire sewer system. Long term measurements of gaseous hydrogen sulfide (H<sub>2</sub>S) within the sewer atmosphere yielded concentrations up to 367 ppm. Interstitial fluids, extracted from deteriorated concrete by squeezing, contained sulfate (SO<sub>4</sub><sup>2-</sup>) concentrations of up to 104 g l<sup>-1</sup> at strong acidic conditions (0.7 > pH > 3.1) and are close to the saturation state of gypsum. This sulfuric acid attack is indicative for a well-established biofilm containing sulfide oxidizing bacteria (SOB), which was analyzed to consist mainly of *Acidithiobacillus thiooxidans*. The micro-structure of the attacked concrete displays a progressing alteration zone, which is caused by microbial induced concrete corrosion (MICC), with a suggested pH gradient from about 13 to < 1, from the intact inner concrete zone to the outermost heavily deteriorated concrete. Calcium sulfate minerals such as gypsum (CaSO<sub>4</sub>·2H<sub>2</sub>O), bassanite (CaSO<sub>4</sub>·1/2H<sub>2</sub>O) and anhydrite (CaSO<sub>4</sub>) are abundant in the altered concrete, which were formed from

the dissolution of the cement phases and Ca-bearing aggregates. Remarkably high corrosion rates of different precast concrete manholes were quantified to reach values greater than  $1 \text{ cm yr}^{-1}$ , despite the fact that  $\text{C}_3\text{A}$ -free cement, fly ash and a w/c of  $\sim 0.35$  was used.

## 2.2. Introduction

Corrosion of concrete-based sewer systems due to the emission of hydrogen sulfide ( $\text{H}_2\text{S}$ ) from wastewater is a worldwide occurring issue with great economical relevance. The so-called microbial induced concrete corrosion (MICC) (Gutiérrez-Padilla et al., 2010; O'Connell et al., 2010) is considered to significantly reduce the lifespan of concrete structures, from expected 100 down to 30-50 years, in extreme cases even down to 10 years (Jensen, 2009). The required remediation actions are often challenging as individual processes linked to MICC still remain uncertain and thus typically generate high costs. It has been estimated in 2002 that the United States need to spend about 390 billion dollars within the following 20 years in order to keep the existing wastewater infrastructure on life support (Gutiérrez-Padilla et al., 2010). In 1996, over 520 million dollars were spent solely in Los Angeles County for restorations of corroded sewer systems, which were directly assigned to MICC (Joseph et al., 2012). Besides economic aspects,  $\text{H}_2\text{S}$  and other volatile components such as ammonia ( $\text{NH}_3$ ), which both are common byproducts of MICC, are extremely toxic even in low concentrations and can cause significant health related consequences (Saracevic, 2008; World Health Organisation, 2000). Additionally,  $\text{H}_2\text{S}$  features an extremely low odor threshold of 0.0035 ppm, thus often being subject to community appeals due to emerging odor problems (WHO, 2001). Although, the earliest studies of MICC date back to 1900 (Olmstead and Hamlin, 1900) the environmental controls, processes, and corrosion rates of MICC are still in debate.

The deterioration of concrete that is subjected to MICC is attributed to a chain of complex biotic and abiotic chemical reactions: (i) Sulfate-reducing bacteria (SRB), e.g. *Desulfovibrio spp.* and *Desulfomaculum spp.* (Dinh et al., 2004; Hvitved-Jacobsen et al., 2002), develop in the organic-rich wastewater and colonize the adjacent sewer walls and sediment layers. The SRB colonize within an anaerobic biofilm, wherein organic matter breaks down and sulfate is progressively reduced to gaseous  $\text{H}_2\text{S}$  (Alexander et al., 2013). (ii) Accordingly,  $\text{H}_2\text{S}$  degases into the sewer atmosphere and subsequently accumulates in the pore space of the concrete via gaseous diffusion and subsequent absorption in the interstitial solution. Since concrete made with ordinary Portland cement (OPC) is a strongly alkaline media with an average pH value of  $\sim 13.5$  in the pore solution (Tritthart, 1989), chemical acid-base reactions, such as carbonation and in particular  $\text{H}_2\text{S}$  acidification successively cause the pH to drop. Starting from pH 9.5, progressive colonization of the concrete walls with strains of sulfur-oxidizing bacteria (SOB) occurs. SOB use  $\text{H}_2\text{S}$  either directly (Jensen et al., 2011) or via different key precursors,

e.g. thiosulfate ( $S_2O_3$ ) or elemental sulfur ( $S^0$ ) as an electron donor (Islander et al., 1991). These reactions finally result in the formation of sulfuric acid ( $H_2SO_4$ ), which attacks the concrete and leads to a variety of dissolution processes, besides enhancing some neo-formation reactions of sulfate mineral phases within the cementitious matrix (Nielsen et al., 2008; Yousefi et al., 2014). (iii) The dissociation of  $H_2SO_4$  goes almost to completion and thus strongly reduces pH for stimulating the dissolution of silicate, hydroxide and carbonate minerals. In addition, by providing  $SO_4^{2-}$  the precipitation of sulfate minerals such as gypsum ( $CaSO_4 \cdot 2H_2O$ ) and ettringite ( $(CaO)_3 \cdot Al_2O_3 \cdot (CaSO_4)_3 \cdot 32H_2O$ ) is promoted (Zhang et al., 2008; Soleimani et al., 2013). The formation of gypsum and ettringite is well known to cause intense microstructural damage by high crystallization pressures (Mittermayr et al., 2015; Jiang et al., 2014; Roberts et al., 2002). (iv) As the interstitial solution pH of the initially damaged concrete decreases progressively, different strains of bacteria colonize the pores of the concrete, with *Acidithiobacillus thiooxidans* being the most aggressive one (Okabe et al., 2007).

Many laboratory studies were carried out focusing on the deterioration mechanisms related to MICC on different types of concrete (Gutiérrez-Padilla et al., 2010; Nielsen et al., 2008; De Belie et al., 2004; Herisson et al., 2013; Ešťokov et al., 2012), but so far field studies on MICC are rare (Nielsen et al., 2006). Although, the results from laboratory experiments have been widely used to draw conclusions about MICC processes in natural environments, it is almost impossible to reproduce field environmental conditions of MICC in the lab. The aim of the present case study is to contribute to a deeper understanding of reaction paths, environmental controls, and corrosion rates related to MICC in a modern Austrian sewer system by introducing an advanced multi proxy approach that comprises gaseous, hydro-geochemical, bacteriological, mineralogical and mechanical analyses.

### 2.3. Study site

The investigated sewer system is located mainly in rural areas near the city of Graz in the south-eastern part of Austria. It can be categorized as a combined sewer network (Hvitved-Jacobsen et al., 2013), thus transporting the daily wastewater of around 13,000 citizen as well as the runoff from seasonal storm events. In recent years, the Austrian government demanded the fusion of smaller wastewater systems, which resulted in increasing amounts of longer intercepting sewers. Consistent with this concept, two new power mains were installed in 2004 in order to secure proper wastewater transport in local communities.

The newly built sewer system comprises a concrete storage basin (SB1), where the wastewater from the surrounding sewer channels is collected and pumped through the first power main (PM1), on average, every six hours. The PM1 is made of cast iron and polyethylene (PE) insets, with a sewer

diameter of 200 mm and a sewer length of 4 km. The adjoining PE gravity sewer (GS1), consists of around 50 concrete-based manholes (GS1-1 to GS1-50) and two small income pipes of residential areas, and is about 5 km in length. Subsequently, the wastewater is collected within a second storage basin (SB2) from which it is continuously pumped into another power main (PM2), with a length of 1.8 km and a 300 mm sewer diameter. The last part of the system holds another gravity sewer section (GS2), comprising 30 concrete-based manholes (GS2-1 to GS2-30), before the wastewater finally reaches the purification plant (Figure 1).

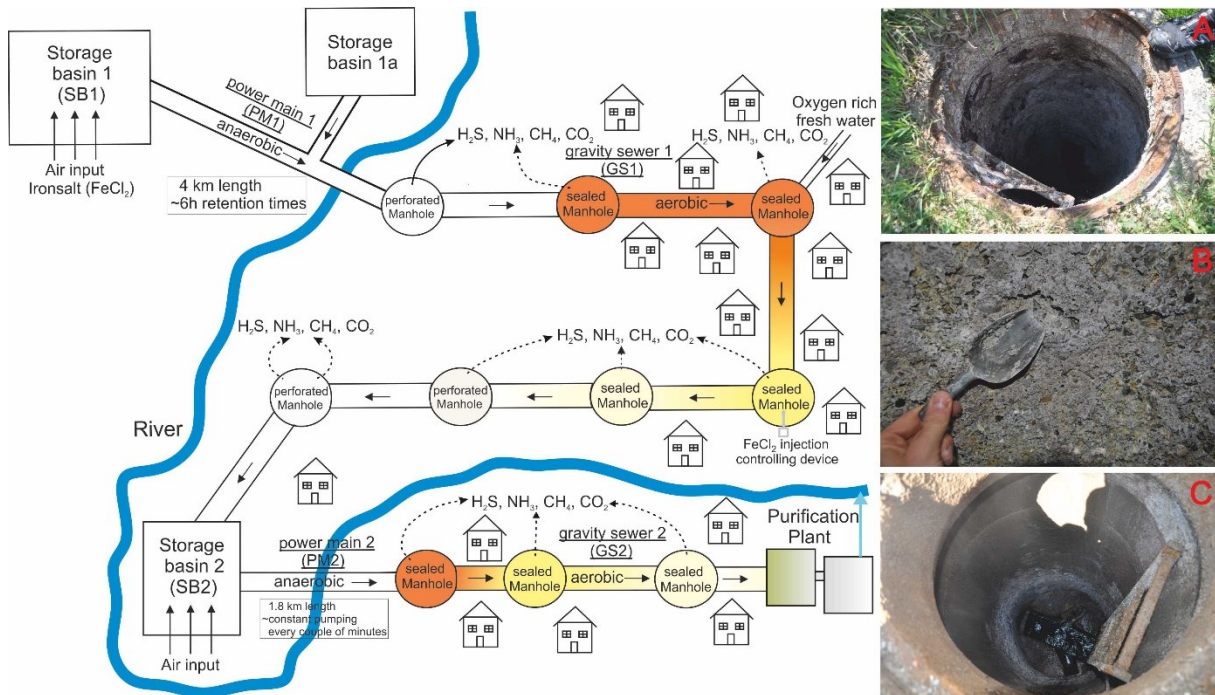


Figure 1: Schematic map of the Austrian sewer network near Graz. The intensity of concrete corrosion is indicated by the orange (intense deterioration) and yellow colour (less deterioration). Note that the highest corrosion level occurs within the sealed manhole covers. Intensive degassing of H<sub>2</sub>S, CO<sub>2</sub>, CH<sub>4</sub>, and NH<sub>3</sub> is indicated with solid arrows within the upper parts of the system and the partly perforated manhole covers, while lower emission is indicated with dotted arrows. Fresh air and iron-salt (FeCl<sub>2</sub>) are constantly added to the storage basin 1 (SB1) to limit the H<sub>2</sub>S concentrations in the atmosphere of the selected manholes by iron sulphide formation. On the right, inserted images A and B show examples of strongly deteriorated concrete of manholes within the upper parts of the gravity sewer sections, while C represents less degraded concrete of manholes within the middle parts of the system.

Both storage basins (SB1 and SB2) are made of concrete; however, no further investigations were conducted on this material since they showed no signs of visual damage. In contrary, some of the manholes in the gravity sewers were strongly deteriorated. In severe cases, the first few centimeters of the concrete revealed a mushy appearance and could be easily scraped off with bare hands. With increasing distance from the power main outlets, the intensity of concrete corrosion decreases, as seen in non-corroded manholes at the end of these sections (see Figure 1, A-C). The manholes are between 30 cm and 400 cm deep with great majority at an average depth of about 200-300 cm, and consist of precast concrete elements. The contract document specified precast elements with a compressive

strength class of C30/37, C<sub>3</sub>A free cement and a minimum water/cement (w/c) ratio of 0.45 to withstand severe aggressive environments (AS2 according to ÖNORM B 2503: Drain and sewer systems - Supplementary specifications for design, construction and testing). This classification corresponds to exposition class XA2 for chemical attack according to ÖNORM B 4710-1 (Concrete - Part 1: Specification, production, use and verification of conformity. Rules for the implementation of EN 206-1 for normal and heavy concrete). According to the precast factory, implemented elements possessed a w/c ratio of ~0.35. CEM I 42.5N (C<sub>3</sub>A-free) plus fly ash and 0.25 wt. % of a PCE based superplasticizer, referred to cement content, were added to the concrete mixture.

The transported wastewater comprises mainly domestic wastewater, although one surface quarry and some minor commercial areas are also discharging into the system. Nevertheless, both the quality and chemical composition of the wastewater fulfills the statutory requirements for communal wastewater. Since the new power mains were installed, community complains of odor rose, which were caused by constant H<sub>2</sub>S emission from the sewer system (Figure 1). As a first countermeasure, the manhole covers in populated areas were sealed, whereas sewer sections in sparsely populated regions remained perforated. Secondly, in order to prevent the establishment of anaerobic conditions (and subsequently H<sub>2</sub>S accumulation) within the power mains, fresh air is pumped into the storage basins. Thirdly, a 15% iron(II)chloride (FeCl<sub>2</sub>) solution is added regularly into the primary storage basin (since 2010) in order to reduce H<sub>2</sub>S formation by precipitation of sulfide ions as iron sulfides (e.g., pyrite, FeS<sub>2</sub>, and ironmonosulfide, FeS).

## 2.4. Materials and Methods

In total 84 samples were collected for this study. This comprises solid and liquid samples (58 in total) from the corroded manholes of GS1 and GS2, as well as, liquid samples of SB1 and SB2 (5 in total). Gas measurements were conducted during the six sampling dates within representative manholes to value the concentrations of H<sub>2</sub>S, CO<sub>2</sub>, and CH<sub>4</sub>. In addition, long term gas observations were carried out in order to determine variations in the total H<sub>2</sub>S volumes. Drill cores (21 in total), of 5 cm in diameter, were taken from heavily damaged and intact concrete to evaluate the concrete composition and corrosion rates. The residual thickness of the altered concrete liner was directly measured and compared with that of unaltered concrete (initially about 13 cm thick) to achieve corrosion rates in cm yr<sup>-1</sup>.

### 2.4.1. Solids

Deteriorated concrete mush from different sites was sampled and shoveled into plastic bags. The samples were dried at 40°C and subsequently grounded in a McCrone micronizing mill for 8 min, together with 10 wt. % ZnO as internal standard. X-ray diffraction (XRD) patterns of randomly oriented



preparations were recorded over the range of  $4-85^{\circ}2\theta$  with a step size of  $0.008^{\circ}2\theta$  and a count time of 40 s/step, using a PANalytical X'Pert PRO diffractometer. The diffractometer was equipped with a Co-tube (40 kV and 40 mA), a spinner stage,  $0.5^{\circ}$  divergence and antiscattering slits, and a Scientific X'Celerator detector. Mineral identification and quantification were carried out based on Rietveld refinement of powder XRD patterns using the PANalytical X'Pert HighScore software (version 2.2e) and pdf-2 database.

Extracted drill cores were used for compressive strength and gross density analysis. Therefore, 5 cm cylinders were cut (non-damaged part), subsequently dried, plane-parallel polished and tested, using a Toni Technik 300 kN testing machine, according to Austrian guidelines ÖNORM EN 12504-1 (Testing concrete in structures – Part1: Cored specimens – Taking, examining and testing in compression).

In order to study mineral alterations and neo-formation features of the concrete, selected samples were analyzed with a Zeiss DSM 982 Gemini scanning electron microscope (SEM), operated at 5kV accelerating voltage, by mounting the samples on standard SEM stubs. Images of the sample material have been taken by using the DISS 5 software package (version 5.9.9.1).

In addition, polished thin sections of various drill core samples were prepared to study the microstructural damage of the concrete by combined back-scattered electron imaging (BSE) and single spot analyses using an electron microprobe (EMPA) JEOL JXA-8200 Superprobe. Single spot analyses were made at an accelerating voltage of 15 kV and 5 nA. Damaged and unaltered concrete samples were analyzed for their sulfur (S) and total organic carbon (TOC, after acidification of samples to remove carbonate) contents using a Leco CS230 analyzer. The analytical error is < 5%.

#### **2.4.2. Liquids**

On site, pH and electric conductivity (EC) were measured using a WTW Multi350i instrument equipped with a SenTix41 and a TetraCon325 electrode.  $O_2$  concentrations and redox potential were measured using a Hach LDO and a SenTix ORP electrode, respectively. For further hydro-chemical analyses, wastewater samples were taken throughout the whole sewer system. In the laboratory, the liquid samples were centrifuged using an Avanti™-J-25I centrifuge and subsequently filtered through  $0.45\ \mu\text{m}$  membranes to remove suspended solids and most of the colloidal fraction. Afterwards, the carbonate alkalinity was measured by potentiometric titration with 0.005 M HCl (analytic error < 3%). The major, minor, and trace element concentrations of filtered samples was measured by a Dionex ICS-3000 ion chromatograph (IC) and a PerkinElmer Optima 8300DV inductively coupled plasma optical emission spectrometer (ICP-OES; samples acidified with 2%  $HNO_3$ ). The analytic error was determined to be < 3% for IC and < 6% for ICP-OES analyses. The dissolved organic carbon content (DOC) was analyzed using a Shimadzu TOC-VcPH+ASI-V Analyzer, with an analytical error below 5%.

Dissolved H<sub>2</sub>S was preserved with 5% Zn acetate solution and directly measured spectrophotometrically at Leibniz Institute for Baltic Sea Research Warnemünde (IOW) according to Cline (1969) (Cline, J, 1969) using a Specord 40 (Analytic Jena) device with an analytical precision of ±2 % (Kowalski et al., 2012).

Hydro-chemical modelling was carried out using the computer code PHREEQCi (version 3.1.5-9133). The minteq database was applied in order to calculate saturation indices of gypsum and anhydrite, whereas Inl database was used for bassanite (Parkhurst and Apello, 1999).

A hydraulic press, in a modified setup of Tritthart (Tritthart, 1989), was used to extract the interstitial solutions of the concrete. Therefore, between 800 and 1100 g of the deteriorated concrete was filled into a steel cylinder of a specially adapted press and pressurized at ~1200 kN. The squeezed solutions were sucked into a syringe. Conductivity and pH measurements were conducted instantly after sampling. The extracted pore solutions were then filtered through a 0.45 µm membrane filter, and analyzed with the methods described above (see more details (Mittermayr et al., 2013)).

### **2.4.3. Microbiological Analyses**

Samples were analyzed to prove the existence of SOB in the sampled concrete. 1 g of deteriorated concrete was suspended in 1 ml 0.9% NaCl solution. 0.5 ml was used to inoculate a 100 ml Erlenmeyer flask containing 20 ml modified growth medium for the enrichment of *Thiobacilli* (Starkley, 1935). The medium contained (NH<sub>4</sub>)<sub>2</sub>SO<sub>4</sub> (0.4), KH<sub>2</sub>PO<sub>4</sub> (0.4), CaCl<sub>2</sub> (0.25), FeSO<sub>4</sub> (0.01), MgSO<sub>4</sub> (0.5) and Na<sub>2</sub>S<sub>2</sub>O<sub>3</sub> (5) salts, reported in g l<sup>-1</sup>, that were dissolved in distilled water. Bacteria, growing in this medium in a shaker-incubator at 25°C for five to seven days, were plated on solid medium with the same composition, but additionally containing 1.5 g l<sup>-1</sup> agar. Bacterial cells harvested by centrifugation from the liquid cultures or from colonies that were suspended in 50 µl water were used to extract DNA. Samples were subjected to heat induced lysis for 10 min at 98°C. The released DNA was used for amplification of a 298 base pair 16S rDNA fragment using primers in conserved regions flanking two highly variable regions V5 and V6 (Chakravorty et al., 2007) in standard PCR reactions using Phusion DNA polymerase (New England Biolabs). Forward primer: GATTAGATACCCTGGTAGTCCACGC; reverse primer: TCTCACGACACGAGCTGACGAC. The sequence of the gel purified DNA fragment was determined using both forward and reverse primers in separate sequencing reactions provided by the Eurofins Genomics (Germany) sequencing service. The resulting DNA sequence was searched in the 16S rRNA database (Bacteria and Archaea) subset at the National Center for Biotechnology using BLASTN 2.2.30+.

#### 2.4.4. Gas Phase Analyses

The concentrations of gaseous H<sub>2</sub>S, CH<sub>4</sub>, and CO<sub>2</sub> within the sewer pipe atmosphere were measured periodically, using a Draeger 3000 gas monitor. Long-term gas observations coupled with temperature records were conducted to monitor the inhibitory effect of FeCl<sub>2</sub> addition into the wastewater on gaseous H<sub>2</sub>S emission. Therefore, several myDataSens1000\_H<sub>2</sub>S gas monitors were installed in consecutively positioned manholes, to monitor the H<sub>2</sub>S concentrations over several weeks.

### 2.5. Results

#### 2.5.1. Wastewater chemistry - Atmospheric sewer composition

Wastewater samples taken throughout the whole system showed a decrease in pH from 8.0 ± 0.2 within the storage basins (SB1 and SB2) down to 7.4 ± 0.3 within the sections of the gravity sewer (GS1 and GS2; Figure 1). Consistently, the redox potential values from +51 mV (SB1) and +32 mV (SB2) decreased down to -248 mV (GS1) and -320 mV (GS2), indicating the progressive evolution from oxidizing to strongly reducing conditions within the wastewater. Individual concentrations of dissolved components in the wastewater are displayed in Table 1.

Table 1: Wastewater chemistry along the flow direction within the sewer system. Samples were gathered from the two storage basins (SB1 and SB2) as well as from the first (GS1-1), 6th (GS1-6-6) and 7th manhole of gravity sewer 1 (GS1-7-2), and from the first manhole of gravity sewer 2 (GS2-1-6). Temperature (T°C), pH, electric conductivity (EC) and redox potential (Eh) were measured directly after sampling. Additionally, concentrations of dissolved organic carbon (DOC) are displayed. Complete concentrations of cations (Na<sup>+</sup>, NH<sub>4</sub><sup>+</sup>, K<sup>+</sup>) and anions (Cl<sup>-</sup>, PO<sub>4</sub><sup>3-</sup>) are displayed within the Appendix.

Sample ID	pH	T °C	EC mS cm <sup>-1</sup>	Eh mV	O <sub>2</sub> mg l <sup>-1</sup>	SO <sub>4</sub> <sup>2-</sup> mg l <sup>-1</sup>	Ca <sup>2+</sup> mg l <sup>-1</sup>	Mg <sup>2+</sup> mg l <sup>-1</sup>	DOC mg l <sup>-1</sup>
SB1-5	8.2	10.0	1.7	51.0	0.8	74.3	65.2	13.9	73.0
GS1-1	7.4	8.0	1.7	-157	1.4	41.2	74.6	14.9	64.5
GS1-6-5	7.4	17.7	1.4	-209	1.6	23.3	66.9	12.2	56.2
GS1-7-2	7.3	9.1	1.5	-248	1.8	152	114	13.2	83.0
SB2-2	7.8	9.6	1.8	32.0	4.3	249	147	14.3	83.0
GS2-1-6	7.6	13.5	0.9	-320	0.5	28.7	49.3	9.90	27.5

Occurring re-oxidation could be quantified within GS1, where O<sub>2</sub> concentrations increased from 1.4 mg l<sup>-1</sup> in the first manhole (GS1-1) up to 4.3 mg l<sup>-1</sup> within SB2. Interestingly, O<sub>2</sub> concentrations at SB1 were extremely low, between 0.2 and 0.8 mg l<sup>-1</sup>. In SB1, sulfate concentrations from 64 to 115 mg l<sup>-1</sup> were measured, which decreased down to 25 ± 15 mg l<sup>-1</sup> of SO<sub>4</sub><sup>2-</sup> in the first manholes of GS1 after the upper power main (PM1) of the system. In GS1 the SO<sub>4</sub><sup>2-</sup> concentration within the wastewater increased continuously with flow distance. Finally, in SB2, concentrations between 23 and 249 mg l<sup>-1</sup>

of  $\text{SO}_4^{2-}$  were analyzed. After the second power main (PM2), low  $\text{SO}_4^{2-}$  concentrations of  $30 \pm 15 \text{ mg l}^{-1}$  occurred again. Sulfide concentrations of  $0.35 \text{ mg l}^{-1}$  were measured within SB1, which decreased after the PM1 down to  $0.06 \text{ mg l}^{-1}$ .

Data of long term gas measurements showed average concentrations of 6 ppm of  $\text{H}_2\text{S}$ , with large variations between 0.1 and 367 ppm, within the 4<sup>th</sup> manhole of GS1 (GS1-4) during  $\text{FeCl}_2$  addition over a 6-week period (closed lid). Without  $\text{FeCl}_2$  addition, the  $\text{H}_2\text{S}$  concentrations at least doubled. Typical  $\text{H}_2\text{S}$  long term concentration, concurrent temperature variations and critical  $\text{H}_2\text{S}$  thresholds for the human beings are presented in Figure 2.

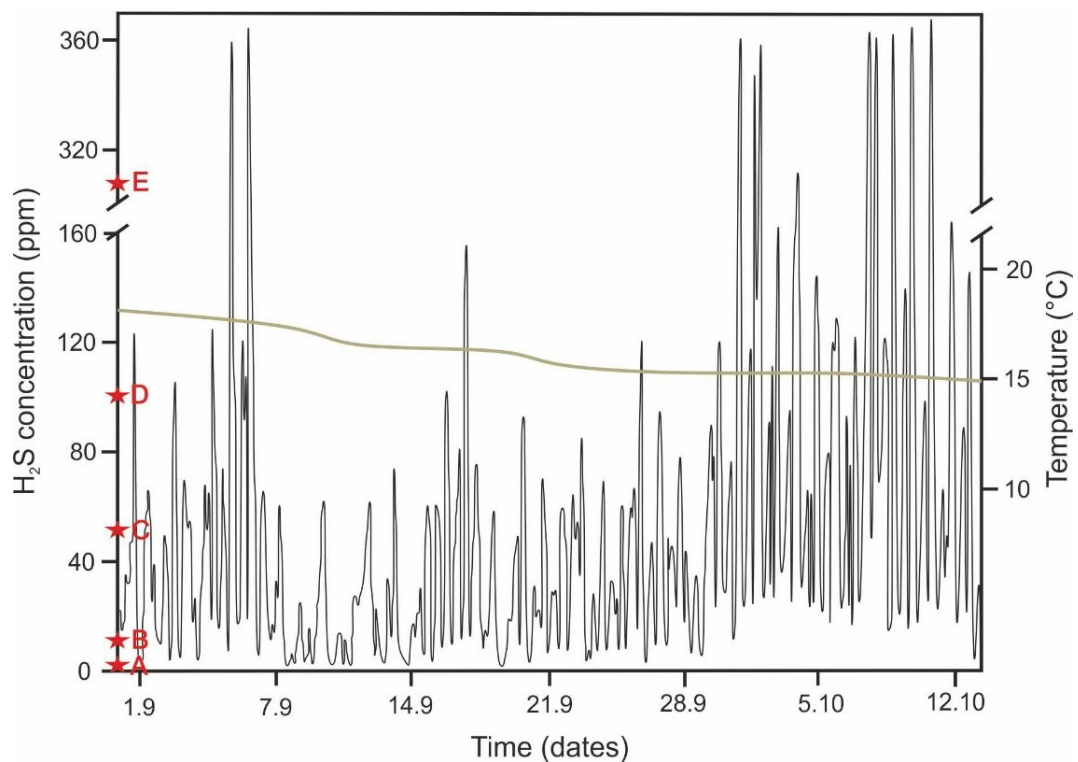


Figure 2: Typical evolution of concentrations of gaseous  $\text{H}_2\text{S}$  within the 4th manhole (GS-1-4) of GS1 (grey line). Internal manhole temperature is displayed in green color. Red stars (A-E) mark important  $\text{H}_2\text{S}$  thresholds for human beings, such as odour threshold (A), eye irritation and headache (B), severe damages of eyes and respiratory systems (C), emerging odourless for human beings (D) and possible death (E) (WHO, 2001).

Gas measurements, conducted during sampling within different manholes, displayed concentrations up to 84 ppm of  $\text{H}_2\text{S}$  (open lids). With flow direction of the wastewater a decrease in gaseous  $\text{H}_2\text{S}$  concentrations was detected, resulting in manholes without any recognizable  $\text{H}_2\text{S}$  emission at the end of GS1 and GS2. Indeed, high  $\text{CO}_2$  concentrations of up to 2600 ppm (typical atmospheric  $\text{CO}_2$  around 370 ppm) were measured throughout the whole system. Additionally,  $\text{CH}_4$  concentrations of up to 1760 ppm were reached in the first few manholes after the two power mains.

### 2.5.2. Sulphuric acid attack and concrete corrosion

Drill cores, extracted from the most heavily corroded manholes in the upper sections of GS1 and GS2, revealed mean corrosion rates of  $0.4 \text{ cm yr}^{-1}$  (Table 2). Significant higher maximum corrosion rates of up to  $>1.0 \text{ cm yr}^{-1}$  were reached in certain strongly deteriorated manholes, e.g. GS2-1. The intact precast concrete of drill cores, extracted from the manholes of GS1 and GS2, showed compressive strengths of  $88 \pm 11 \text{ N/mm}^2$  and residual thickness of 4.0 to 12.5 cm. Therefore, the loss of material within heavily corroded manholes could be determined with up to 9 cm within the last 9 years.

Table 2: Characteristics of drill cores taken from heavily damaged concrete manholes ( $N_{dc}$ = number of cores extracted) showing various states of concrete corrosion. The residual thickness ( $L_{dc}$ ) of each altered concrete liner was directly measured and compared with that of unaltered concrete (13.0 cm) to achieve corrosion rates in  $\text{cm yr}^{-1}$  ( $R_c$ ) and the loss of material (ML). The depth of the different manholes (shaft depth), the compression strength (CS) and density ( $\rho_{concrete}$ ) of the drill cores extracted is additionally reported.

Manhole ID	shaft depth cm	CS $\text{N/mm}^2$	$\rho_{concrete}$ $\text{kg/m}^3$	$N_{dc}$	$L_{dc}$ cm	ML cm	$R_c$ $\text{cm yr}^{-1}$
GS1-4	290	85.1	2370	4	8.5; 9.5; 9.0; 10.0	4.5; 3.5; 4.0; 3.0	0.5; 0.4; 0.4; 0.3
GS1-6	315	97.9	2410	2	9.0; 11.0	4.0; 2.0	0.4; 0.2
GS1-7	273	70.5	2340	2	11.0; 11.5	2.0; 1.5	0.2; 0.2
GS1-26	260	79.9	2330	2	10.0; 12.0	3.0; 1.0	0.3; 0.1
GS1-29	220	90.0	2390	2	12.5; 12.5	0.5; 0.5	0.1; 0.1
GS1-32	170	83.4	2310	2	12.0; 12.5	1.0; 0.5	0.1; 0.1
GS2-1-2	264	106.2	2390	6	4.0; 5.0; 5.0; 6.5; 7.0; 9.5	9.0; 8.0; 8.0; 6.5; 6.0; 3.5	1.0; 0.9; 0.9; 0.7; 0.7; 0.4
GS2-2	274	97.8	2380	1	11.0	2.0	0.2

Mineral compositions of intact concrete were quantified and subsequently compared to compositions of altered concrete. The siliceous compounds of the aggregates remained largely unaffected by corrosion, while the carbonate aggregates were almost completely dissolved or transformed. Analogous, the latter is valid for the cementitious phases, mainly calcium-silicate-hydrate phases (C-S-H) and portlandite ( $\text{Ca(OH)}_2$ ). The alteration of Ca-bearing mineral phases yielded in the precipitation of large quantities of gypsum of up to 42 wt. %. Additionally, significant amounts of anhydrite ( $\text{CaSO}_4$ ;  $16 \pm 1 \text{ wt. } \%$ ) and bassanite ( $\text{CaSO}_4 \cdot 0.5\text{H}_2\text{O}$ ;  $3 \pm 2 \text{ wt. } \%$ ) formed within the corrosion layer of the first two corroded manholes of GS1 (GS1-3 and GS1-4) and the first manhole of GS2 (GS2-1). The change in the quantitative, mineralogical composition of unaltered concrete into strongly deteriorated concrete layers is displayed in Table 3.

Table 3: Mineralogical composition of concrete samples of non-corroded concrete from drill cores, as well as of corroded areas obtained by Rietveld refinement of powder XRD patterns in wt. %, containing quartz (Qz), plagioclase (Pl), alkali feldspar (Kfs), calcite (Cal), muscovite (Ms), portlandite (Port), hornblende (Hbl), clinocllore (Clc), gypsum (Gp), bassanite (Bs), anhydrite (Anh), and x-ray amorphous phases (Amph).

	Sample ID	Qz	Pl	Kfs	Cal	Ms	Port	Hbl	Clc	Gp	Bs	Anh	Amph	R <sub>wp</sub>
Intact	GS1-4-4	41.3	20.2	6.7	5.4	5.2	1.8	0.0	0.7	0.9	0.0	0.0	17.9	5.79
	GS1-6-2	42.2	19.4	4.9	6.8	4.8	2.4	1.4	1.0	0.0	0.0	0.0	17.1	5.54
	GS1-7-2	44.2	13.6	3.3	6.8	4.3	1.6	0.6	0.6	1.2	0.0	0.0	23.9	5.38
	GS1-25-2	40.7	13.5	3.9	9.7	3.5	2.0	1.1	0.4	2.7	0.0	0.0	22.5	5.33
	GS1-28-2	40.2	18.4	5.6	6.7	3.9	1.1	1.4	0.0	2.2	0.0	0.0	20.4	5.34
	GS1-31-2	37.0	15.4	4.4	12.9	4.1	2.7	0.0	0.7	0.6	0.0	0.0	22.2	5.44
	GS2-1-3	41.3	14.1	3.3	12.1	3.9	2.2	1.7	0.7	0.6	0.0	0.0	20.1	5.35
	GS2-2-1	38.9	15.6	5.8	7.0	3.6	1.9	0.6	0.6	0.0	0.0	0.0	26.1	5.53
Corroded	GS1-3-1	27.2	6.6	2.8	0.0	0.0	0.0	0.0	0.0	25.5	1.5	15.2	11.6	7.02
	GS1-4-1	42.0	10.4	0.0	0.0	3.9	0.0	0.0	0.0	12.0	0.8	10.2	10.7	6.05
	GS1-5-1	32.7	13.6	6.6	0.0	0.0	0.0	8.3	0.0	27.8	0.0	0.0	10.7	7.41
	GS1-6-2	33.1	12.5	0.0	0.0	4.4	0.0	2.2	0.0	30.2	0.0	0.0	16.8	7.17
	GS1-8-1	34.0	18.8	0.0	0.0	0.0	0.0	0.0	0.0	33.8	0.0	0.0	12.9	7.18
	GS2-1-1	34.0	13.4	1.8	0.0	2.6	0.0	0.0	0.0	24.3	4.9	17.3	1.8	7.35
	GS2-1-2	31.4	14.5	0.0	0.0	0.0	0.0	0.0	0.0	43.0	0.0	0.0	10.8	7.14

The amount of TOC in the deteriorated concrete ranged between 0.12 and 0.51 wt. %, while TOC quantities between 0.09 and 0.25 wt. % were analyzed for non-deteriorated, respectively.

Microprobe analyses clearly displayed proceeding transformation of the cementitious matrix into gypsum, as well as continuing dissolution and leaching of the cementitious phases. Carbonate aggregates were gradually dissolved and transformed into gypsum, whereas, within GS1-3, GS1-4 and GS2-1 additionally anhydrite and bassanite formation occurred. Secondary electron images (SEI) clearly showed gypsum formation within the deteriorated cementitious matrix (Figure 3).

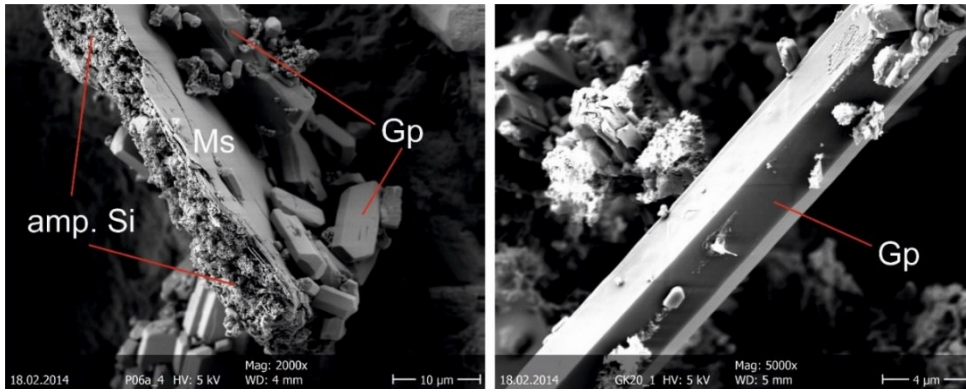


Figure 3: SE-images showing neo-formed gypsum (Gp) crystals due to propagating MICC, as well as amorphous silica (amp. Si) and relicts of mica such as muscovite (Ms).

Residuals of the aggregates, mainly quartz, feldspar (plagioclase and K-feldspar) and mica (muscovite/biotite) as well as distinct Fe-bearing phases like Ferro hornblende ( $(Ca_2Fe_5Al(SiAlO_{22})(OH)_2)$ ) and ilmenite ( $TiFeO_3$ ) remained unaltered. A sharp transition zone (width about 100  $\mu m$ ) can be seen between the initial pristine concrete and highly altered cementitious matrixes, displaying massive occurrences of gypsum, bassanite and anhydrite (Figure 4).

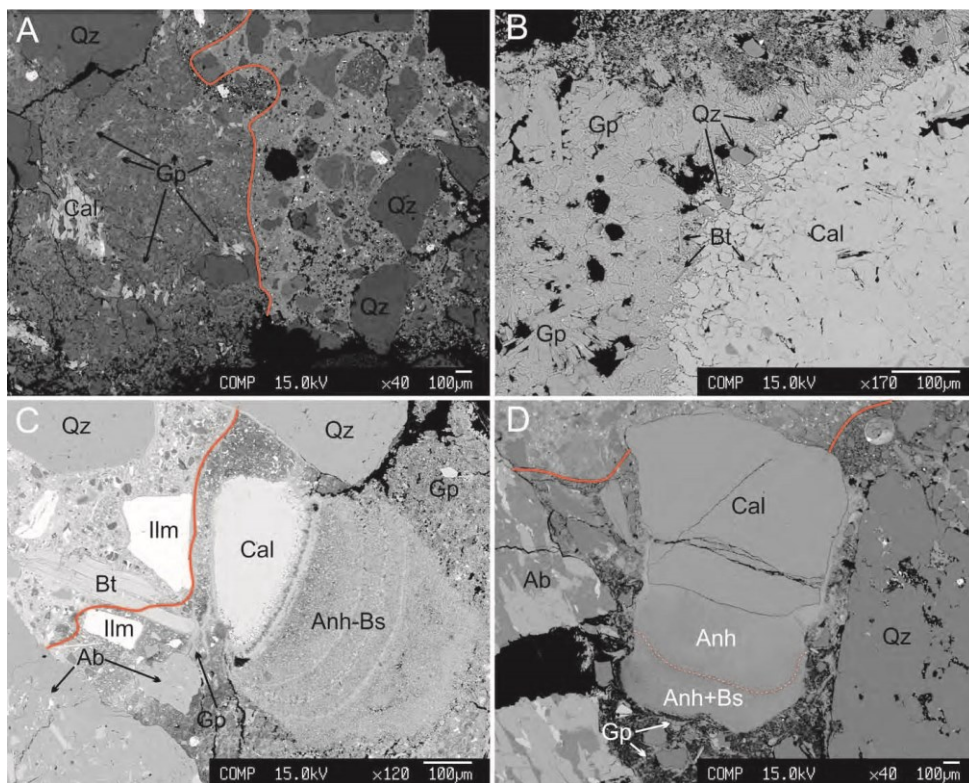


Figure 4: BSE images of partly altered concrete. Top left (A) shows the sharp transition zone between strongly deteriorated concrete with abundant gypsum (Gp) on the left side and less altered concrete on the right side (red line). Top right (B) displays the gradual replacement of calcite (Cal) by gypsum (Gp). Bottom left (C) shows a corrosion front progressing from the right to the left side, causing dissolution of calcite and precipitation of gypsum, anhydrite (Anh) and bassanite (Bs), while grains of the additives like quartz (Qz), ilmenite (Ilm), biotite (Bt) and Albite (Ab) remain largely unaffected. Bottom left (D) displays an enlarged view of a calcite grain, which is transformed into anhydrite and bassanite. Gypsum occurs within the corroded matrix.

Interstitial solutions, extracted from the deteriorated concrete, showed extremely low pH values between 0.7 and 3.1, while concentrations of  $\text{SO}_4^{2-}$  reached high values between 2 and 104  $\text{g l}^{-1}$ . Additionally, high concentrations of  $\text{Ca}^{2+}$  ( $550 \pm 100 \text{ mg l}^{-1}$ ),  $\text{Mg}^{2+}$  (52 to 4321  $\text{mg l}^{-1}$ ) and  $\text{NH}_4^+$  (63 to 2994  $\text{mg l}^{-1}$ ) were measured. In general, a strong and positive correlation between a decrease in pH and elevated dissolved ion concentrations is evident. The Ca-concentration does not follow this trend, but displayed quite constant concentrations. All interstitial solutions were saturated with respect to gypsum ( $\text{SI}_{\text{Gp}}$  between 0.02 and 0.41) and anhydrite ( $\text{SI}_{\text{Anh}}$  between 0.01 and 0.43) while being slightly under-saturated with respect to bassanite ( $\text{SI}_{\text{Bs}}$  between -0.94 and -0.52). Typical enrichment trends in dissolved components, as well as saturation indices for relevant sulfate minerals are summarized in Table 4.

Table 4: Chemical composition of expressed interstitial solutions (PF) from strongly deteriorated concrete of GS1 and GS2. The pH and electrical conductivity (EC) were measured under laboratory conditions at 23 °C. Saturation indices (SI) for gypsum (Gp), bassanite (Bs) and anhydrite (Anh) were calculated using the computer code PHREEQC. The ion mass balance error (in %) is reported.

Sample ID	pH	EC $\text{mS cm}^{-1}$	$\text{Na}^+$ $\text{mg l}^{-1}$	$\text{NH}_4^+$ $\text{mg l}^{-1}$	$\text{K}^+$ $\text{mg l}^{-1}$	$\text{Mg}^{2+}$ $\text{mg l}^{-1}$	$\text{Ca}^{2+}$ $\text{mg l}^{-1}$	$\text{Sr}^{2+}$ $\text{mg l}^{-1}$	Cr $\text{mg l}^{-1}$	Fe $\text{mg l}^{-1}$
GS1-3-PF1	0.9	59.5	97.8	296	122	115	680	5.88	24.5	1527
GS1-4-PF1	0.9	64.2	91	152	266	243	584	5.69	30.2	2080
GS1-5-PF1	2.4	5.7	182	80.8	33.3	51.8	577	3.26	1.90	151
GS1-5-PF2	3.1	4.6	167	62.7	55.2	61.9	638	3.98	1.31	164
GS1-6-PF1	2.7	8.7	109	236	186	309	542	13.7	9.87	838
GS1-6-PF2	1.6	20.4	103	315	163	206	621	15.0	17.6	1005
GS1-6-PF3	2.3	11.3	100	341	194	343	508	8.10	43.0	1721
GS1-6-PF4	1.6	18.3	75.4	370	111	126	494	3.54	12.4	643
GS1-6-PF5	1.8	12.7	59.2	284	108	92.2	469	3.04	11.3	658
GS2-1-PF1	1.0	102.0	2978	2994	1383	4322	551	14.9	138	15693
GS2-1-PF2	1.1	69.5	404	635	534	1521	575	6.53	65.7	6241
GS2-1-PF3	0.7	101.0	573	210	330	990	567	4.54	48.1	2818
GS2-1-PF4	0.9	66.4	523	198	346	931	520	8.47	59.6	2943



Table 4: Continued

Sample ID	Zn mg l <sup>-1</sup>	Al mg l <sup>-1</sup>	F- mg l <sup>-1</sup>	Cl- mg l <sup>-1</sup>	NO <sub>3</sub> <sup>-</sup> mg l <sup>-1</sup>	SO <sub>4</sub> <sup>2-</sup> mg l <sup>-1</sup>	PO <sub>4</sub> <sup>3-</sup> mg l <sup>-1</sup>	SI Gp	SI Bs	SI Anh
GS1-3-PF1	4.22	311	bdl.	44.6	29.0	13605	198	0.11	-0.84	0.10
GS1-4-PF1	3.47	540	bdl.	168	15.0	18139	156	0.14	-0.80	0.14
GS1-5-PF1	1.58	21.2	bdl.	120	8.75	2719	0.89	0.06	-0.89	0.05
GS1-5-PF2	1.23	23	bdl.	112	11.7	2730	0.50	0.11	-0.84	0.10
GS1-6-PF1	4.89	394	9.20	15.4	52.2	7127	3.74	0.10	-0.85	0.09
GS1-6-PF2	3.90	305	5.23	15.9	45.1	9951	17.02	0.15	-0.80	0.14
GS1-6-PF3	4.46	401	8.12	23.4	45.1	9436	15.08	0.10	-0.85	0.09
GS1-6-PF4	1.61	139	bdl.	20.8	28.5	7750	7.19	0.04	-0.91	0.03
GS1-6-PF5	1.55	122	bdl.	17.0	22.4	6092	7.06	0.02	-0.94	0.01
GS2-1-PF1	152	5720	40.6	1648	6.58	104210	555	0.41	-0.52	0.43
GS2-1-PF2	70	1675	20.0	316	1.99	44090	345	0.23	-0.72	0.23
GS2-1-PF3	23	998	bdl.	376	5.35	40818	161	0.11	-0.83	0.11
GS2-1-PF4	18	919	bdl.	380	3.85	32717	141	0.10	-0.85	0.09

Bacteria, enriched from deteriorated concrete samples, were isolated and identified as SOB belonging to the species *Acidithiobacillus thiooxidans*. The sequenced 16S rDNA fragment was 99.6 % identical to the sequence of *Acidithiobacillus thiooxidans* ATCC 19377 (database entry NR\_044920.1). A search against NCBI's (National Center for Biotechnology Information) complete non-redundant nucleotide collection revealed several hits with 100 % sequence identity to 16sDNA fragments from uncultured bacteria (e.g. accession number KF845940) present in biofilms associated with concrete corrosion in the USA, for instance a 98.5 % genetic conformity was determined for *Acidithiobacillus ferrooxidans* (Ling et al., n.d.).

## 2.6. Discussion

The results obtained in the present case study verified that the underlying mechanisms of concrete corrosion are attributed to microbial induced concrete corrosion (MICC). Measured redox potentials down to -320 mV as well as low oxygen levels in the wastewater clearly indicated prevailing anaerobic conditions and associated bacterial activity within PM1 and PM2. There, anaerobic autotrophic organisms, mainly of the genus *Desulfovibrio spp.* and *Desulfomaculum spp.* oxidized organic matter using sulfate as electron acceptor in the absence of oxygen and nitrate (Jensen, 2009) (Figure 5). This process resulted in the formation of sulfide species, including H<sub>2</sub>S, at prevailing pH values between 7 and 8. The sulfide production is accompanied by a significant decrease in the concentration of dissolved sulfate, from about 105 to 14 mg l<sup>-1</sup>, throughout the power mains. Subsequently, H<sub>2</sub>S was liberated from the wastewater into the manholes atmospheres, where concentrations of up to 367 ppm of H<sub>2</sub>S were reached. FeCl<sub>2</sub> addition has proven to trigger iron sulfide precipitation, e.g. FeS<sub>2</sub> and FeS, thus reducing H<sub>2</sub>S concentrations down to an average value of 6 ppm. However, partial re-oxidation of metastable FeS into SO<sub>4</sub><sup>2-</sup> ions within GS1 due to re-aeration resulted in elevated SO<sub>4</sub><sup>2-</sup> concentrations of up to 247 mg l<sup>-1</sup> within SB2. Subsequently, the sulfate ions are reduced within PM2 resulting in high sulfide production rates and consistently high H<sub>2</sub>S emission within GS2-1. Concentrations of CO<sub>2</sub> up to 2600 ppm and CH<sub>4</sub> up to 1760 ppm were quantified in the sewer atmosphere.

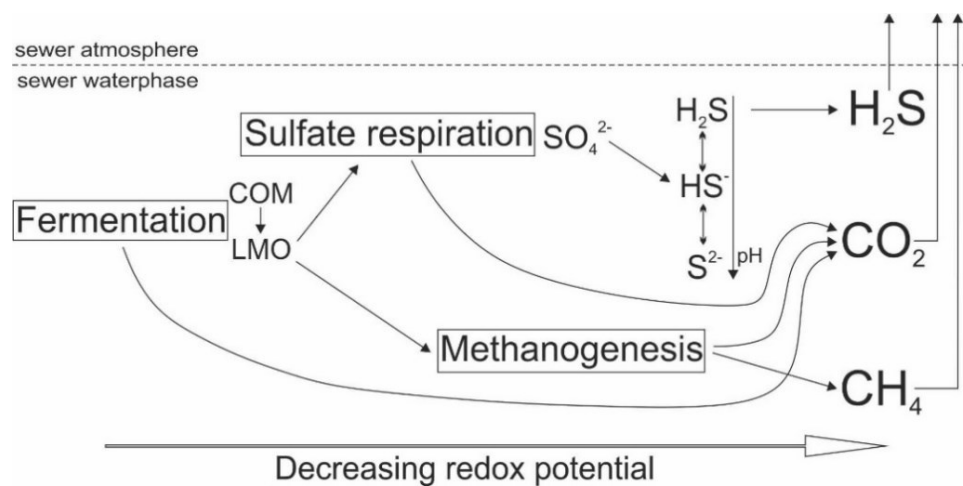


Figure 5: Schematic view of the 3 microbial processes occurring under anaerobic conditions (Hvitved-Jacobsen et al., 2013). Initial transformation from complex organic molecules (COM) into low molecular organics (LMO) takes place through a series of reduction and oxidation processes. LMO are consumed by sulphate-reducing bacteria as well as methane-producing bacteria resulting in the formation of sulphide species, beside methane (CH<sub>4</sub>) and CO<sub>2</sub> production. Note that each individual process is limited to a distinct redox potential.

CH<sub>4</sub> is a common byproduct of methanogenesis, which typically proceeds under extremely reducing conditions that are validated by redox potentials below -200 mV (Hvitved-Jacobsen et al., 2013). CH<sub>4</sub> production is reported in areas within the power main, where sulfate depletion occurred, indicating

complete reduction of  $\text{SO}_4^{2-}$  into sulfide species within parts of PM1 and PM2 (Cappenberg, 1974). A schematic view of the main anaerobic microbial processes is given in Figure 5.

The liberation of volatile components from the wastewater is controlled by surrounding partial gas pressure, temperature and flow turbulences (Saracevic, 2008; Jensen et al., 2011). The latter seemed to engage in a central role concerning the degassing rapidity of the volatile components. Increased corrosion could be quantified in manholes of GS1 (GS1-3, GS1-4), where turns are enhancing flow turbulences and associated higher degassing rates of  $\text{H}_2\text{S}$ ,  $\text{CO}_2$  and  $\text{CH}_4$ . Moreover, after PM2 the wastewater entered GS2 two meters above the channel bottom, creating a waterfall. With increasing flow direction, a significant increased decline in  $\text{H}_2\text{S}$  concentrations within the atmosphere of the concrete based manholes was measured. Simultaneously, the highest corrosion rates of about  $1 \text{ cm yr}^{-1}$  were measured in the first manhole of GS2 (GS2-1). Hence, in GS2 the intensities of cement corrosion decreased much faster with flow distance, compared to GS1 (Figure 6).

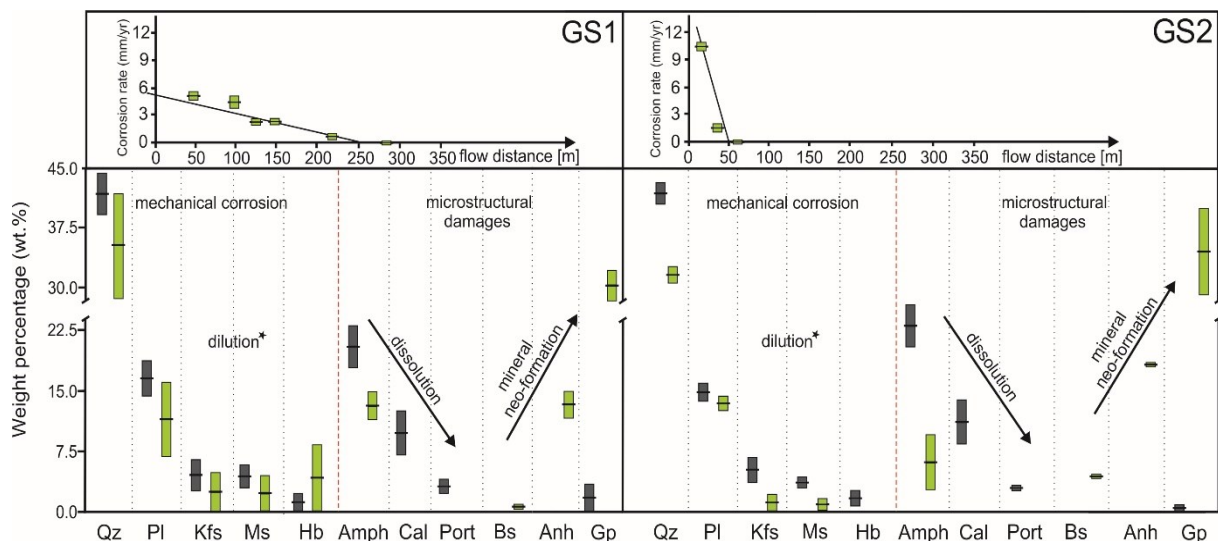


Figure 6: Change in the quantitative, mineralogical composition of unaltered (grey) versus heavily damaged concrete (green), related to MICC. The concrete corrosion rate with flow distance within GS1 and GS2 is reported on top of the figure. Note the significantly highly localized concrete damage in GS2. \*Ongoing dissolution of the supporting cementitious matrix is causing dilution of siliceous compounds such as quartz (Qz), plagioclase (Pl), K-feldspar (Kfs), muscovite (Ms) and hornblende (Hb). Decrease of carbonate and cementitious phases like calcite (Cal) and portlandite (Port) can be attributed to dissolution and subsequent mineral neo-formation of gypsum (Gp), anhydrite (Anh) and bassanite (Bs) formation, which causes intense microstructural damage of the concrete. X-ray amorphous phases (Amph), mainly represent the CSH phases of the cement.

After entering the sewer atmosphere within the manholes,  $\text{H}_2\text{S}$  was absorbed into the interstitial solutions of the outer layer of the concrete walls, where it oxidized through complex reaction paths (De Belie et al., 2004)(Alexander et al., 2013), with  $\text{H}_2\text{SO}_4$  being the final product. It is suggested that the uptake and transformation of gaseous  $\text{H}_2\text{S}$  into  $\text{H}_2\text{SO}_4$  is more efficient in manholes with sealed covers, since ventilation out of the manhole atmosphere is hampered and 100% water saturation within the pore structure of the concrete is reached, creating an environment similar to a bioreactor. Quantification of how much exactly sealed covers attribute towards intensifying corrosion is difficult,

since all those strongly deteriorated manholes are situated within the first part of GS1 and GS2, where simultaneously most intensive degassing occurred. However, no visible corrosion could be seen within the first two manholes of GS1 (GS1-1, GS1-2), which are coated with perforated covers, whereas the following strongly deteriorated manholes, (GS1-3 and following), matched those with sealed covers. Additionally, the straight course within this first 50 meters of GS1 promoted a calm wastewater flow with minor flow turbulences and consequential low degasification rates. During the early stages of the MICC attack carbonation due to the interaction between CO<sub>2</sub>, condensed water, the calcium hydrate phases (C-H) and C-S-H phases of the cementitious matrix took place. Additionally, abiotic oxidation of H<sub>2</sub>S occurred, producing thiosulfuric and polythionic acids (Islander et al., 1991). Both processes reduced the pH from initially ~13 down to ~9.5. Below the latter pH, progressive colonization of aerobic heterotrophic bacteria results in biotic H<sub>2</sub>SO<sub>4</sub> production. Through ongoing decrease of pH different strains of neutrophil SOB colonized the pore system. Starting from pH 5, acidophil bacteria appeared. The bacteria extracted from the deteriorated concrete were identified as *Acidithiobacillus thiooxidans*, which thrive until pH 0.2, if sulfate concentrations exceed about 74 g l<sup>-1</sup> (Lee et al., 2006). In our pore fluids the sulfate concentrations were up to 104 g l<sup>-1</sup>.

It is likely that the bacteria *Acidithiobacillus ferrooxidans* play a central role in intensifying the corrosion rate of concrete in the present case study. These sulfur-oxidizing chemolithotrophs have the ability to use ferric iron as an electron acceptor, if oxygen supply is limited. This ability potentially favors the production of H<sub>2</sub>SO<sub>4</sub> in deeper, anoxic layers of the concrete, thereby accelerating the deterioration of the cementitious phases (Rawlings et al., 2002). Huge amounts of dissolved iron of up to 15.6 g l<sup>-1</sup> were determined within the interstitial solution of deteriorated concrete (Table 4). The metabolism of *Acidithiobacillus thiooxidans* and, most likely *Acidithiobacillus ferrooxidans*, press ahead with the H<sub>2</sub>SO<sub>4</sub> production and adherent concrete deterioration. According to Islander et al. 1991 (Islander et al., 1991), only within this last stage of MICC, where acidophil bacteria are adopting the pore volume at pH below 5, intense concrete breakdown takes place. Considering higher corrosion rates as MICC progresses, it can be taken for granted that during the last years the corrosion rates within the system significantly exceeded the measured average rates of up to 1 cm yr<sup>-1</sup>. This is due to the fact that the measured rates reflect the mean annual loss of concrete wall material since the installation of the sewer system in 2004, whereas concrete alteration in the first years of service is considered low (Table 2). Measured TOC concentrations within the concrete of the initial precast elements confirm the application of superplasticizers, i.e. polycarboxylate ether based superplasticizer (PCEs), which might promote the development of SOB by providing an additional carbon source for bacterial metabolism, beside of CO<sub>2</sub>.

The produced  $\text{H}_2\text{SO}_4$  triggered the dissolution of the cementitious matrix and carbonate aggregates, as well as the neo-formation of gypsum, bassanite and anhydrite. In general, the degradation of the concrete can be assigned to coupled chemical reactions, as well as mechanical and microstructural processes (Figure 6). Quantitative XRD analysis showed the gradual reduction of the C-S-H phases (amorphous content), portlandite and carbonates. The dissolution of these phases resulted in high concentrations of total dissolved solids and associated oversaturation of the interstitial solutions towards calcium sulfate minerals, thus triggering massive neo-formation of gypsum of up to 42 wt. %. Due to proceeding dissolution of the supporting cementitious matrix, silica aggregates break out, which caused a decrease in their abundances, although virtually not affected by MICC. Expected ettringite formation lacked due to its high solubility at the present low pH values and the fact that  $\text{C}_3\text{A}$ -reduced concrete was used in the concrete mixture. Bassanite and anhydrite formation within the most heavily corroded manholes (GS1-3, GS1-4 and GS2-1) could be explained by wetting and drying cycles and subsequent variable  $\text{SO}_4^{2-}$  and  $\text{H}_2\text{O}$  activities within the interstitial solutions of the concrete (for detail see chapter 4). According to Lawrence et al., 1967 (Hardie, 1967), transformation of gypsum into anhydrite occurs within a 4 molar  $\text{H}_2\text{SO}_4$  solution at 1 atm pressure and 23°C. Microprobe analysis support the concept of gradual depletion of the C-S-H phases within the cementitious matrix, adherent dissolution of portlandite and calcite, as well as massive Ca-mineral neo-formation due to propagating corrosion (Figure 4). Moreover, progressing sulfate ion diffusion into the initially damaged concrete matrix is accompanied with a depletion of Si- and Mg-bearing cementitious phases, whereas Ca concentrations remained largely constant due to precipitation as (hydrated) Ca-sulfates. The mobilization and uptake of  $\text{SO}_4^{2-}$  ions proceeded along cracks and grain boundaries between the aggregates and the cement matrix, before propagating throughout the whole matrix.

Possible remediation strategies for the present case system are referred to the application of calcium aluminate cement (CAC) based concrete, as they show better performances in systems exposed to MICC, compared to OPC concrete (Herisson et al., 2013, 2014a, 2014b). Here, the composition of the applied cement plays a major role concerning the establishment of biofilms within concrete pore volumes. CAC reveals inhibitory effects on the activity of the neutrophil bacteria since Al is known to have bacteriostatic characteristics (Goyns and Alexander, 2014). Additionally, the hydrated alumina phases react with the  $\text{H}_2\text{SO}_4$ , to form an alumina gel layer, which significantly decreases the porosity and permeability and hence the diffusion rates in particular within the concrete surface layers. Since the alumina gel layer forms instantaneously, significant lower  $\text{H}_2\text{S}$  diffusion rates, as well as lower oxygen penetration depths could be achieved, thereby limiting biofilm adhesion (Herisson et al., 2014a). Furthermore, the higher acid neutralization capacity of  $\text{Al}(\text{OH})_3$  compared to Ca-hydroxide/carbonate minerals decelerates the pH decrease of the concrete within corrosive

environments. In this context, it is crucial to adapt the Austrian standards for sanitary engineering (e.g. ÖNORM B 2503 in Austria), which currently neither value critical  $\text{H}_2\text{S}_{\text{gas}}$  levels for constructive materials, nor other potentially relevant gaseous components, such as  $\text{CO}_2$  and  $\text{NH}_3$ . Additionally, suggested  $\text{C}_3\text{A}$ -free concrete contains higher  $\text{Fe}_2\text{O}_3$  contents, which might favor the development of *Acidithiobacillus ferrooxidans*, thus increasing biotic  $\text{H}_2\text{SO}_4$  production.

## 2.7. Summary and Conclusion

In the present study, a multi proxy approach, including mineralogical, mechanical, chemical, and biological analyses, was used as a highly powerful tool to investigate the complex reaction mechanisms and controlling environmental parameters for progressing MICC. The deterioration of concrete in the studied Austrian sewer system was accordingly identified to be attributed to bacteriogenically induced sulfuric acid attack, associated with the formation and degassing of high quantities of  $\text{H}_2\text{S}$ . Long retention times of the wastewater within the power mains combined with sealed manhole covers and low discharge rates created “bioreactor conditions”, which resulted in high microbial activity, abundant sulfate reduction, subsequently  $\text{H}_2\text{S}$  degassing and  $\text{H}_2\text{SO}_4$  production.  $\text{H}_2\text{SO}_4$  accumulation in the interstitial solutions of the concrete resulted in pH values between 0.7 and 3.1. This extremely aggressive (micro)environment enhanced the dissolution of the cement matrix and in particular the breakdown of non-siliceous aggregates as well as the neo-formation of potentially expandable alteration products, i.e. gypsum, bassanite and anhydrite. In the present case, the expected ettringite formation lacked due to very low pH values and the application of  $\text{C}_3\text{A}$ -free concrete used for the concrete mixture. High concrete corrosion rates exceeding  $1 \text{ cm y}^{-1}$  were obtained, which caused large parts of the present sewer system to be strongly deteriorated after only 9 years of usage, although highly sulfate resistant concrete plus fly ash (w/c 0.35;  $\text{C}_3\text{A}$ -free cement) was applied.

## 2.8. Acknowledgements

The authors gratefully thank the Graz University of Technology (Austria) scientific grant program for financial support, as well as the scientific input of Josef Tritthart. Additionally, special thanks to Peter Rappold and the Department of Water Resources Management, Styria, as well as to Heinz Lackner and the Department of Energy, Residential Constructions and Technology, Styria, for their financial support. Mineralogical and chemical analyses were carried out at the NAWI Graz Central Lab for Water, Minerals and Rocks. Bacterial isolation and identification were conducted with the expert technical assistance of Karin Bischof at the Institute of Molecular Biosciences, University of Graz (Austria). Jason Prabitz of Kirchdorfer Fertigteilverteilung GmbH and Johannes Kaissl of VTA GmbH are acknowledged for their technical support.

## 2.9. Bibliography

- Alexander, M., Bertron, A., De Belie, N., 2013. Performance of Cement-Based Materials in Aggressive Aqueous Environments, 1st ed. Springer, Ghent. doi:10.1007/978-94-007-5413-3
- Cappenberg, T.E., 1974. Interrelations between sulfate-reducing and methane-producing bacteria in bottom deposits of a fresh-water lake. *J. Microbiol.* 40, 285–95.
- Chakravorty, S., Helb, D., Burday, M., Connell, N., Alland, D., 2007. A detailed analysis of 16S ribosomal RNA gene segments for the diagnosis of pathogenic bacteria. *J. Microbiol. Methods* 69, 330–9.
- Cline, J. D., 1969. Spectrophotometric determination of hydrogen sulfide in natural waters. *Limnol. Oceanogr.* 14, 454–458.
- De Belie, N., Monteny, J., Beeldens, a., Vincke, E., Van Gemert, D., Verstraete, W., 2004. Experimental research and prediction of the effect of chemical and biogenic sulfuric acid on different types of commercially produced concrete sewer pipes. *Cem. Concr. Res.* 34, 2223–2236. doi:10.1016/j.cemconres.2004.02.015
- Dinh, H.T., Kuever, J., Mußmann, M., Hassel, A.W., 2004. Iron corrosion by novel anaerobic microorganisms. *Nature* 829–832. doi:10.1038/nature0234912345678910
- Ešťokov, A., Harbuláková, V.O., Luptáková, A., Številová, N., 2012. Study of the Deterioration of Concrete Influenced by Biogenic Sulphate Attack. *Procedia Eng.* 42, 1731–1738. doi:10.1016/j.proeng.2012.07.566
- Goyns, A.M., Alexander, M., 2014. Performance of various concretes in the Virginia experimental sewer over 20 years. *Calcium Aluminates*. Balkema.
- Gutiérrez-Padilla, M.G.D., Bielefeldt, A., Ovtchinnikov, S., Hernandez, M., Silverstein, J., 2010. Biogenic sulfuric acid attack on different types of commercially produced concrete sewer pipes. *Cem. Concr. Res.* 40, 293–301. doi:10.1016/j.cemconres.2009.10.002
- Hardie, L.A., 1967. The gypsum-anhydrite equilibrium at one atmosphere pressure. *Am. Mineral.* 52.
- Herisson, J., Gueguen-Minerbe, M., Van Hullebusch, E.D., Chaussadent, T., 2014a. Biogenic corrosion mechanism: Study of parameters explaining calcium aluminate cement durability., in: *Calcium Aluminates*. Balkema, pp. 645–58.
- Herisson, J., Guéguen-Minerbe, M., van Hullebusch, E.D., Chaussadent, T., 2014b. Behaviour of different cementitious material formulations in sewer networks. *Water Sci. Technol.* 69, 1502–8. doi:10.2166/wst.2014.009
- Herisson, J., van Hullebusch, E.D., Moletta-Denat, M., Taquet, P., Chaussadent, T., 2013. Toward an accelerated biodeterioration test to understand the behavior of Portland and calcium aluminate cementitious materials in sewer networks. *Int. Biodeterior. Biodegradation* 84, 236–243. doi:10.1016/j.ibiod.2012.03.007
- Hvitved-Jacobsen, T., Vollertsen, J., Nielsen, A.H., 2013. *Sewer Processes - Microbial and Chemical Process Engineering of Sewer Networks*, 2nd ed. CRC Press, London.
- Hvitved-Jacobsen, T., Vollertsen, J., Yongsiri, C., Nielsen, A.H., 2002. Sewer microbial processes, emissions and impacts, in: *Sewer Processes and Networks*. Paris, p. 13.
- Islander, B.R.L., Deviny, J.S., Member, A., Mansfeld, F., Postyn, A., Shih, H., 1991. Microbial ecology of crown corrosion in sewers. *J. Environ. Eng.* 117, 751–770.
- Jensen, H.S., 2009. PhD thesis; Hydrogen sulfide induced concrete corrosion of sewer networks. Aalborg University.

- Jensen, H.S., Lens, P.N.L., Nielsen, J.L., Bester, K., Nielsen, A.H., Hvitved-Jacobsen, T., Vollertsen, J., 2011. Growth kinetics of hydrogen sulfide oxidizing bacteria in corroded concrete from sewers. *J. Hazard. Mater.* 189, 685–91. doi:10.1016/j.jhazmat.2011.03.005
- Jiang, G., Wightman, E., Donose, B.C., Yuan, Z., Bond, P.L., Keller, J., 2014. The role of iron in sulfide induced corrosion of sewer concrete. *Water Res.* 49, 166–74. doi:10.1016/j.watres.2013.11.007
- Joseph, A.P., Keller, J., Bustamante, H., Bond, P.L., 2012. Surface neutralization and H<sub>2</sub>S oxidation at early stages of sewer corrosion: influence of temperature, relative humidity and H<sub>2</sub>S concentration. *Water Res.* 46, 4235–45. doi:10.1016/j.watres.2012.05.011
- Kowalski, N., Dellwig, O., Beck, M., Grunwald, M., Dürselen, C.-D., Badewien, T.H., Brumsack, H.-J., van Beusekom, J.E.E., Böttcher, M.E., 2012. A comparative study of manganese dynamics in the water column and sediments of intertidal systems of the North Sea. *Estuar. Coast. Shelf Sci.* 100, 3–17. doi:10.1016/j.ecss.2011.03.011
- Lee, E.Y., Lee, N.Y., Cho, K.-S., Ryu, H.W., 2006. Removal of hydrogen sulfide by sulfate-resistant *Acidithiobacillus thiooxidans* AZ11. *J. Biosci. Bioeng.* 101, 309–14. doi:10.1263/jbb.101.309
- Ling, A.L., Robertson, C.E., Pace, N.R., Hernandez, M.T., n.d. *Microbial and Chemical Characterization of Concrete Corrosion Biofilms of Wastewater Infrastructure in Ten Cities.* (Unpublished).
- Mittermayr, F., Baldermann, A., Kurta, C., Rinder, T., Klammer, D., Leis, A., Tritthart, J., Dietzel, M., 2013. Evaporation — a key mechanism for the thaumasite form of sulfate attack. *Cem. Concr. Res.* 49, 55–64. doi:10.1016/j.cemconres.2013.03.003
- Mittermayr, F., Rezvani, M., Baldermann, A., Hainer, S., Breitenbücher, P., Juhart, J., Graubner, C.-A., Proske, T., 2015. Sulfate resistance of cement-reduced eco-friendly concretes. *Cem. Concr. Compos.* 55, 364–373. doi:10.1016/j.cemconcomp.2014.09.020
- Nielsen, A.H., Vollertsen, J., Jensen, H.S., Madsen, H.I., Hvitved-Jacobsen, T., 2006. Aerobic and Anaerobic Transformations of Sulfide in a Sewer System – Field Study and Model Simulations. *Proc. Water Environ. Fed.* 2006, 3654–3670. doi:10.2175/193864706783751447
- Nielsen, A.H., Vollertsen, J., Jensen, H.S., Wium-Andersen, T., Hvitved-Jacobsen, T., 2008. Influence of pipe material and surfaces on sulfide related odor and corrosion in sewers. *Water Res.* 42, 4206–14. doi:10.1016/j.watres.2008.07.013
- O’Connell, M., McNally, C., Richardson, M.G., 2010. Biochemical attack on concrete in wastewater applications: A state of the art review. *Cem. Concr. Compos.* 32, 479–485. doi:10.1016/j.cemconcomp.2010.05.001
- Olmstead, W.M., Hamlin, H., 1900. Converting portions of the Los Angeles outfall sewer into a septic tank. *Eng. News* 971–980.
- Parkhurst, D.L., Apello, C.A.J., 1999. *User’s guide to PHREEQC (V2).*
- Rawlings, D.E., Dew, D., Plessis, C., 2002. Biomineralization of metal-containing ores and concentrates 7799, 4–5.
- Roberts, D.J., Nica, D., Zuo, G., Davis, J., 2002. Quantifying microbially induced deterioration of concrete: initial studies. *Int. Biodeterior. Biodegradation* 49, 227–234. doi:10.1016/S0964-8305(02)00049-5
- Saracevic, E., 2008. PhD thesis; Zur Kenntnis der Schwefelwasserstoffbildung und -vermeidung in Abwasserdruckleitungen. TU Wien.
- Soleimani, S., Isgor, O.B., Ormeci, B., 2013. Resistance of biofilm-covered mortars to microbiologically influenced deterioration simulated by sulfuric acid exposure. *Cem. Concr. Res.* 53, 229–238. doi:10.1016/j.cemconres.2013.06.016



- Starkley, R.L., 1935. Isolation of some bacteria which oxidize thiosulfate. *Soil Sci.* 39, 197–220.
- Tritthart, J., 1989. Chloride binding in cement I. Investigations to determine the composition of porewater in hardened cement. *Cem. Concrete Res.* 19, 586–94.
- World Health Organisation, 2001. Air Quality Guidelines 40, 9823. doi:10.1002/1521-3773(20010316)
- World Health Organisation, 2000. Hydrogen Sulfide, in: *Air Quality Guidelines for Europe*. Copenhagen, p. 7.
- Yousefi, A., Allahverdi, A., Hejazi, P., 2014. Accelerated biodegradation of cured cement paste by *Thiobacillus* species under simulation condition. *Int. Biodeterior. Biodegradation* 86, 317–326. doi:10.1016/j.ibiod.2013.10.008
- Zhang, L., De Schryver, P., De Gusseme, B., De Muynck, W., Boon, N., Verstraete, W., 2008. Chemical and biological technologies for hydrogen sulfide emission control in sewer systems: a review. *Water Res.* 42, 1–12. doi:10.1016/j.watres.2007.07.013

## 2.10. Appendix

Appendix A1: Chemical composition of wastewater samples taken from different manholes within GS1 and GS2 as well as from SB1 and SB2. DOC: total dissolved organic carbon, where values are referred to wt. % of C.

Sample ID	Na <sup>+</sup> mg l <sup>-1</sup>	NH <sub>4</sub> <sup>+</sup> mg l <sup>-1</sup>	K <sup>+</sup> mg l <sup>-1</sup>	Mg <sup>2+</sup> mg l <sup>-1</sup>	Ca <sup>2+</sup> mg l <sup>-1</sup>	Cl <sup>-</sup> mg l <sup>-1</sup>	SO <sub>4</sub> <sup>2-</sup> mg l <sup>-1</sup>	PO <sub>4</sub> <sup>3-</sup> mg l <sup>-1</sup>	DOC mg l <sup>-1</sup>
SB1-1	85.4	76.9	23.1	12.9	69.0	104	64.0	2.77	n.a.
SB1-4	72.9	85.4	21.4	13.0	83.7	90.4	115	0.45	61.1
SB1-5	142	104	24.9	13.9	65.2	237	74.3	1.84	73.0
GS1-1	136	73.3	25.9	14.9	74.6	228	41.2	6.34	64.5
GS1-6-1	39.6	23.5	8.62	4.76	27.3	46.3	14.3	3.88	82.5
GS1-6-2	37.3	22.7	8.26	4.86	38.0	43.8	41.4	3.97	59.4
GS1-6-3	28.6	41.3	9.55	7.91	27.7	25.9	21.5	8.02	56.2
GS1-6-4	93.4	56.8	25.2	11.2	71.5	102	40.9	7.80	n.a.
GS1-6-5	92.0	70.0	25.7	12.2	66.9	102	23.3	14.8	n.a.
GS1-6-6	68.6	50.4	18.3	10.1	79.4	87.3	79.7	8.13	50.2
GS1-6-7	67.9	50.0	18.0	9.75	70.5	86.4	51.0	9.43	48.0
GS1-6-8	70.8	58.6	18.4	10.8	73.0	94.3	57.2	7.23	46.2
GS1-6-9	138	74.9	23.9	15.2	73.6	223	48.8	5.32	65.0
GS1-7-1	95.5	70.9	23.6	13.2	81.5	89.7	64.4	18.6	83.7
GS1-7-2	95.9	70.3	24.3	13.2	114	91.0	152	16.8	83.0
GS1-8-1	27.9	28.2	9.21	6.71	26.3	29.9	15.4	4.03	52.4
SB2-1	34.8	23.5	8.18	4.82	30.3	40.2	23.3	3.55	38.7
SB2-2	110	83.9	32.9	14.3	147.5	104	249	15.3	83.0
GS2-1-1	36.3	25.3	8.38	5.18	28.2	43.5	13.8	5.09	56.5
GS2-1-2	77.9	68.3	24.1	17.0	77.4	85.2	45.0	10.5	n.a.
GS2-1-5	60.9	51.1	20.8	10.1	49.9	64.1	30.8	11.3	25.5
GS2-1-6	59.5	49.9	20.1	9.87	49.3	62.8	28.7	11.2	27.5
GS2-1-7	94.9	70.9	21.0	13.2	76.2	89.1	44.4	19.0	73.2
GS2-1-8	94.0	71.6	21.2	13.0	69.7	88.6	23.8	19.4	77.3
GS2-1-9	152	77.4	22.6	14.3	63.8	214	32.0	11.1	69.2

## Chapter 3

### The decisive role of acidophilic bacteria in concrete sewer networks: A new model for fast progressing microbial concrete corrosion

Grengg, C.<sup>1</sup>, Mittermayr, F.<sup>2</sup>, Koraimann, G.<sup>3</sup>, Konrad, F.<sup>1</sup>, Szabó M.<sup>4</sup>, Demeny A.<sup>4</sup>, Dietzel, M.<sup>1</sup>

<sup>1</sup> Institute of Applied Geosciences, Graz University of Technology, Rechbauerstraße 12, 8010, Graz, Austria

<sup>2</sup> Institute of Technology and Testing of Construction Materials, Graz University of Technology, Inffeldgasse 24, 8010, Graz, Austria

<sup>3</sup> Institute of Molecular Biosciences, University of Graz, Humboldtstraße 50, 8010, Graz, Austria

<sup>4</sup> Institute for Geological and Geochemical Research, Hungarian Academy of Science, Budaörsi Street 45, H-1112, Budapest, Hungary

Keywords: Concrete; sulphuric acid; EMPA; Micro XRD; acid corrosion; microbiological corrosion;

#### 3.1. Abstract

This study introduces a novel approach intertwining analytics of spatial microbial distribution with chemical, mineralogical and (micro)structural related aspects in corroded concrete sewer environments. Samples containing up to 4cm thick corrosion layers were collected from concrete manholes and analyzed using hydro-geochemical, microbiological, biochemical and mineralogical methods. Opposed to the current opinion DNA and RNA indicating microbial activity were found throughout the entire deterioration layer down to the corrosion front. Elemental distributions of corresponding areas revealed a dynamic pH- and diffusion-controlled system in which a distinct succession of elemental accumulations was unequivocally correlated with responding pH levels, associated dissolution and precipitation of solids, as well as with the spatially resolved presence of microbes. Microbial activity further coincided with massive iron deposition zones, within the inner anoxic to anaerobic corrosion layers. As a possible microbial catalyst for iron oxidation and in-situ acid production in this zone, we propose *Acidithiobacillus ferrooxidans* which were isolated from the deteriorated concrete. Based on the data we propose a new model in which biogenic induced in-situ acid production is a decisive factor, steering high concrete corrosion rates of  $>1\text{cm yr}^{-1}$ .

#### 3.2. Introduction

The degradation of sewer systems due to microbial induced concrete corrosion (MICC) has been one of the main problems of modern society's subsurface infrastructure within the last century

(Jensen, 2009; O'Connell et al., 2010; Olmstead and Hamlin, 1900). Besides of huge economic relevance, also health related concerns due to hazardous gas production and associated odor problematic are recognized (Hvitved-Jacobsen et al., 2002; Joseph et al., 2012; Nielsen et al., 2008, 2006). The general process mechanisms have been subject to numerous studies, and can be summarized as a complex chain of coupled biotic and abiotic redox reactions (Grenng et al., 2015; Islander et al., 1991; Okabe et al., 2007; Vincke et al., 2000; Vollertsen et al., 2008). Initial sulfate reduction proceeds within anaerobic sediment layers, which accumulate along the bottom of preferentially slow flowing sewer pipes and power mains holding long retention times (Alexander et al., 2013; Herisson et al., 2013; Jayaraman et al., 1999). There, various species of sulfate reducing bacteria (SRB) lead to hydrogen sulfide (H<sub>2</sub>S) production, which is accompanied by fermentation processes producing carbon dioxide (CO<sub>2</sub>) and volatile organic compounds (VOC's) (Gao et al., 2016; Liu et al., 2016; van Loosdrecht et al., 2016). Gaseous compounds produced, are liberated into the atmosphere of the concrete pipes and manholes, where they partly dissolve into the condensates along the concrete walls and subsequently diffuse into the concrete pore structure. After an initial period of abiotic pH reduction due to acid-base reactions involving CO<sub>2</sub> and H<sub>2</sub>S in the alkaline concrete environment, secondary H<sub>2</sub>S re-oxidation by a succession of sulfur oxidizing bacteria (SOB) results in biogenic sulfuric acid (H<sub>2</sub>SO<sub>4</sub>) production and subsequent concrete deterioration (Alexander et al., 2013; De Belie et al., 2004). In order to efficiently control MICC, it is central to understand the succession, distribution and interaction of various species of microorganisms involved combined with the chemical, mineralogical and material related aspects of concrete degradation. A mutualistic relationship between different autotroph SOB and heterotrophs, e.g. *Acidiphilium*, has been reported (Hernandez et al., 2002; Islander et al., 1991; Okabe et al., 2007). Cho and Mori (Cho and Mori, 1995) described the interaction of autotrophic bacteria and acid-resistant fungi which oxidize H<sub>2</sub>S to thiosulfate (S<sub>2</sub>O<sub>3</sub><sup>2-</sup>). The latter thiosulfate ions again can be utilized by *Acidithiobacilli spp.* Current models suggest the highest cell concentrations at and close to the concrete surface within oxygen (O<sub>2</sub>), CO<sub>2</sub> and H<sub>2</sub>S rich layers. O<sub>2</sub> concentrations are reported to decrease drastically with depth in the corrosion layer of the concrete, mainly due to chemical oxygen consumption, reaching anoxic conditions at 400 to 600 μm. Cell accumulations are described to decrease accordingly (Okabe et al., 2007; Satoh et al., 2009). However, these models are based on observations, drawn from bulk samples of various in situ testing sites, with limited information regarding spatially resolved microbial distribution throughout the interior of corrosion layers. Limited information is found in the literature describing MICC processes drawn from field studies and field observations. Analysis of data obtained from samples originating from real sewer environments is central in order to enhance in-depth knowledge of MICC and enables development of possible counteracting measures.

This field study aims to investigate the presence and spatial distribution of microorganisms throughout up to 4 cm thick deterioration layers of a strongly corroded concrete sewer system, which has been recently described in (Grenng et al., 2015). For that purpose, concrete samples, cut from several, strongly deteriorated concrete manholes (see Figure 1), and were analyzed by in situ nucleic acid (DNA and RNA) staining in combination with fluorescence microscopy. In order to obtain extensive information, microbial accumulations were linked to element distributions of the same areas, which were measured using an electron microprobe. High resolution spot analyses of mineralogical composition throughout the corrosion fronts were analyzed, using Micro-XRD, in order to determine the spatial distribution of newly formed mineral phases. This dataset was integrated into a new model for fast progressing MICC. Intriguingly, DNA and RNA indicating microbial activity was found not only at the surface but also deeply inside the deteriorated concrete at the transition zone to intact concrete. Since we were able to isolate *Acidithiobacillus ferrooxidans* from the material, a bacterial species capable of chemoautotrophic anaerobic growth, iron oxidation and acid production, we propose that this bacterial species plays a decisive role in the progression of MICC.

### **3.3. Study site, Materials and Methods**

#### **3.3.1. Study site description and concrete properties**

Concrete samples investigated in this study were extracted from strongly deteriorated concrete manholes of an Austrian sewer system. A detailed description of the system, including concrete properties, corrosion rates, wastewater chemistry, microbial aspects and interstitial fluid chemistry has been recently described in Ref. (Grenng et al., 2015). In brief, the system investigated is handling the wastewater of around 13 000 people, with a daily average wastewater discharge of around 300 m<sup>3</sup>. In 2004, two new power mains were integrated into the system in the course of the fusion of two separated gravity sewers lines. Ever since, community complains about odor rose, which were accompanied by heavy degradation of several concrete manholes within the gravity sewer sections. Measured corrosion rates of up to >1 cm yr<sup>-1</sup> led to a required replacement of affected manholes after a service life of only 10 years. Material analytics of non-corroded implemented precast elements revealed a mean comprehensive strength of  $88 \pm 11$  N/mm<sup>2</sup> and a w/c ratio of ~0.35. CEM I 42.5N (C<sub>3</sub>A-free) plus fly ash and 0.25 wt. % of a PCE based superplasticizer, referred to the cement content, was used for concrete production. This classification corresponds to exposition class XA2 for chemical attack according to ÖNORM B 4710-1 (Concrete - Part 1: Specification, production, use and verification of conformity. Rules for the implementation of EN 206-1 for normal and heavy concrete), thus exceeding the requirements postulated in European concrete standard regulations (EN 206-1).

From heavily corroded manholes expressed interstitial concrete solutions showed low pH levels between 0.7 and 3.1 with extremely high concentrations of dissolved ions e.g. sulfate up to 104 g l<sup>-1</sup> (for representative values see Table 1).

Table 1: Representative mineralogical characterization of the implemented concrete and expressed interstitial fluids within this system. Showing the mineralogical composition of non-deteriorated (CM 1 and CM 2) and strongly corroded (CM<sub>c</sub> 1 and CM<sub>c</sub> 2) concrete samples in wt. %, containing quartz (Qz), plagioclase (Pl), alkali feldspar (Kfs), calcite (Cal), muscovite (Ms), portlandite (Port), hornblende (Hbl), clinocllore (Clc), gypsum (Gp), bassanite (Bs), anhydrite (Anh) and X-ray amorphous phases (Amph), together with the analytical error (R<sub>wp</sub>). Additionally, chemical compositions of expressed interstitial solutions (IS1, IS2 and IS3) from strongly deteriorated concrete manholes are shown together with pH and electrical conductivity (EC). For a complete dataset see Grengg et al. (Grengg et al., 2015).

#### Concrete composition

	ID	Qz	Pl	Kfs	Cal	Ms	Port	Hbl	Clc	Gp	Bs	Anh	Amph	R <sub>wp</sub>
Intact	CM1	41.3	20.2	6.7	5.4	5.2	1.8	0.0	0.7	0.9	0.0	0.0	17.9	5.79
	CM2	42.2	19.4	4.9	6.8	4.8	2.4	1.4	1.0	0.0	0.0	0.0	17.1	5.54
Corroded	CM <sub>c</sub> 1	27.2	6.6	2.8	0.0	0.0	0.0	0.0	0.0	25.5	1.5	15.2	11.6	7.02
	CM <sub>c</sub> 2	31.4	14.5	0.0	0.0	0.0	0.0	0.0	0.0	43.0	0.0	0.0	10.8	7.14

#### Interstitial fluid chemistry

ID	pH	EC mS cm <sup>-1</sup>	Na <sup>+</sup> mg l <sup>-1</sup>	NH <sub>4</sub> <sup>+</sup> mg l <sup>-1</sup>	K <sup>+</sup> mg l <sup>-1</sup>	Mg <sup>2+</sup> mg l <sup>-1</sup>	Ca <sup>2+</sup> mg l <sup>-1</sup>	Fe mg l <sup>-1</sup>	Zn mg l <sup>-1</sup>	Al mg l <sup>-1</sup>	Cl <sup>-</sup> mg l <sup>-1</sup>	NO <sub>3</sub> <sup>-</sup> mg l <sup>-1</sup>	SO <sub>4</sub> <sup>2-</sup> mg l <sup>-1</sup>
IS 1	0.9	64	91	152	266	243	584	2080	3.47	540	168	15.0	18139
IS 2	1.0	102	2978	2994	1383	4322	551	15693	152	5720	1648	6.58	104210
IS 3	0.7	101	573	210	330	990	567	2818	23	998	376	5.35	40818

Between non-deteriorated and strongly affected concrete, a complete depletion of cement phases, e.g. portlandite and C-S-H phases, as well as of carbonate aggregates was observed. Simultaneously, massive formation of sulfate salts, mainly gypsum (Gp, up to 29 wt. %), but also anhydrite (Anh, up to 15 wt. %) and bassanite (Bas, up to 1.5 wt. %) proceeded. Representative values are summarized in Table 1. Bacteria, enriched from the deteriorated concrete samples of the same manholes were identified as *Acidithiobacillus thiooxidans*.

### 3.3.2. Concrete extraction, visual observations and analyses

Concrete pieces with dimensions of several 10th of cm were cut with an angle grinder from the exhumed manholes and dried at 40 °C for several days. In order to stabilize the 3.5 to 4 cm thick mushy deterioration layers, the whole samples were covered in a two-component epoxy resin (Buehler;

EpoThin 2 Hardener) under vacuum conditions. Thereafter, several 0.5 cm thick cross sections were cut from the sample and again covered in epoxy resin in order to guarantee stability for pursuing thick section preparations (Figure 1). High-resolution mappings throughout the thick sections were conducted using a Keyence VHX-5000 Digital-Microscope with a 100-fold optical magnification.

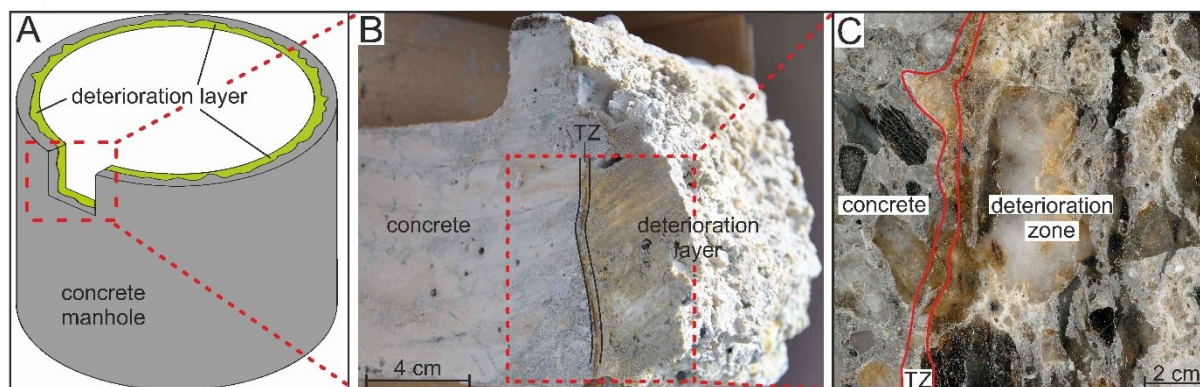


Figure 1: Schematic description of the sampling campaign. Samples were cut from several concrete manholes (A). Notice the sharp transition zone (TZ) and up to 4 cm thick deterioration layer (B). Samples were dried and subsequently embedded into a two component epoxy resin in order to guarantee stability for further analyses and imaging (C).

### 3.3.3. Element Mappings

Quantitative elemental distribution images of aluminum, calcium, iron, magnesium, silicon and sulfur were recorded by electron probe microanalysis (EPMA) using a JEOL JXA-8200 Superprobe (JEOL, Tokyo, Japan). The wavelength-dispersive analytical mode with 15 kV acceleration voltage and a beam current of 30 nA was used. 1024 x 1024 point analyses and a step size of 3  $\mu\text{m}$  yielded elemental distribution mappings of 3072 x 3072  $\mu\text{m}$ . Figure. 2 is stitched from 9 such images, with an overlap of 100 pixels between each mapping, resulting in a 9016 x 9016-pixel graphic. The quantification of the individual mappings in wt. % was performed against mineral standards from SPI (Pyrope for Al, Si and Fe; Anhydrite for Ca and S (SPI).

### 3.3.4. Micro XRD analyses

A Rigaku DMAX-Rapid II micro diffraction system with a rotating Cu anode and micro-focus optics was used to carry out point mineralogical analyses on flat cut surfaces of the samples. X-rays were generated at 50 kV and 0.6 nA and collimated to 800 microns on the samples surface according to the textural and mineralogical characteristics of the analyzed spots with a dwell time of 600 seconds. Corresponding spot areas were  $\sim 0.5 \text{ mm}^2$  as calculated from collimator sizes and incident angles. Diffraction patterns were collected onto a 2D detector and transformed to conventional intensity vs. 2theta patterns using the Rigaku 2DP data processing software. Mineralogical phase identifications were carried out using PANalytical X'Pert HighScore software (version 2.2e) and pdf-2 crystal structure database.



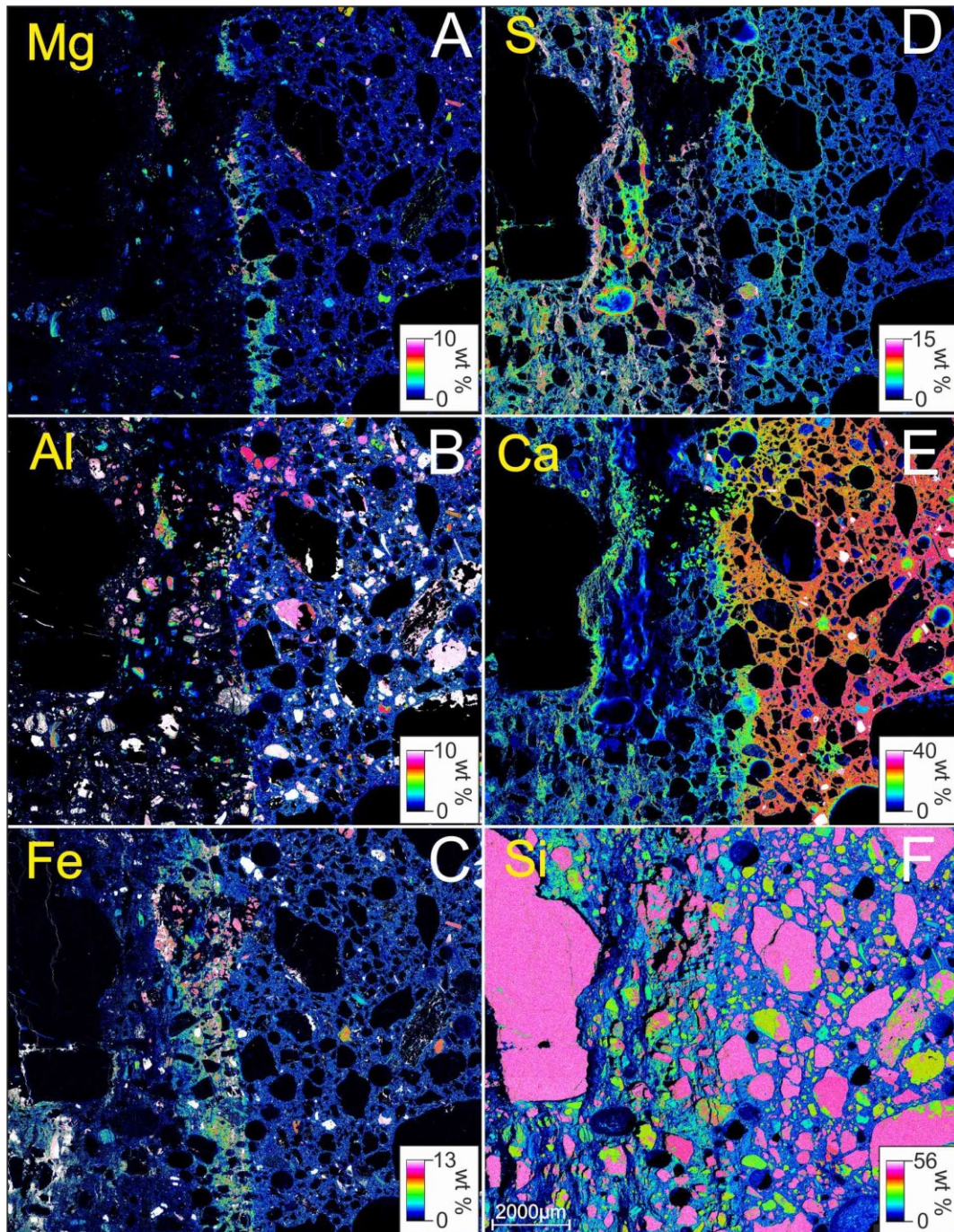


Figure 2: Displaying the element distributions from non-corroded concrete (right side) throughout the corrosion front and heavily corroded layers (left side). Notice the succession of S, (D, up to 15 wt.%), Mg (A, up to 10 wt.%), Al (B, up to 10 wt.%), and Fe (C, up to 13 wt.%) accumulation areas throughout the transition zone from non- deteriorated concrete, which is characterized by high Ca concentrations (E, up to 40 wt.%) and Si (F, up to 56 wt.%) concentrations, to strongly corroded concrete.

### 3.3.5. Fluorescent staining and imaging

To directly visualize the distribution of microbial activity throughout the deteriorated concrete sample a mixture of two dyes that show fluorescence when bound to nucleic acids (DNA and/or RNA) was applied. The dye consisted of SYTO9 (green fluorescence, 480 nm excitation, 500 nm emission) and propidium iodide (PI, red fluorescence, 490 nm excitation, 635 nm emission) which are



components of the LIVE/DEAD BacLight bacterial viability kit (Molecular Probes). Whereas SYTO9 is a DNA dye that enters all cells, PI can only penetrate into dead cells. 1.5  $\mu$ L of each dye were diluted in 5 mL PBS. The surface of the concrete block was covered with the solution and kept in the dark for 1h. Afterwards, the surface was carefully rinsed with distilled water and then dried before detecting fluorescent signals using a ChemiDoc MP (BioRad) imaging system. To detect fluorescent signals blue or green excitation LEDs together with fluorescein or rhodamine filter sets were used, respectively. Exposure times for fluorescein, rhodamine or white were 0.036, 0.428 or 0.081 sec, respectively. Multichannel images were created by overlay and further processed using Image Lab 4.0 software (BioRad). Identical image parameters were used for all color channels and exported into jpg format.

### **3.3.6. Fluorescence microscopy**

Epifluorescence microscopy images were obtained directly from the stained surface of the concrete sample block (see above) using a Nikon Eclipse Ti microscope with a 10x objective (Plan Fluor 10x DIC L N1). The motorized sample holder was used to determine x/y coordinates to align the images to the exact positions on the surface of the sample block. For each position three images with three different filter sets (blue 360/460 DAPI, green 480/535 FITC, red 559.5/645.5 Texas Red) and identical exposure times of 100 ms were taken. Images were analyzed using NIS-Elements software. Identical image parameters were used for all color channels and overlays were exported into jpg format.

### **3.3.7. Growth and enrichment of *Acidithiobacillus ferrooxidans***

1 g of concrete extracted from the inner corrosion layers of the deteriorated manholes was suspended in 1 mL of 0.9% NaCl solution. 0.5 mL was used to inoculate a 100 mL Erlenmeyer flask containing 20 mL growth medium for the enrichment of *Acidithiobacillus ferrooxidans* (according to ATCC Medium 2039 and (Silverman and Lundgren, 1959)). The growth medium was prepared by combining 4 volumes of sterile solution A (800 mL containing 1 g  $(\text{NH}_4)_2\text{SO}_4$ , 1 g  $\text{MgSO}_4 \times 7 \text{H}_2\text{O}$ , 0.5 g  $\text{KH}_2\text{PO}_4$ , 0.1 g KCl; adjusted to pH 2.3 with  $\text{H}_2\text{SO}_4$ ) and 1 volume of freshly prepared sterile solution B (200 mL containing 20 g  $\text{FeSO}_4$ ). Microorganisms growing aerobically in this medium in a shaker-incubator (180 rpm) at 25°C for five to seven days were transferred to fresh medium to allow further enrichment of *A. ferrooxidans*. Growth of *A. ferrooxidans* was indicated by oxidized Fe and a distinct orange color of the liquid medium. In addition, the presence of bacterial cells was monitored by light microscopy (see Appendix 1, Figure A.1).

### **3.3.8. DNA isolation, PCR amplification and sequencing**

Bacterial cells from 10 mL of the cultures were harvested by a two-step centrifugation protocol. Precipitates present in the medium were removed by a 2 min centrifugation at low speed (180 x g).

Cells present in the supernatant were harvested by centrifugation for 15 min at 4500 x g and washed several times with phosphate buffered saline (PBS). DNA was extracted from the cells using the Meta-G-Nome DNA Isolation Kit following to the manufacturer's protocol (Epicentre, Madison, Wisconsin). The extracted DNA was used as a template for amplification and sequence determination of a 298 base pair 16S rDNA fragment covering variable regions V5 and V6 (Vasileiadis et al., 2012) as recently described (Grengg et al., 2015).

## 3.4. Results

### 3.4.1. Structural observations and element distributions

Non-corroded concrete showed typical pattern of silicate and carbonate aggregates of various sizes, which are embedded in a fine grained, greyish cementitious matrix. The transition zone (TZ) to strongly deteriorated concrete was marked by a sharp horizon of a width of 2 to 3 mm at a depth of up to  $3 \pm 1$  cm, followed by a sequence of shifting reddish/brownish and whitish layers, accompanied by massive crack formations (Figure 1, B and C). Element mappings of Al, Ca, Fe, Mg, S and Si throughout these corrosion fronts revealed a clearly defined element succession path (Figure 2). Element distributions within the cementitious matrix of non-corroded concrete were dominated by high concentrations of Ca and Si, whereas significantly lower abundances of Al, Mg and Fe could be measured. Most of the larger aggregates contained exclusively Si representing quartz (Qz), while smaller ones showed a more diverse chemistry, incorporating Al, Ca, Fe and Mg in different quantities, representing feldspar (Fsp), calcite (Cal), plagioclase (Pl), muscovite (Ms) and hornblende (Hb). A profile through the TZ was characterized by decreasing Ca concentrations and first S incorporation, mainly along grain boundaries and cracks. Subsequently, an accumulation zone of predominately Mg which was linked to brucite ( $\text{Mg}(\text{OH})_2$ ) precipitates, with an average of 1 mm width established, which was cut off by a sharp ( $< 0.1$  mm) Al rich layer, consisting mainly of gibbsite ( $\text{Al}(\text{OH})_3$ ) (Figure 2, A, B and Appendix 1 Figure A2 and Figure A3). The following next 1 to 2 mm contained a zone of massive Fe accumulation (Figure 2C). Ferric iron ( $\text{Fe}^{3+}$ ) containing precipitates were identified as goethite ( $\alpha\text{-FeO}(\text{OH})$ ), lepidocrocite ( $\gamma\text{-FeO}(\text{OH})$ ) and parabutlerite ( $\text{Fe}(\text{SO}_4)(\text{OH})\cdot 2\text{H}_2\text{O}$ ) by high resolution Micro-XRD analyses (Figure 3). The outermost 2-3 cm of the deterioration layer were characterized by alternating filamentary S, Ca, representing sulfate salts (Gp, Anh, Bas) and Fe accumulation zones, while complete depletion of Mg and Al were observed (Figure 2 and Appendix Figure A2). Although significant Si concentrations were measured within this strongly deteriorated matrix, no mineral incorporating significant amounts of Si was detected by XRD analyses, implying amorphous silica as the main corrosion product, reflected by the X-ray amorphous content of up to 11.6 wt. % (Table 1). Zones of Si depletion correspond to areas of crack formations and associated calcium sulfate

accumulation zones. Throughout the entire corrosion front no change in Si abundances within the aggregates could be observed, while partly depletion of Al, Mg and Fe occurred within smaller mineral aggregates, e.g. Fsp and Ms, distributed within the corrosion layer.

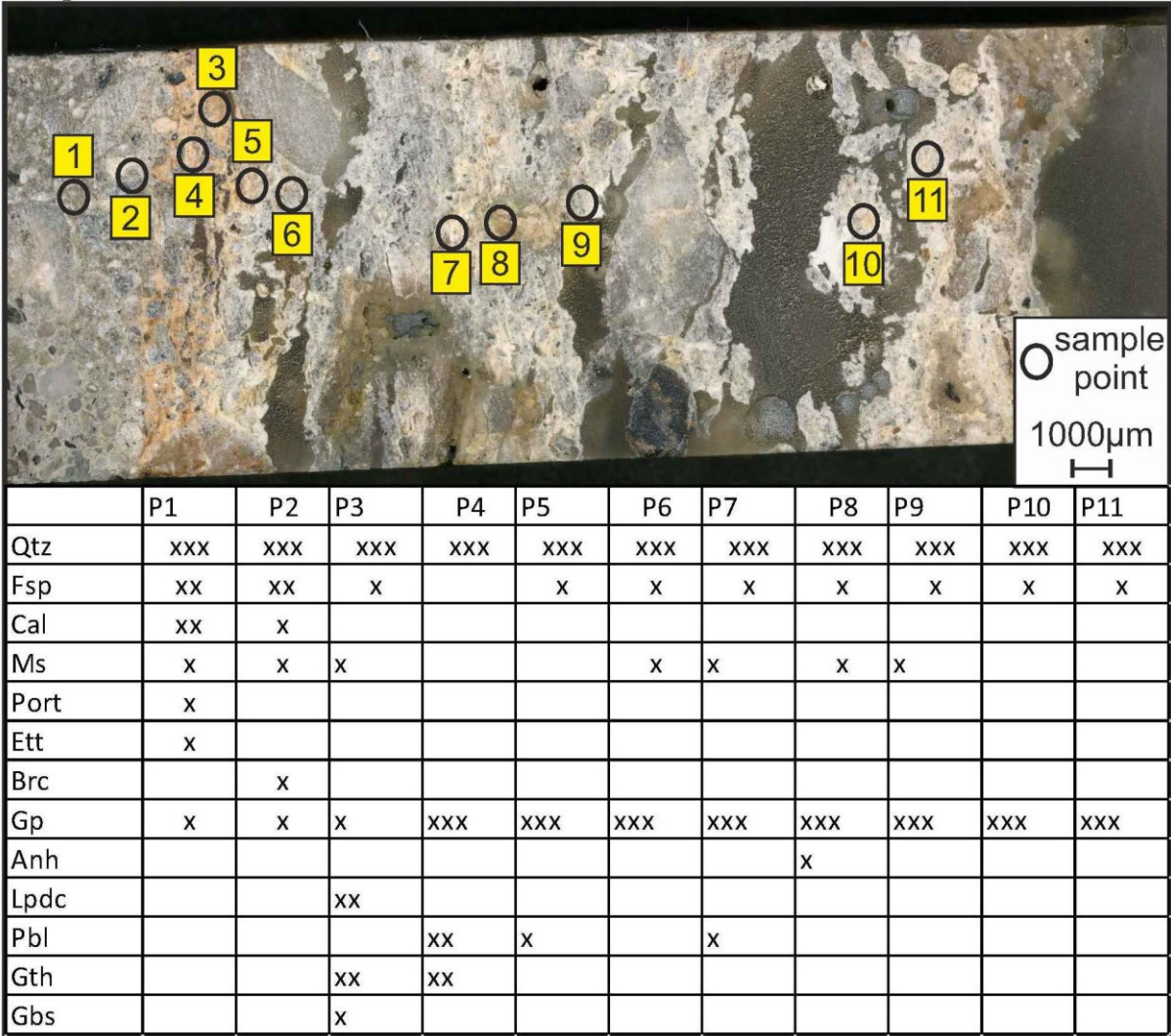


Figure 3: Micro XRD spot analyses throughout a corrosion front. Spot analyses were conducted from the left (intact concrete, Point 1 and 2) to the right (corroded concrete, Points 3-11), showing quartz (Qtz), feldspar (Fsp), Calcite (Cal), muscovite (Ms), portlandite (Port), ettringite (Ett), brucite (Brc), gypsum (Gp), anhydrite (Anh), lepidocrocite (Lpdc), parabutlerite (Pbl), goethite (Gth) and gibbsite (Gbs). Relative abundances are indicated by x-scale, where xxx represents high abundances, while x indicates trace contents.

**3.4.2. Microbial distribution**

Epifluorescence images of the stained surface revealed unevenly distributed clusters of high fluorescence throughout the whole corrosion layer, implying cell accumulations within the entire deterioration zone (see Figure 4). Three areas of high fluorescence intensities could be subcategorized: (i) clusters of high intensities within the first 0.5 cm from the surface, (ii) clusters at an average depth

of about 2.0 to 2.5 cm and, (iii) clusters located directly at the transition zone to non-corroded concrete at a depth of about 3.5 to 4.0 cm.

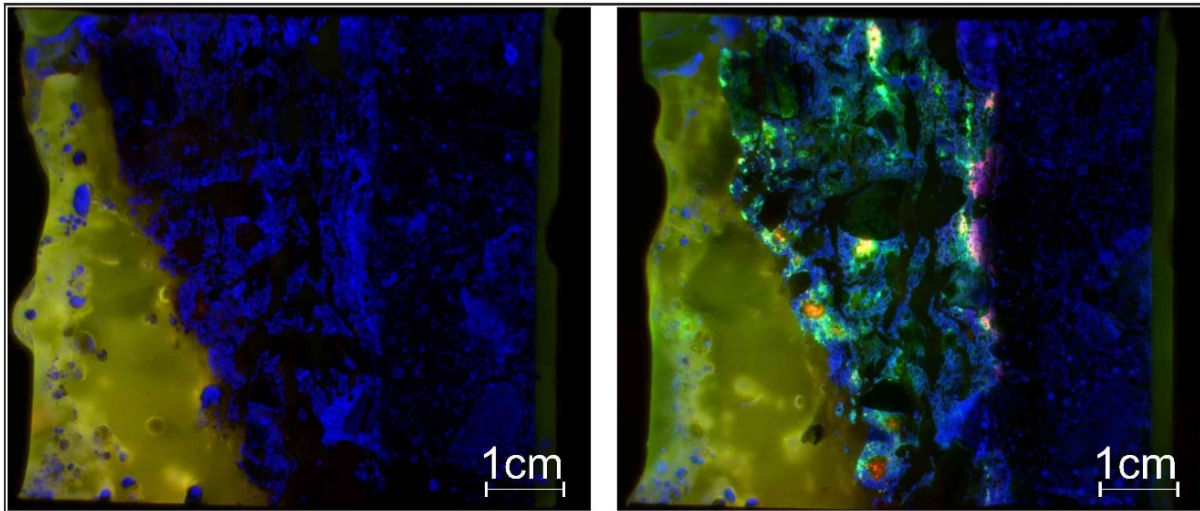


Figure 4: Fluorescent images taken from unstained (left image) and stained (right image) concrete sample block. Background (green and red) is only visible in the epoxy material used for embedding the concrete. In the concrete part, there is no background fluorescence before staining. Fluorescence indicating presence of microorganisms and microbial activity is only visible in deteriorated areas of the stained concrete sample block (right image).

Contrary to previous work (Okabe et al., 2007), no decrease in intensities and corresponding cell concentrations with depth could be recognized. High resolution spot analyses within the corrosion layer revealed strongly elevated intensities (arbitrary units) with an average of 2578 for the green and 643 for the red filter set, corresponding to nucleic acids (DNA and RNA) originating from microbial cells (Figure 5, points 1,2,3,5,6,7,8,9,10,12,13,14,16). Significantly higher peak intensities of up to 5662 for the green and 1708 for the red filter set were measured in cluster areas showing high fluorescence (Figure 5, points 5,7,8,9). Control measurements within the non-corroded concrete showed average intensities of  $409 \pm 11$  and  $391 \pm 2$  representing green and red background fluorescence, respectively (Figure 5, points 4,11,15). A complete dataset of the mean fluorescence intensities is provided in the Appendix 1, Table A.1. The presence of bacterial cells was also inferred from images obtained by light microscopy (see Appendix 1, Figure A.1). Material from the inner layers of the deteriorated concrete samples were used for inoculation of a medium selective for *A. ferrooxidans*. Indeed, we were able to cultivate bacteria in that medium as can be seen in Appendix 1, Figure A.1. In addition, we observed a distinct orange color within the liquid medium indicating the presence of oxidized Fe. To unambiguously identify the bacterial species growing in liquid medium, DNA was isolated from cells present in the culture and further used as a template for amplification and sequence determination of a 298 base pair 16S rDNA fragment, encompassing V5 and V6 variable regions (Vasileiadis et al., 2012). Megablast (Johnson et al., 2008) sequence searches in the NCBI DNA database revealed 100% sequence identity with several uncultured *A. ferrooxidans* bacteria, among them samples from volcanic



lake water (accession number KP972193), volcanic soil (accession number KP972205) or acid mine drainage waters (accession number JF815498).

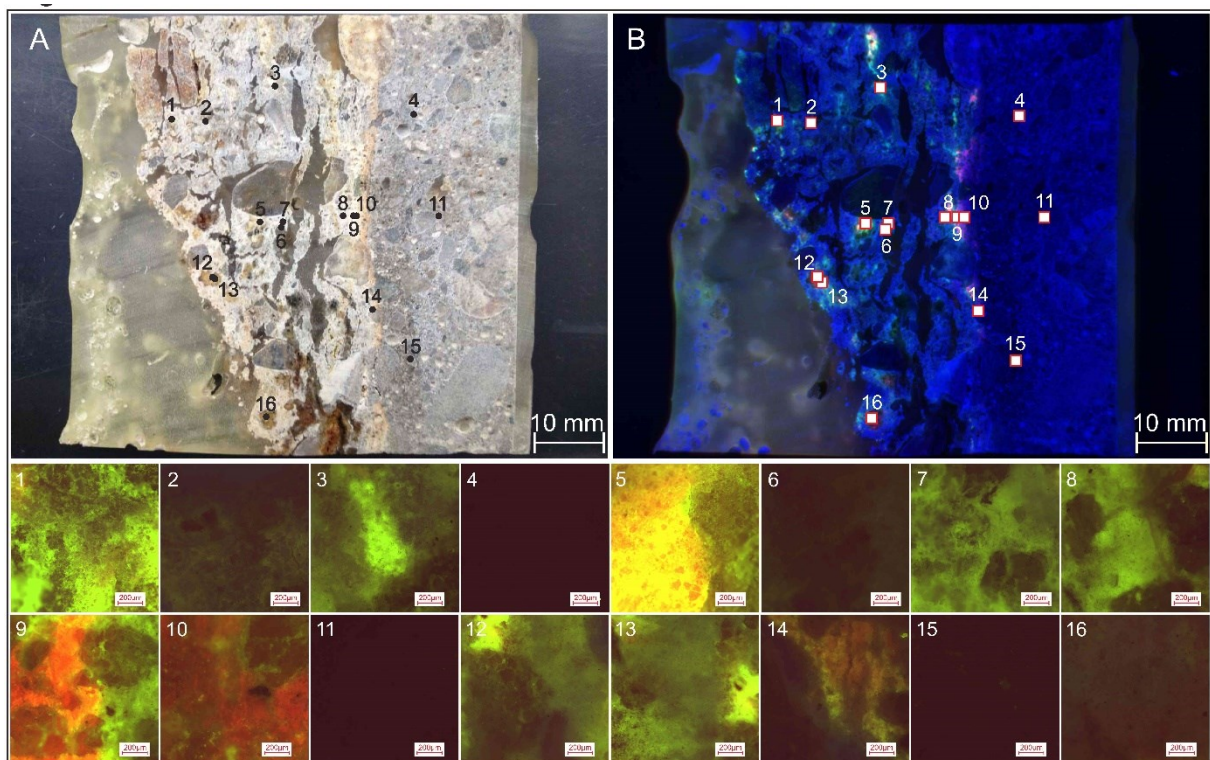


Figure 5: Microbial activity on deteriorated concrete revealed by SYTO9 and PI nucleic acid staining. The surface of the same concrete sample block is shown in A and B. A: Color image. B: Fluorescent image. The 16 images shown below were produced using a fluorescence microscope at the positions (circles and squares) indicated in A and B. Green, red and yellow areas on the surface arise from the nucleic acid intercalating dyes and indicate the presence of microbes in those areas. The bars in 1-16 are 200 µm each.

### 3.5. Discussion

The aim of this study was to determine the exact process mechanisms responsible for those exceptionally high corrosion rates ( $>1 \text{ cm yr}^{-1}$ ) observed within this system, based on a combined mineralogical, hydro-geochemical and biological approach. Based on the results obtained we propose a new model combining the complex mineral dissolution and re-precipitation reactions occurring during advanced MICC propagation with the spatial microbial distribution, ultimately steering corrosion progression of the system.

Opposed to the current hypothesis (Okabe et al., 2007; Satoh et al., 2009), microorganisms were not limited to the oxygen rich uppermost layers of the deteriorated concrete, but were distributed throughout the whole corrosion zone up to a depth of 4 cm, as clearly demonstrated by epifluorescence analyses (Figure 4 and Figure 5). Microbial nucleic acids were detected in patches throughout the whole deterioration layers with high concentrations especially at and close to the corrosion front, as well as at a depth of around 2.5 cm from the concrete surface. Bacteria enriched

and isolated from the deteriorated concrete were identified as acidophilic SOB of the genus *Acidithiobacillus spp.* (*A. Thiooxidans* and *A. ferrooxidans*). While *A. thiooxidans* is widely approved as the dominant SOB species at strongly acidic (pH <2) conditions during advanced MICC (Jiang et al., 2016a; Ling et al., 2015, 2014; Okabe et al., 2007; Satoh et al., 2009; Yamanaka et al., 2002; Yousefi et al., 2014), the role of *A. ferrooxidans* is still under debate. Few reports have mentioned the presence of *A. ferrooxidans* within MICC environments, but its impact on corrosion propagation remained unclear (Jiang et al., 2016b; Maeda et al., 1999; Yamanaka et al., 2002). *A. ferrooxidans* are gram negative, rod-shaped, autotroph bacteria, which obtain carbon by fixing inorganic carbon (mainly CO<sub>2</sub>). They are acidophilic with a growth optimum at pH 1.5 to 2.5. Under aerobic conditions, oxygen is used as electron acceptor and energy is obtained by the oxidation of ferrous iron to ferric iron or reduced sulfur compounds to sulfuric acid. If oxygen is lacking and reduced sulfur compounds are used as the electron donor, ferric iron serves as the electron acceptor (Rawlings and Kusano, 1994). In our study, cell accumulations, observed at and close to the corrosion front, as well as at a depth of 2.5 cm, were correlated with significant Fe accumulation zones. Previous studies reported oxygen depletion to establish at a depth of around 400 to 600 μm (Okabe et al., 2007), therefore overall anoxic to anaerobic conditions can be assumed within the inner ~3 cm of the corrosion layers. Those O<sub>2</sub> limited conditions, in combination with massive Fe accumulations would inhibit the growth of aerobic *A. thiooxidans*, while favoring the growth of *A. ferrooxidans*. Therefore, it is likely that *A. thiooxidans* mainly occupies the oxygen rich outermost layers while *A. ferrooxidans* dominate within the interior of the corroded concrete, where oxygen supply is temporarily limited (depending on changing RH conditions), but iron accumulation takes place. Hence, *A. ferrooxidans* are likely to play a central role within MICC propagation within the observed system, by supplying in situ produced H<sub>2</sub>SO<sub>4</sub> within the inner deterioration layer at and close to the corrosion front.

Previous studies recognized the significance of single element concentrations regarding MICC propagation. For instance, Al content was linked to the bioreceptivity of concrete applied (Goyns and Alexander, 2014; Herisson et al., 2013), while Fe was correlated with crack formation (Jiang et al., 2014). However, to date no model exists combining the role of all major elements, their fate with corrosion progression and their impact on microbial activity. In this study, element distributions, monitored throughout the corroded concrete layers revealed a dynamic pH and diffusion controlled system, in which a distinct succession of elemental accumulations was unequivocally correlated with responding pH levels, associated dissolution and precipitation of solids, as well as with the spatially resolved presence of microbes. Since *A. thiooxidans* and *A. ferrooxidans*, were found in the material we consider these bacteria to be key players in the process (Figure 6).

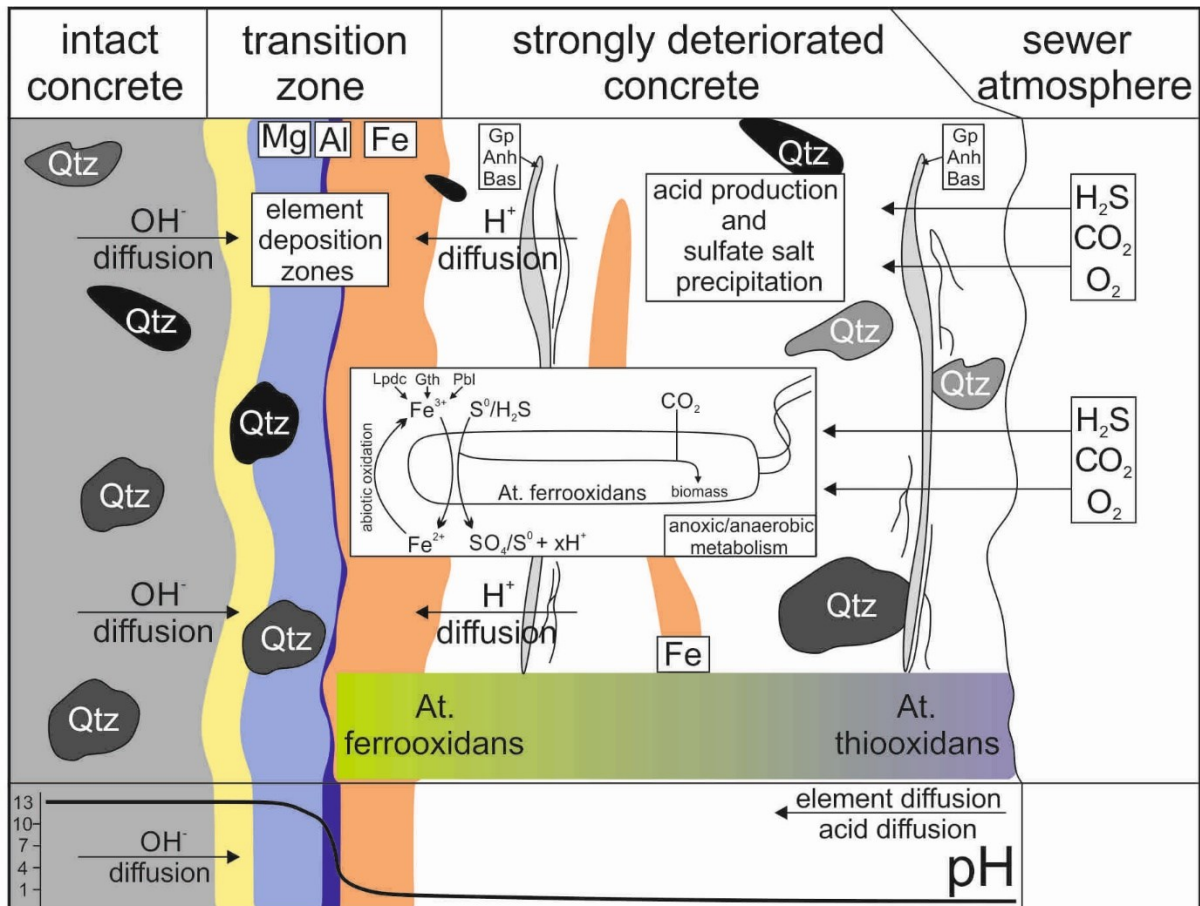


Figure 6: pH and diffusion controlled model showing the succession of element accumulations together with associated microbiological activity within a progressive corrosion front from the left to the right side. Initial sulfate incorporation marks the beginning of the transition zone in which the pH drops from 13 to below 1. Mg accumulations indicate pH >9, while Al deposition is associated with a strong pH decrease from 9 to 4. Fe deposition zones can be linked with the anaerobic metabolism of *A. ferrooxidans* within the deeper corrosion layers, where Fe<sup>3+</sup>, present in iron hydroxides and sulfates, e.g. Lpdc, Gth, Pbl, gets reduced to Fe<sup>2+</sup> during oxidation of reduced sulfur compounds.

The inner, non-corroded concrete was dominated by a matrix of Ca and Si rich phases like portlandite (Ca(OH)<sub>2</sub>) and calcium silicate hydrates (C-S-H phases), framing siliceous and carbonate aggregates, e.g. Qtz, Fsp, Cal and Ms, at strongly alkaline conditions (pH ~13) (Table 1) (Vollpracht et al., 2015). The transition zone (TZ) between non-corroded and the strongly affected concrete was limited to 2-3 mm, in which the pH dropped from initial ~13 to below 1, causing dynamic dissolution and precipitation of single phases, characterized by single element concentrations (Figure 2). The inner border of TZ was marked by decreasing Ca concentration due to acid penetration. Simultaneously, sulfate incorporation along grain boundaries proceeded, which could be linked to the interfacial transition zone and associated higher portlandite (Ca(OH)<sub>2</sub>) content (Scrivener et al., 2004). As a consequence, microstructural damage to the cement matrix occurred due to the formation of expansive sulfate phases (Mittermayr et al., 2015). Within the initial zone of Ca depletion, Mg accumulations took place due to the precipitation of Mg hydroxides e.g. brucite (Mg(OH)<sub>2</sub>). Thereby, hydroxide (OH<sup>-</sup>) diffused from high pH areas within the non-corroded concrete while Mg ion diffusion was triggered by Mg

precipitation and associated concentration gradient. Since the stability of expected Mg bearing precipitates is limited to strongly alkaline conditions, a pH minimum of around 9 marked the end of Mg precipitation (White, 2013). Thickness and Mg concentrations of the accumulation zone could be directly correlated to the prevailing pH gradient and subsequently used as an indicator for the corrosion progression rate. Thick Mg layers correspond to low pH gradients and low acid diffusion rates, whereas the high Mg concentration would imply significant mass transport and associated high corrosion intensity of the affected concrete. Subsequently, a sharp, poorly pronounced Al accumulation horizon indicated the strong drop in pH from around 9 to 4. Due to its amphoteric behavior, with low solubility between pH 9 and 4, Al precipitation as gibbsite ( $\text{Al}(\text{OH})_3$ ) was triggered by the change from alkaline to acidic conditions (Appelo and Postma, 2005; White, 2013). Consequently, at pH <4 complete depletion of Al within the cementitious matrix was observed (Figure 2). The first Fe accumulation zone developed within the low pH border zone of Al accumulation. There, due to the vicinity to the TZ and expected  $\text{OH}^-$  diffusion from alkaline regions, slightly elevated pH levels (pH 3-4) initiated Fe precipitation as various  $\text{Fe}^{3+}$  oxyhydroxides, like lepidocrocite, goethite and parabutlerite under oxidizing conditions present. All Fe accumulation zones could be linked to areas of high microbial activity, pointing to a possible central role of *A. ferrooxidans* and iron during advanced MICC within this system. Under prevailing anoxic to anaerobic conditions Fe was utilized by *A. ferrooxidans*, which used ferric iron ( $\text{Fe}^{3+}$ ) as electron acceptor to form ferrous iron ( $\text{Fe}^{2+}$ ) during oxidation of reduced sulfur speciation.  $\text{Fe}^{2+}$  produced shows significant higher solubility and associated high mobility in respect to ferric iron speciation (Appelo and Postma, 2005). With progressing corrosion, soluble  $\text{Fe}^{2+}$  diffused into the inner layers of the corrosion front due to an expected concentration gradient, where it was re-oxidized by  $\text{H}_2\text{SO}_4$  and subsequently re-precipitated as Fe hydroxides and hydrated  $\text{Fe}^{3+}$  sulfates (Figure 6). Areas of Fe accumulation, framing various aggregates within strongly acidic layers could be explained due to additional Fe input from mica and feldspar grains, partly affected by the extremely aggressive interstitial solutions with pH as low as 0.7 (Table 1). Fe rich layers and clusters represented favorable environments for *A. ferrooxidans* and were correspondingly adopted (Figure 4). Quartz grains were not affected throughout the whole corrosion front, indicating the resistivity of quartz at strongly acidic environments. The outermost 2-3 cm of the corroded layers were characterized by a matrix of filamentous Ca and S layers, representing the secondarily precipitated sulfate salts Gp, Anh, Bas, while Si rich layers consist of amorphous silica. With progressing corrosion and associated shift of single pH levels and diffusion gradients towards deeper concrete layers, dynamic re-dissolution and conditionally re-precipitation of element accumulation zones proceeded.



### 3.6. Conclusion

This study described a novel model for advanced MICC within a strongly deteriorated sewer system, intertwining biological, mineralogical, (micro)structural and hydro-geochemical factors. Controlled by pH and diffusion a dynamic micro-system developed which was dominated by ongoing mineral dissolution and re-precipitation and subordinated microbial distribution. Opposed to current opinions, microbial activity within this system was not limited to the surface near, oxygen rich corrosion layers, but expanded throughout the entire deterioration zone. No decrease in microbial activity with depth could be identified, with high cell accumulations at and close to the corrosion front at a depth of four cm. *A. ferrooxidans* were isolated from the inner deteriorated concrete layers and are suggested to be linked with Fe accumulation zones within the deeper anoxic to anaerobic corrosion layers, which triggered suggested in situ  $H_2SO_4$  production, thereby changing corrosion dynamics within this system. Accordingly, the central role of iron regarding bioreceptivity and associated durability of concrete affected by MICC should be emphasized. In our model *A. thiooxidans* are likely to dominate the oxygen rich zones close to the surface, while *A. ferrooxidans* are proposed to adopt the pore spaces within deeper, anaerobic, corrosion layers. In fact, in situ acid production at and close to the corrosion front have to be recognized as one central factor, steering high corrosion rates  $> 1 \text{ cm yr}^{-1}$  and associated failure of several concrete manholes after a service life less than 10 years. Further research in different environments is required in order to ensure the general validation of the model.

### 3.7. Acknowledgement

The authors gratefully thank the Graz University of Technology (Austria) scientific grant program for financial support, as well as the scientific input of Josef Tritthart and Joachim Juhart. Special thanks to Peter Rappold and the Department of Water Resources Management, Styria, as well as to Heinz Lackner and the Department of Energy, Residential Constructions and Technology, Styria, for their financial support. Mineralogical and chemical analyses were carried out at the NAWI Graz Central Lab for Water, Minerals and Rocks. Bacterial isolation and identification were conducted with the expert technical assistance of Karin Bischof and Sarah Pycha at the Institute of Molecular Biosciences, University of Graz (Austria). Spot analyses of mineralogical compositions were carried out at the Institute for Geological and Geochemical Research, Hungarian Academy of Science, in Budapest.

### 3.8. Bibliography

Alexander, M., Bertron, A., De Belie, N., 2013. Performance of Cement-Based Materials in Aggressive Aqueous Environments, 1st ed. Springer, Ghent. doi:10.1007/978-94-007-5413-3

- Appelo, C.A.J., Postma, D., 2005. *Geochemistry, groundwater and pollution*, 2nd ed. A.A. Balkema Publishers, Amsterdam.
- Cho, K.-S., Mori, T., 1995. A newly isolated fungus participates in the corrosion of concrete sewer pipes. *Water Sci. Technol.* 31, 263–271. doi:10.1016/0273-1223(95)00343-L
- De Belie, N., Monteny, J., Beeldens, a., Vincke, E., Van Gemert, D., Verstraete, W., 2004. Experimental research and prediction of the effect of chemical and biogenic sulfuric acid on different types of commercially produced concrete sewer pipes. *Cem. Concr. Res.* 34, 2223–2236. doi:10.1016/j.cemconres.2004.02.015
- Gao, S.-H., Ho, J.Y., Fan, L., Richardson, D.J., Yuan, Z., Bond, P.L., 2016. Antimicrobial effects of free nitrous acid on *Desulfovibrio vulgaris* : implications for sulfide induced concrete corrosion. *Appl. Environ. Microbiol.* AEM.01655-16. doi:10.1128/AEM.01655-16
- Goyns, A.M., Alexander, M., 2014. Performance of various concretes in the Virginia experimental sewer over 20 years. *Calcium Aluminates*. Balkema.
- Grengg, C., Mittermayr, F., Baldermann, a., Böttcher, M.E., Leis, a., Koraimann, G., Grunert, P., Dietzel, M., 2015. Microbiologically induced concrete corrosion: A case study from a combined sewer network. *Cem. Concr. Res.* 77, 16–25. doi:10.1016/j.cemconres.2015.06.011
- Herisson, J., van Hullebusch, E.D., Moletta-Denat, M., Taquet, P., Chaussadent, T., 2013. Toward an accelerated biodeterioration test to understand the behavior of Portland and calcium aluminate cementitious materials in sewer networks. *Int. Biodeterior. Biodegradation* 84, 236–243. doi:10.1016/j.ibiod.2012.03.007
- Hernandez, M., Marchand, E.A., Roberts, D., Peccia, J., 2002. In situ assessment of active *Thiobacillus* species in corroding concrete sewers using uorescent RNA probes. *Int. Biodeterior. Biodegradation* 49, 271–276.
- Hvitved-Jacobsen, T., Vollertsen, J., Yongsiri, C., Nielsen, A.H., 2002. Sewer microbial processes, emissions and impacts, in: *Sewer Processes and Networks*. Paris, p. 13.
- Islander, B.R.L., Devanny, J.S., Member, A., Mansfeld, F., Postyn, A., Shih, H., 1991. Microbial ecology of crown corrosion in sewers. *J. Environ. Eng.* 117, 751–770.
- Jayaraman, A., Mansfeld, F.B., Wood, T.K., 1999. Inhibiting sulfate-reducing bacteria in biofilms by expressing the antimicrobial peptides indolicidin and bactenecin. *J. Ind. Microbiol. Biotechnol.* 22, 167–175. doi:10.1038/sj.jim.2900627
- Jensen, H.S., 2009. PhD thesis; Hydrogen sulfide induced concrete corrosion of sewer networks. Aalborg University.
- Jiang, G., Wightman, E., Donose, B.C., Yuan, Z., Bond, P.L., Keller, J., 2014. The role of iron in sulfide induced corrosion of sewer concrete. *Water Res.* 49, 166–74. doi:10.1016/j.watres.2013.11.007
- Jiang, G., Zhou, M., Chiu, T.H., Sun, X., Keller, J., Bond, P.L., 2016a. Wastewater-Enhanced Microbial Corrosion of Concrete Sewers. doi:10.1021/acs.est.6b02093
- Jiang, G., Zhou, M., Chiu, T.H., Sun, X., Keller, J., Bond, P.L., 2016b. Wastewater-Enhanced Microbial Corrosion of Concrete Sewers. *Environ. Sci. Technol.* 50, 8084–8092. doi:10.1021/acs.est.6b02093
- Johnson, M., Zaretskaya, I., Raytselis, Y., Merezhuk, Y., McGinnis, S., Madden, T.L., 2008. NCBI BLAST: a better web interface. *Nucleic Acids Res.* 36, W5-9. doi:10.1093/nar/gkn201
- Joseph, A.P., Keller, J., Bustamante, H., Bond, P.L., 2012. Surface neutralization and H<sub>2</sub>S oxidation at early stages of sewer corrosion: influence of temperature, relative humidity and H<sub>2</sub>S concentration. *Water Res.* 46, 4235–45. doi:10.1016/j.watres.2012.05.011

- Ling, A.L., Robertson, C.E., Harris, J.K., Frank, D.N., Kotter, C. V, Stevens, M.J., Pace, N.R., Hernandez, M.T., 2015. High-resolution microbial community succession of microbially induced concrete corrosion in working sanitary manholes. *PLoS One* 10. doi:10.1371/journal.pone.0116400
- Ling, A.L., Robertson, C.E., Harris, J.K., Frank, D.N., Kotter, C. V, Stevens, M.J., Pace, N.R., Hernandez, M.T., 2014. Carbon Dioxide and Hydrogen Sulfide Associations with Regional Bacterial Diversity Patterns in Microbially Induced Concrete Corrosion. *Environ. Sci. Technol.* 48, 7357–7364. doi:10.1021/es500763e
- Liu, Y., Tugtas, A.E., Sharma, K.R., Ni, B.J., Yuan, Z., 2016. Sulfide and methane production in sewer sediments: Field survey and model evaluation. *Water Res.* 89. doi:10.1016/j.watres.2015.11.050
- Maeda, T., Negishi, A., Komot, H., Oshima, Y., Kamimura, K., Sugi, T., 1999. Isolation of Iron-Oxidizing Bacteria from Corroded Concretes of Sewage Treatment Plants. *Biosci. Bioeng.* 4, 300–305.
- Mittermayr, F., Rezvani, M., Baldermann, A., Hainer, S., Breitenbücher, P., Juhart, J., Graubner, C.-A., Proske, T., 2015. Sulfate resistance of cement-reduced eco-friendly concretes. *Cem. Concr. Compos.* 55, 364–373. doi:10.1016/j.cemconcomp.2014.09.020
- Nielsen, A.H., Vollertsen, J., Jensen, H.S., Madsen, H.I., Hvitved-Jacobsen, T., 2006. Aerobic and Anaerobic Transformations of Sulfide in a Sewer System – Field Study and Model Simulations. *Proc. Water Environ. Fed.* 2006, 3654–3670. doi:10.2175/193864706783751447
- Nielsen, A.H., Vollertsen, J., Jensen, H.S., Wium-Andersen, T., Hvitved-Jacobsen, T., 2008. Influence of pipe material and surfaces on sulfide related odor and corrosion in sewers. *Water Res.* 42, 4206–4214. doi:10.1016/j.watres.2008.07.013
- O’Connell, M., McNally, C., Richardson, M.G., 2010. Biochemical attack on concrete in wastewater applications: A state of the art review. *Cem. Concr. Compos.* 32, 479–485. doi:10.1016/j.cemconcomp.2010.05.001
- Okabe, S., Odagiri, M., Ito, T., Satoh, H., 2007. Succession of sulfur-oxidizing bacteria in the microbial community on corroding concrete in sewer systems. *Appl. Environ. Microbiol.* 73, 971–980. doi:10.1128/AEM.02054-06
- Olmstead, W.M., Hamlin, H., 1900. Converting portions of the Los Angeles outfall sewer into a septic tank. *Eng. News* 971–980.
- Rawlings, D.E., Kusano, T., 1994. Molecular Genetics of *Thiobacillus ferrooxidans*. *Microbiol. Rev.* 58, 39–55.
- Satoh, H., Odagiri, M., Ito, T., Okabe, S., 2009. Microbial community structures and in situ sulfate-reducing and sulfur-oxidizing activities in biofilms developed on mortar specimens in a corroded sewer system. *Water Res.* 43, 4729–39. doi:10.1016/j.watres.2009.07.035
- Scrivener, K.L., Crumbie, A.K., Laugesen, P., 2004. The Interfacial Transition Zone (ITZ) Between Cement Paste and Aggregate in Concrete. *Interface Sci.* 12, 411–421.
- Silverman, M.P., Lundgren, D.G., 1959. Studies on the chemoautotrophic iron bacterium *ferrobacillus ferrooxidans*. *J. Bacteriol.* 77, 642–647.
- van Loosdrecht, M.C.M., Nielsen, P.H., Lopez-Vazquez, C.M., Brdjanovic, D., 2016. *Experimental Methods in Wastewater Treatment*. IWA Publishing, London.
- Vasileiadis, S., Puglisi, E., Arena, M., Cappa, F., Cocconcelli, P.S., Trevisan, M., 2012. Soil bacterial diversity screening using single 16S rRNA gene V regions coupled with multi-million read generating sequencing technologies. *PLoS One* 7. doi:10.1371/journal.pone.0042671
- Vincke, E., Monteny, J., Beeldens, A., De Belie, N., Taerwe, L., Van Gemert, D., Verstraete, W.H., 2000. Recent developments in research on biogenic sulfuric acid attack of concrete, in: *Environmental Technologies to Treat Sulfur Pollution: Principles and Engineering*. IWA Publishing, pp. 515–541.

- Vollertsen, J., Nielsen, A.H., Jensen, H.S., Wium-Andersen, T., Hvitved-Jacobsen, T., 2008. Corrosion of concrete sewers--the kinetics of hydrogen sulfide oxidation. *Sci. Total Environ.* 394, 162–70. doi:10.1016/j.scitotenv.2008.01.028
- Vollpracht, A., Lothenbach, B., Snellings, R., Haufe, J., 2015. The pore solution of blended cements: a review. *Mater. Struct.* doi:10.1617/s11527-015-0724-1
- White, W.M., 2013. *Geochemistry*, 1st ed. John Wiley & Sons, Oxford.
- Yamanaka, T., Aso, I., Togashi, S., Tanigawa, M., 2002. Corrosion by bacteria of concrete in sewerage systems and inhibitory effects of formates on their growth. *Water Res.* 36, 2636–2642.
- Yousefi, A., Allahverdi, A., Hejazi, P., 2014. Accelerated biodegradation of cured cement paste by *Thiobacillus* species under simulation condition. *Int. Biodeterior. Biodegradation* 86, 317–326. doi:10.1016/j.ibiod.2013.10.008

### 3.9. Appendix 1

Table A.1: Mean fluorescence intensities (arbitrary units) per pixel of fluorescence microscopy images (1608 x 1608 pixels) shown in Fig. 3. Position denotes the exact location of the magnified image. Green and red fluorescence above background values of  $409 \pm 11$  and  $391 \pm 2$ , respectively, indicate the presence of nucleic acids from microbial cells.

Position	blue	green	red
1	548	4633	618
2	527	1125	424
3	506	2745	442
4	392	404	390
5	493	5662	1708
6	437	824	396
7	488	2879	405
8	418	2571	420
9	419	3465	1111
10	413	1645	805
11	392	401	390
12	543	2499	518
13	535	3173	544
14	476	1299	514
15	396	421	394
16	499	996	455

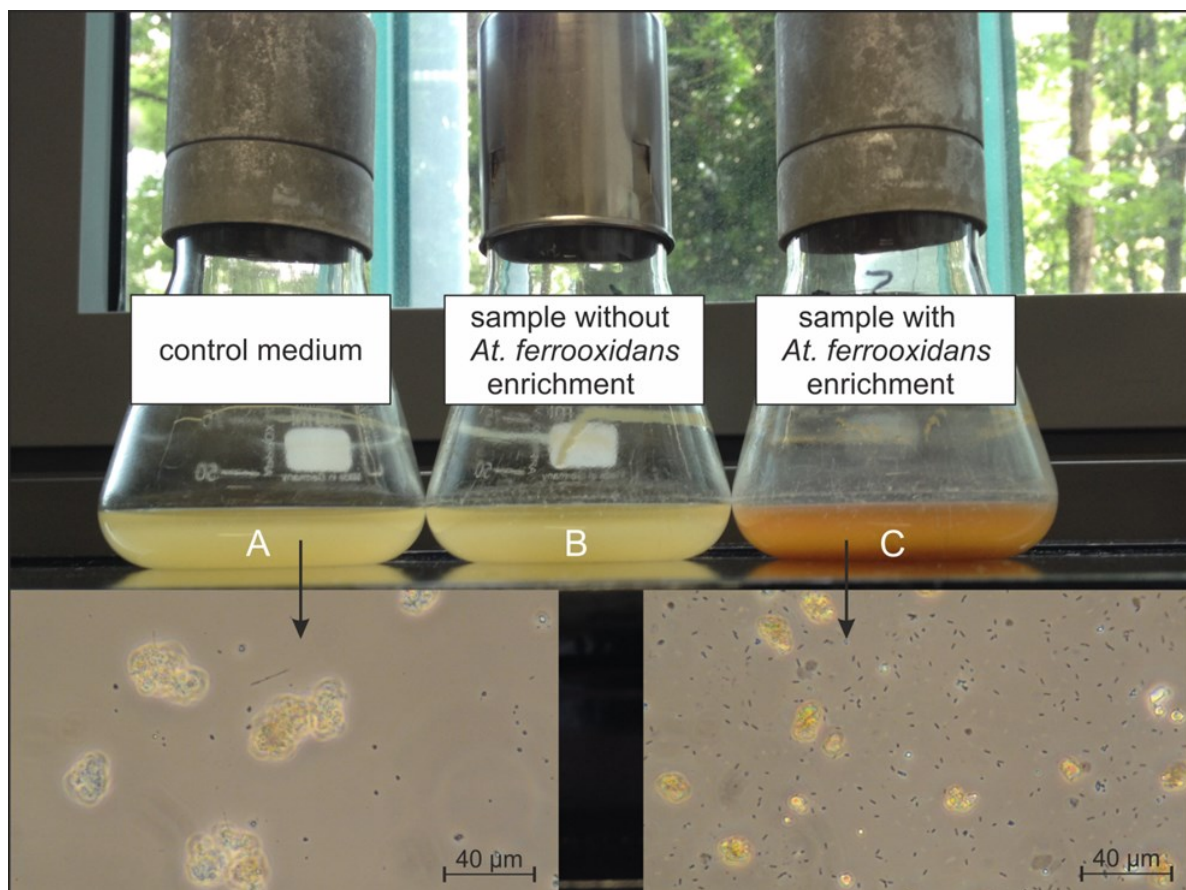


Figure A.1: Enrichment of *A. ferrooxidans*. Growth of bacteria in *A. ferrooxidans* medium is indicated by an orange color arising from oxidized Fe. Microscopy shows the presence of uniformly shaped bacterial cells in flask C. No bacteria were present in the control, flask (A). No growth was observed in a sample from a different sampling site (B).



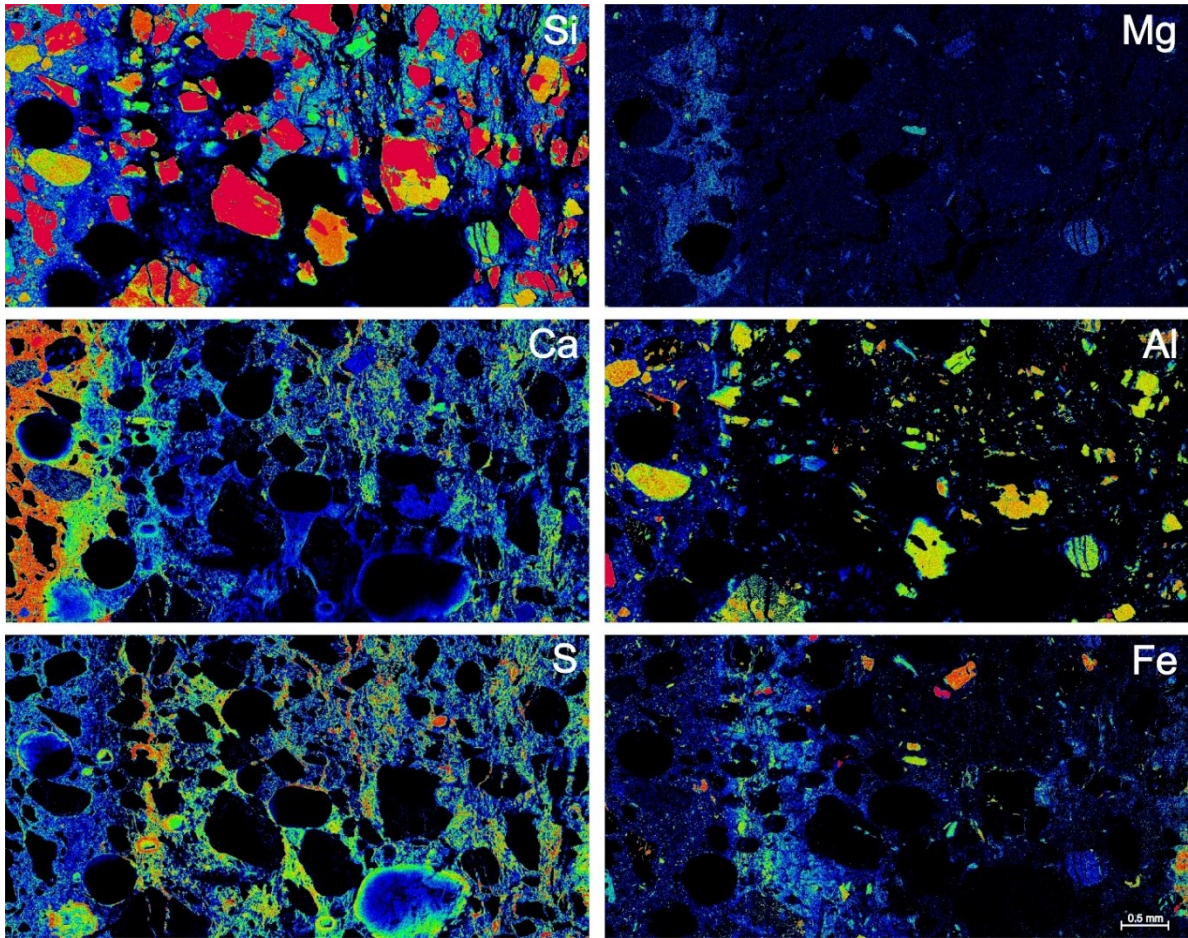


Figure A.2: Displaying the element (Si, Ca, S, Mg, Al, Fe) distributions from intact concrete (left side) throughout the corrosion front and heavily corroded concrete (right side). Notice the accumulation zone of Mg, Al and Fe within the transition zone between intact concrete and heavily corroded concrete.

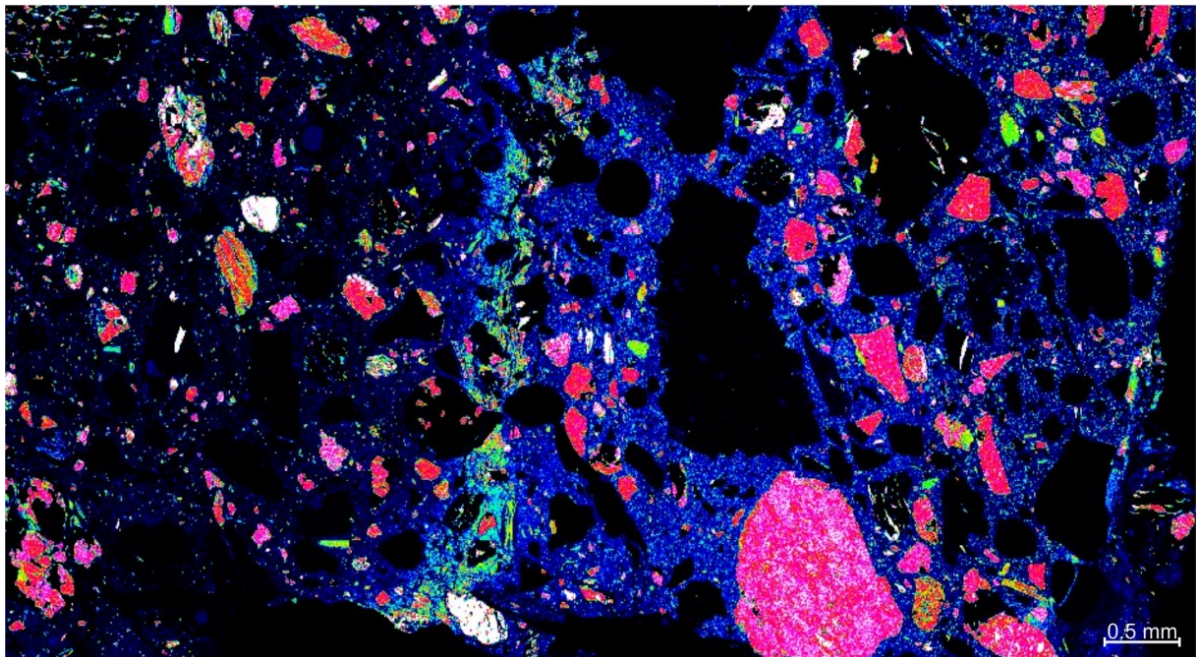


Figure A.3: Displaying the Al accumulation horizon within the transition between intact concrete (right side) and heavily corroded concrete (left side).

## Chapter 4

### How stable isotopes can be used to decipher reaction mechanisms within microbial induced concrete corrosion environments

Grengg, C.<sup>1</sup>, Mittermayr, F.<sup>2</sup>, Baldermann, A.<sup>1</sup>, Böttcher, M. E.<sup>3</sup>, Leis, A.<sup>4</sup>, Koraimann, G.<sup>5</sup> & Dietzel, M.<sup>1</sup>

<sup>1</sup> *Institute of Applied Geosciences, Graz University of Technology, Rechbauerstraße 12, 8010, Graz, Austria*

<sup>2</sup> *Institute of Technology and Testing of Construction Materials, Graz University of Technology, Inffeldgasse 24, 8010, Graz, Austria*

<sup>3</sup> *Geochemistry & Isotope- Biogeochemistry, Leibniz Institute for Baltic Sea Research (IOW), Seestraße 15, D-18119 Warnemünde, Germany*

<sup>4</sup> *RESOURCES – Institute for Water, Energy and Sustainability, Joanneum Research, Elisabethstraße 18/2, 8010, Graz, Austria*

<sup>5</sup> *Institute of Molecular Biosciences, Graz Karl-Franzens University, Heinrichstraße 26, 8010, Graz, Austria*

Keywords: concrete corrosion, sulfur isotopes, bacteria

#### 4.1. Abstract

Understanding the causes, the underlying reaction mechanisms and environmental controls of MICC is crucial in order to provide sustainable restoration strategies. In this study we analyzed different stable isotope systems in combination with conventionally used hydro-geochemical, mineralogical and microbiological analytics within a heavily damaged sewage system, exposed to microbial induced concrete corrosion (MICC). Various decisive parameters for detecting alteration features were determined in the field and laboratory including (i) temperature, pH, chemical characterization of the wastewater and expressed interstitial solutions of the deteriorated concrete, (ii) concentration of gaseous H<sub>2</sub>S, CH<sub>4</sub> and CO<sub>2</sub> within the sewer pipe atmosphere and, (iii) long term monitoring of temperature and H<sub>2</sub>S concentrations within different sewer manholes. Data obtained were interrelated with stable sulfur, oxygen and hydrogen isotope measurements in order to decipher individual microbiological and mineralogical reaction mechanisms.

#### 4.2. Introduction

Within the last decades, the application of stable isotope geochemistry in different geological environmental and geochemical settings, such as (paleo-)climatology, petrology or bio-geochemistry has established itself as an essential tool to broaden the understanding of complex process



mechanisms (Hoefs, 2009). Within recent years, different stable isotope systems could also be successfully applied to answer complex questions arising in the field of engineering and material sciences. For instance, Mittermayr et al., 2012 could successfully decipher the source of sulfur in two railway tunnels, strongly affected by secondary sulfate salt formation, by using stable sulfur isotopes. Accordingly, the application of stable isotope geochemistry in sewer environment affected by MICC represents a promising approach in order to address specific problems within (i) the biochemical sulfur cycle and (ii) to decipher changes in environmental conditions present and associated impact on process dynamics. Since MICC can be described as a chain of biochemical sulfur reduction and subsequent re-oxidation sequences, valuable information regarding the complex biochemical reaction mechanisms leading to severe concrete degradation can be drawn by studying the signatures of stable sulfur isotopes. Large fractionation of up to -46 ‰ are known to proceed during biogenic dissimilatory sulfate reduction and associated H<sub>2</sub>S production (Antler et al., 2014, Deusner et al., 2013). Microbial metabolism processes, potentially causing sulfur fractionation within MICC environments are summarized in Figure 1.

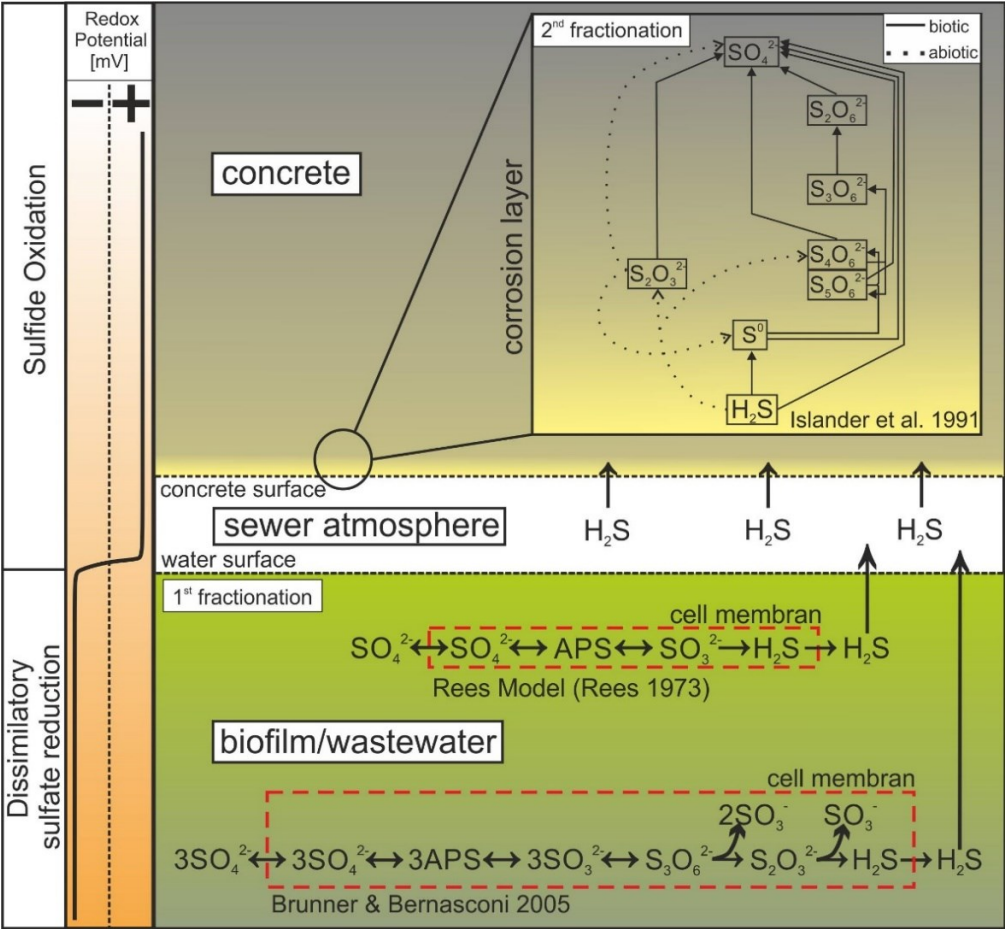


Figure 1: Expected 1<sup>st</sup> biogenic fractionation within the anaerobic wastewater during dissimilatory sulfate reduction described by the Rees Model (Rees, 1973) and an adopted model by Brunner and Bernasconi (Brunner and Bernasconi, 2005). Also possible 2<sup>nd</sup> biogenic fractionation during the re-oxidation by SOBs within the humid pore structure of the concrete, following the model by Islander et al., (1991) is presented.



Additionally, signals of stable oxygen and hydrogen isotopes were used to explain changes in environmental parameters present, together with its impact on the formation of secondary sulfate salts and process dynamics.

### 4.3. Field Site

The investigated sewer system is located near the city of Graz in the south-eastern parts of Austria. It can be categorized as a combined sewer network, thus transporting the daily wastewater flow of around 13000 citizens as well as the runoff from eventual storm events. In 2004 two new power mains were installed in order to secure a proper wastewater drain. Ever since community complaints about odor rose and subsequently deterioration of the concrete within the parts of the gravity sewer started. A detailed description of the system including hydro-chemical, mineralogical and microbiological aspects has been described by Grengg et al., (2015, 2017) and is also subject to this thesis (for a detailed description of the system see Chapter 2.3).

### 4.4. Methods

Liquids were sampled throughout the whole sewer system together with drinking water from the surrounding area in order to gain reference data for chemical analyses. On site measurements of pH, electric conductivity, O<sub>2</sub> concentration and redox potential were carried out. In the lab, the solutions were filtered using 0.45 µm membranes prior to alkalinity analyses by potentiometric titration with 0.02 M HCl. The concentration of dissolved components was measured by a Dionex ICS-3000 ion chromatograph (IC) and a PerkinElmer Optima 8300 DV inductively coupled plasma optical emission spectrometer (ICP-OES).

Deteriorated concrete samples from various manholes were dried at 40°C and subsequently grounded for mineralogical analysis using a PANalytical X'Pert PRO diffractometer (XRD). Mineral phase identification was carried out with the PANalytical X'Pert HighScore software (version 2.2e). A hydraulic press was used to extract the pore fluids of the concrete for the above chemical analyses (Tritthart 1989).

The concentrations of gaseous H<sub>2</sub>S, CH<sub>4</sub>, O<sub>2</sub> and CO<sub>2</sub> within the sewer pipe atmosphere were measured periodically, using a Draeger 3000 gas monitor. Gas samples of the sewer atmosphere were taken using gas sampling tubes.

The stable sulfur isotope ratios (<sup>34</sup>S/<sup>32</sup>S) were analyzed by combustion of BaSO<sub>4</sub>, Ag<sub>2</sub>S or ZnS using a Thermo Finnigan 253 mass spectrometer. The δ<sup>34</sup>S values, gained from BaSO<sub>4</sub>, represent sulfate isotope ratios extracted from the wastewater, as well as from pore fluids of the damaged concrete. Thereby, dissolved sulfate from collected wastewater and interstitial pore solutions was precipitated

as  $\text{BaSO}_4$  due to the addition of  $\text{BaCl}_2$ . Solid samples of the deteriorated concrete layers were dissolved using double distilled  $\text{HNO}_3$ , subsequently filtrated using  $0.45 \mu\text{m}$  membranes and finally re-precipitated as  $\text{BaSO}_4$  by the addition of  $\text{BaCl}_2$ .  $\delta^{34}\text{S}$  values obtained from  $\text{Ag}_2\text{S}$  and  $\text{ZnS}$  reflect the signature of gaseous  $\text{H}_2\text{S}$ , which was captured within Woulff bottles by bubbling through a  $0.1 \text{ M}$  silver nitrate or a  $5\%$  zinc acetate solution, respectively (Figure 2).



Figure 2: The device build for  $\text{H}_2\text{S}$  precipitation, including two interconnected Woulff bottles filled with a  $0.1 \text{ M}$  silver nitrate or  $5\%$  zinc acetate solution through which  $\text{H}_2\text{S}$  bearing sewer atmosphere was bubbled using a hydraulic aquarium pump.

Results are given according to  $\delta^{34}\text{S}$ -notation in ‰ relative to the Vienna-Canyon Diablo Troilite (V-CDT) standard.

Stable hydrogen and oxygen ratios of the wastewater, extracted at specific manholes along the sewer system, and of expressed interstitial solutions, from different deteriorated concrete manholes, were analyzed by wavelength-scanned cavity ring-down spectroscopy (WS-CRDS), using a L2120-I system from Picarro. Results are given in  $\delta^2\text{H}$  and  $\delta^{18}\text{O}$ -notations in ‰ relative to the Vienna Mean Ocean Water (V-SMOW).

## 4.5. Results and Discussion

Low oxygen levels of  $0.3 \text{ mg l}^{-1}$  within the storage basin, together with low pumping rates resulted in oxygen depletion and the establishment of anaerobic conditions within the power mains. Consequently, sulfate reduction by sulfate reducing bacteria (SRB), e.g. *Desulfovibrio spp.* and *Desulfobulbus spp.* (Jensen et al., 2011), proceeded, resulting in  $\text{H}_2\text{S}$  concentrations of up to 400 ppm and  $\text{CO}_2$  concentrations of up to 2800 ppm within the atmosphere of the concrete manholes. The significant decrease of sulfate concentration with flow direction from 250 to  $15 \text{ mg l}^{-1}$  verified the reduction of sulfate to sulfide species due to bacterial activity (see in detail chapter 2.5 and 2.10) (Grenng et al., 2015). The gaseous  $\text{H}_2\text{S}$  and  $\text{CO}_2$  are considered to be rapidly absorbed into the moist pore structure of the concrete, thereby continuously lowering the concrete pH due to abiotic acid-base reactions (Satoh et al., 2009; Islander et al., 1991). Once a pH of 9.5 was reached, the colonization of different strains of SOB occurred and biotic  $\text{H}_2\text{SO}_4$  production started. With persistent decreasing pH new strains of bacteria developed and colonized the surface of the manholes (Okabe et al., 2007). The expressed pore fluid from the corroded concrete yielded pH values between 0.7 and 3.1 (see 2.5, Table 4), generating an extremely aggressive environment. The bacteria extracted from the deteriorated concrete were identified as *A. thiooxidans* and *A. ferrooxidans* (Grenng et al., 2015, 2017). These aggressive interstitial solutions reacted with the cementitious matrix of the concrete, which consist mainly of calcium hydroxide ( $\text{Ca}(\text{OH})_2$ ) and calcium silicate phases (C-S-H), to form mainly gypsum ( $\text{CaSO}_4 \cdot 2\text{H}_2\text{O}$ ), but also bassanite ( $\text{CaSO}_4 \cdot 0.5\text{H}_2\text{O}$ ) and anhydrite ( $\text{CaSO}_4$ ) (Grenng et al. 2015). In this context especially the formation of anhydrite under ambient environmental conditions has to be subject of further thermodynamic considerations. Under atmospheric pressure the conversion between gypsum and anhydrite is a function of temperature and activity of  $\text{H}_2\text{O}$  ( $\alpha_{\text{H}_2\text{O}}$ ) (Hardie, 1967). Accordingly, the formation of significant amounts of anhydrite can either be achieved by an increase in temperature up to around  $58^\circ\text{C}$ , a decrease in  $\alpha_{\text{H}_2\text{O}}$  to around 0.77 (Hardie, 1967), or a combination of the two. Since  $58^\circ\text{C}$  within the pore fluids were never reached within the system (see 2.4, Figure 2), partial decrease in  $\alpha_{\text{H}_2\text{O}}$  is likely to have taken place. Nevertheless, higher temperatures in summer would have positively contributed towards anhydrate formation. Hence, signatures of stable H and O isotopes extracted from the interstitial pore solutions of deteriorated concrete layers were plotted against the pH and the local meteoric water line (Figure 3).

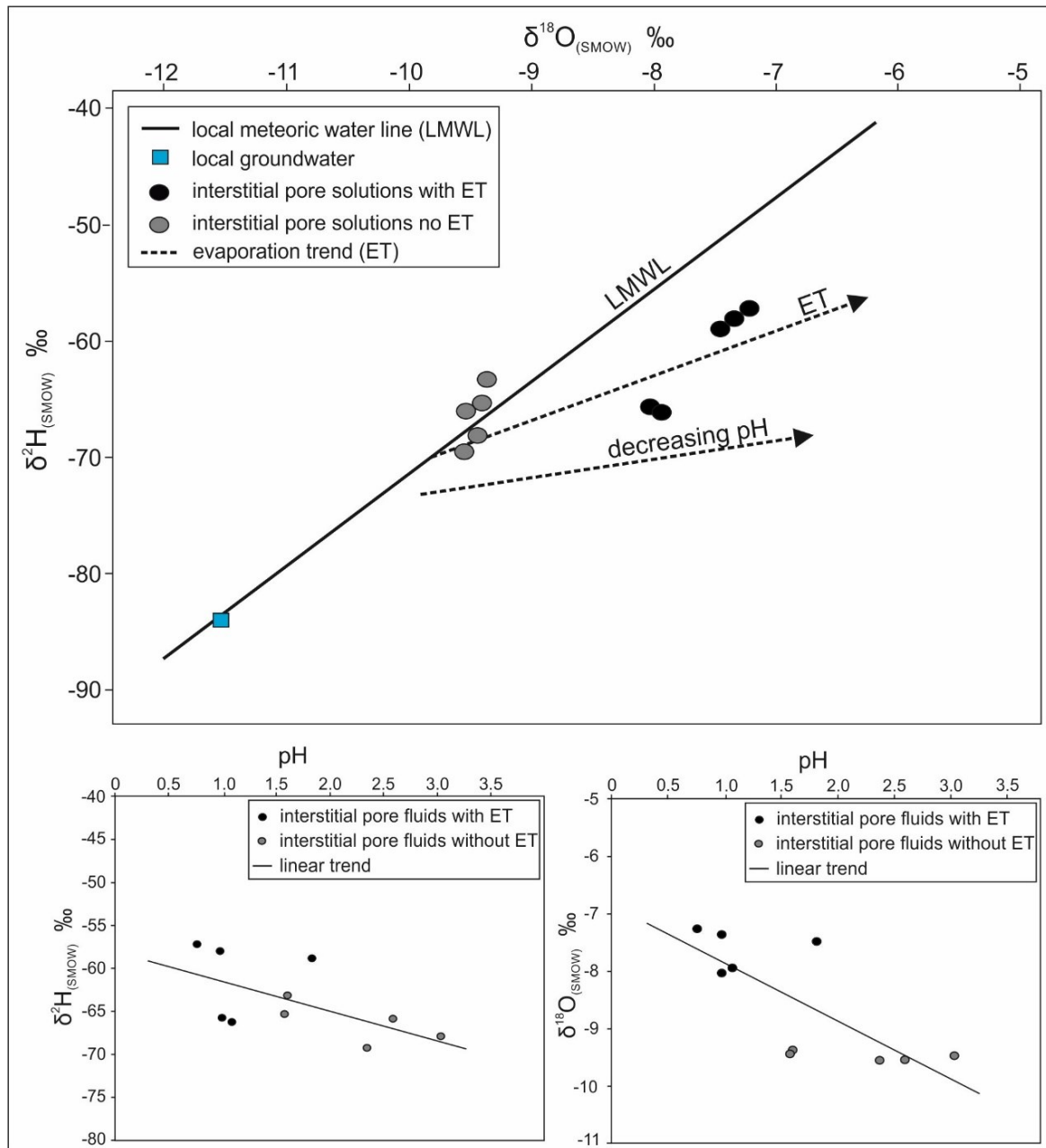


Figure 3: Signatures of stable H and O isotope extracted from interstitial pore solutions of deteriorated concrete layers. A clear enrichment in heavy H and O isotopes could be observed with decreasing pH, which led to corresponding evaporation trend (ET) when plotted against the local meteoric water line for interstitial solutions with pH < 1.5 (black data points). No fractionation could be observed for interstitial pore fluids with pH > 1.5 (grey data points).

Results obtained clearly demonstrate the enrichment of heavy stable H and O isotopes within interstitial pore fluids with decreasing pH. At the same time an evaporation trend could be observed within the same samples when compared to the local meteoric water line. Accordingly, the formation of anhydrite could be clearly attributed to changing humidity levels within the concrete manholes in combination with increasing internal temperatures in summer, corresponding enrichment in dissolved species within the interstitial pore solutions and associated decreasing pH and  $\alpha_{\text{H}_2\text{O}}$ . Observations described were additionally confirmed by measurements of RH and T within such manholes, clearly

emphasizing frequent high fluctuations in RH and T within concrete manholes. Figure 4 shows the negative correlation between T and RH within an Austrian manhole over the period of one week. The measurements were taken within March 2016, during winter season, therefore temperatures are expected to rise significantly during summer months.

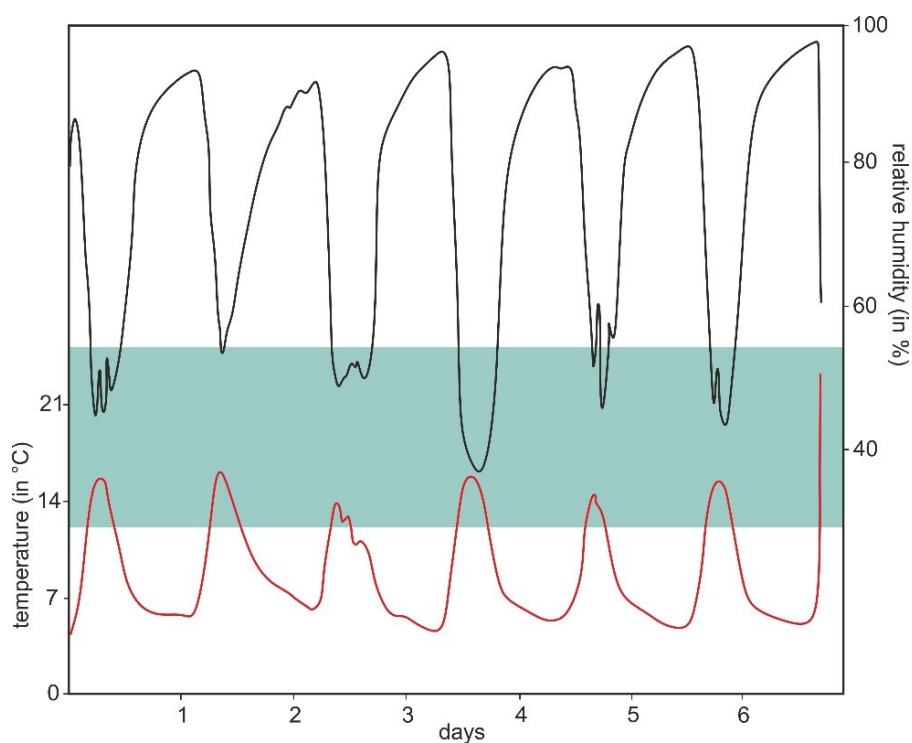


Figure 4: Correlating changes in relative humidity (RH) and temperature within one sewer manhole over the period of one week. In green conditions potentially favoring anhydrite formation due to higher temperatures and low RH and associated low  $\alpha\text{H}_2\text{O}$ .

Furthermore, the impact of RH fluctuations would not only influence mineral neo formation but would also have a large impact on the diffusion of hazardous gases, associated biogenic activity and acid production. In this context signatures of stable H and O isotopes can be recognized as a valuable tool to reconstruct former environmental sewer conditions, responsible for sewer degradation.

The primary reduction of sulfate and subsequent re-oxidation due to SRB and SOB, respectively, within the sewer system resulted in fractionation trends for stable sulfur isotopes (Figure 5). Proceeding dissimilatory sulfate reduction within the anaerobic sediment layers of the power mains resulted in fractionation between the sulfate of the wastewater and the samples captured by  $\text{Ag}_2\text{S}$  and  $\text{ZnS}$ , representing the signal of gaseous  $\text{H}_2\text{S}$ . While we obtained  $\delta^{34}\text{S}$  values between 3.0 and 8.5 ‰ for the wastewater,  $\text{H}_2\text{S}$  signals were in the range of -1 and 3 ‰ (Appendix A1). Compared to fractionations of up to -46‰, as described during dissimilatory sulfate reduction in the literature (Brunner and Bernasconi, 2005), the fractionation observed within this system seems insignificant. This supports the assumption of nearly quantitative conversion of sulfate, present within the power mains, to  $\text{H}_2\text{S}$ , as

non-quantitative transformation would have resulted in large kinetically controlled fractionation effects. Measured extremely low redox potentials of as low as -320 mV, strongly decreasing sulfate concentrations after the power mains and occasionally measured methane concentrations would also militate in that favor (for detail see 2.5).

A second fractionation trend towards light sulfur signals could be observed within pore fluids and the newly formed sulfate salts. Both displayed  $\delta^{34}\text{S}$  values between 0.0 and -4.2 ‰, with no further distinction between one and the other (Figure 5 and Appendix A1). This second kinetic fractionation during the biogenic re-oxidation of reduced sulfur compounds, is in contrast with current observations described in the literature where nearly indistinguishable  $\delta^{34}\text{S}$  are reported (Smith et al., 2011).

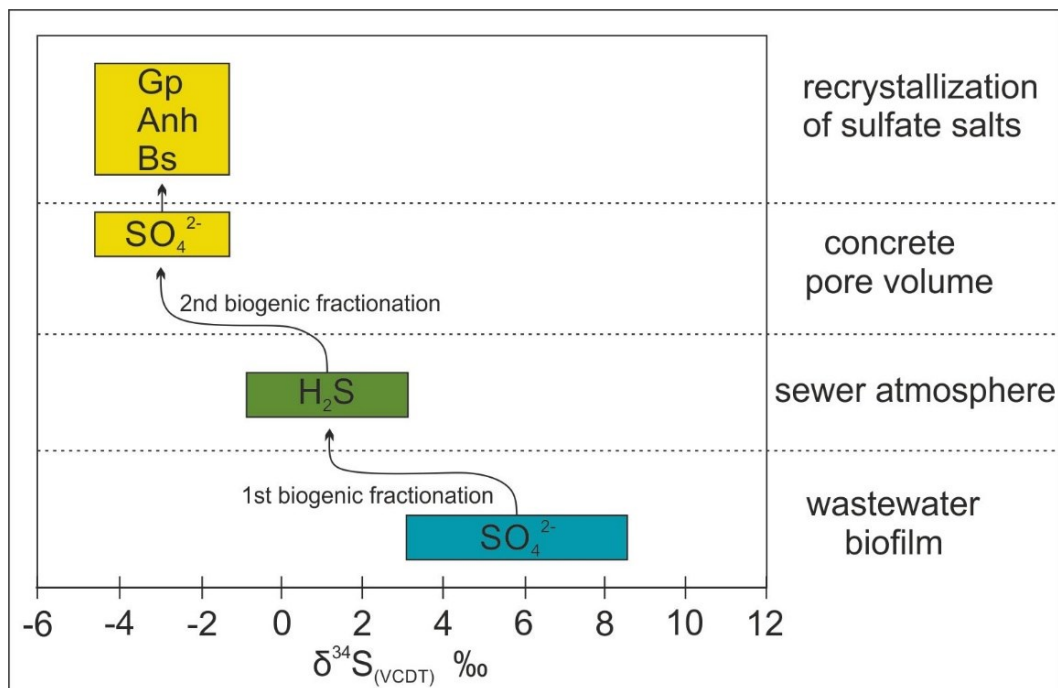


Figure 5: Signatures of stable sulfur isotopes extracted from the wastewater, gaseous H<sub>2</sub>S (via precipitation as Ag<sub>2</sub>S or ZnS), pore fluids and newly formed sulfate salts, together with the two observed biogenic fractionation processes during dissimilatory sulfate reduction (1<sup>st</sup> biogenic fractionation) and subsequent re-oxidation by SOB (2<sup>nd</sup> biogenic fractionation).

#### 4.6. Conclusion

The application of stable sulfur, oxygen and hydrogen isotopes could be successfully applied to decipher individual reaction mechanisms within MICC environments. Fractionation trends within the biochemical sulfur cycle could be clearly assigned to bacterial activity of SRB and SOB. Comparatively small fractionation during dissimilatory sulfate reduction indicated high bacterial activities within the power mains and almost complete conversion rates of sulfate present in the wastewater. This assumption is supported by extremely low redox potentials as low as -320 mV, strongly decreasing sulfate concentrations after the power mains and partial methane production. Interestingly, a second sulfur fractionation during bacterial re-oxidation of reduced sulfur species could be observed, which

should be subject to further research. No distinction in sulfur isotope ratios between the pore fluids and the newly formed sulfate minerals could be observed.

The formation of anhydrite could be explained by evaporation trends of stable H and O isotope trends and associated decreasing  $\alpha_{\text{H}_2\text{O}}$  within the interstitial pore solution of the deteriorated concrete layers.

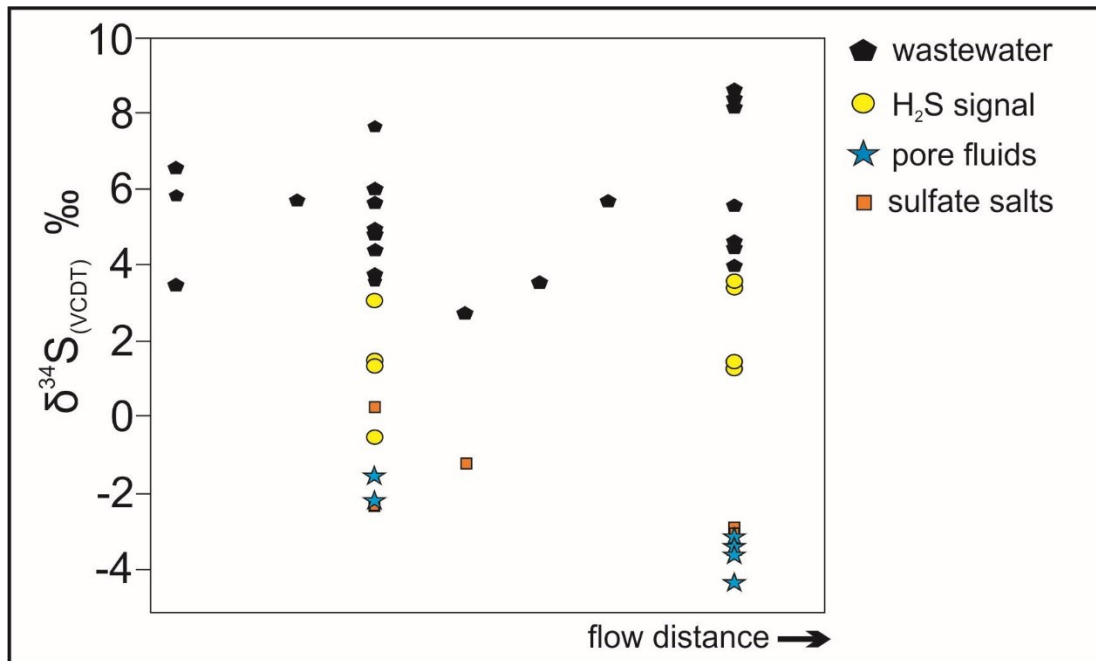
#### 4.7. Bibliography

- Alexander, M., Bertron, A. & De Belie, N., 2013. Performance of Cement-Based Materials in Aggressive Aqueous Environments 1st ed. M. Alexander, A. Bertron, & N. De Belie, eds., Ghent: Springer.
- Antler, G., Turchyn, A. V., Rennie, V., Herut, B., Sivan, O., 2013. Coupled sulfur and oxygen isotope insight into bacterial sulfate reduction in the natural environment. *Geochim. Cosmochim. Acta* 118, 98–117. doi:10.1016/j.gca.2013.05.005
- Brunner, B., Bernasconi, S.M., 2005. A revised isotope fractionation model for dissimilatory sulfate reduction in sulfate reducing bacteria. *Geochim. Cosmochim. Acta* 69, 4759–4771. doi:10.1016/j.gca.2005.04.015
- Deusner, C., Holler, T., Arnold, G.L., Bernasconi, S.M., Formolo, M.J., Brunner, B., 2014. Sulfur and oxygen isotope fractionation during sulfate reduction coupled to anaerobic oxidation of methane is dependent on methane concentration. *Earth Planet. Sci. Lett.* 399, 61–73. doi:10.1016/j.epsl.2014.04.047
- Grengg, C., Mittermayr, F., Baldermann, a., Böttcher, M.E., Leis, a., Koraimann, G., Grunert, P., Dietzel, M., 2015. Microbiologically induced concrete corrosion: A case study from a combined sewer network. *Cem. Concr. Res.* 77, 16–25. doi:10.1016/j.cemconres.2015.06.011
- Haaning Nielsen, A., Lens, P., Vollertsen, J., Hvitved-Jacobsen, T., 2005. Sulfide-iron interactions in domestic wastewater from a gravity sewer. *Water Res.* 39, 2747–55. doi:10.1016/j.watres.2005.04.048
- Hardie, L.A., 1967. The gypsum-anhydrite equilibrium at one atmosphere pressure. *Am. Mineral.* 52, 171–200.
- Hoefs J. *Stable Isotopes Geochemistry*. Berlin Heidelberg: Springer; 2009.
- Islander, B.R.L., Devanny, J.S., Member, A., Mansfeld, F., Postyn, A., Shih, H., 1991. Microbial ecology of crown corrosion in sewers. *J. Environ. Eng.* 117, 751–770.
- Jensen, H.S., Lens, P.N.L., Nielsen, J.L., Bester, K., Nielsen, A.H., Hvitved-Jacobsen, T., Vollertsen, J., 2011. Growth kinetics of hydrogen sulfide oxidizing bacteria in corroded concrete from sewers. *J. Hazard. Mater.* 189, 685–91. doi:10.1016/j.jhazmat.2011.03.005
- Joseph, A.P., Keller, J., Bustamante, H., Bond, P.L., 2012. Surface neutralization and H<sub>2</sub>S oxidation at early stages of sewer corrosion: influence of temperature, relative humidity and H<sub>2</sub>S concentration. *Water Res.* 46, 4235–45. doi:10.1016/j.watres.2012.05.011
- Mittermayr, F., Bauer, C., Klammer, D., Boettcher, M.E., Leis, A., Escher, P., und Dietzel, M., Concrete under sulphate attack: an isotope study on sulphur sources. *Isotopes in Environmental and Health Studies*, 2012. 48(1): p. 105-117.
- Mittermayr, F., Baldermann, A., Kurta, C., Rinder, T., Klammer, D., Leis, A., Tritthart, J., und Dietzel, M., Evaporation — a key mechanism for the thaumasite form of sulfate attack. *Cement and Concrete Research*, 2013. 49(0): p. 55-64.
- O’Connell, M., McNally, C. & Richardson, M.G., 2010. Biochemical attack on concrete in wastewater

applications: A state of the art review. *Cement and Concrete Composites*, 32(7), pp.479–485.

- Okabe, S., Odagiri, M., Ito, T., Satoh, H., 2007. Succession of sulfur-oxidizing bacteria in the microbial community on corroding concrete in sewer systems. *Appl. Environ. Microbiol.* 73, 971–980. doi:10.1128/AEM.02054-06
- Satoh, H., Odagiri, M., Ito, T., Okabe, S., 2009. Microbial community structures and in situ sulfate-reducing and sulfur-oxidizing activities in biofilms developed on mortar specimens in a corroded sewer system. *Water Res.* 43, 4729–39. doi:10.1016/j.watres.2009.07.035
- Smith, L. a., Jim Hendry, M., Wasseenaar, L.I., Lawrence, J., 2012. Rates of microbial elemental sulfur oxidation and 18O and 34S isotopic fractionation under varied nutrient and temperature regimes. *Appl. Geochemistry* 27, 186–196. doi:10.1016/j.apgeochem.2011.10.003
- Tritthart, J., 1989. Chloride binding in cement I. Investigations to determine the composition of porewater in hardened cement. *Cement and Concrete Research*, 19(4), pp.586–94.
- Vincke, E., Monteny, J., Beeldens, A., De Belie, N., Taerwe, L., Van Gemert, D., Verstraete, W.H., 2000. Recent developments in research on biogenic sulfuric acid attack of concrete, in: *Environmental Technologies to Treat Sulfur Pollution: Principles and Engineering*. IWA Publishing, pp. 515–541.
- Yuan, H., Dangla, P., Chatellier, P., Chaussadent, T., 2015. Degradation modeling of concrete submitted to biogenic acid attack. *Cem. Concr. Res.* 70, 29–38. doi:10.1016/j.cemconres.2015.01.002
- Yuan, H., Dangla, P., Chatellier, P., Chaussadent, T., 2013. Degradation modelling of concrete submitted to sulfuric acid attack. *Cem. Concr. Res.* 53, 267–277. doi:10.1016/j.cemconres.2013.08.002

#### 4.8. Appendix



Appendix A1: Signals of stable sulfur isotopes extracted from the wastewater, H<sub>2</sub>S, interstitial pore fluids and newly formed sulfate salts.



Table A1:  $\delta^{34}\text{S}$  extracted from seven manholes (M1 – M7) from the wastewater,  $\text{H}_2\text{S}$  (precipitation via  $\text{Ag}_2\text{S}$  and  $\text{ZnS}$ ), interstitial pore fluids and secondary sulfate salts.

Location	$\delta^{34}\text{S}$ wastewater (‰)	$\delta^{34}\text{S}$ $\text{H}_2\text{S}$ (‰)	$\delta^{34}\text{S}$ pore fluids (‰)	$\delta^{34}\text{S}$ sulfate salts (‰)
M1	3.5; 5.9; 6.7	n.a.	n.a.	n.a.
M2	5.8	n.a.	n.a.	n.a.
M3	3.6; 3.9; 4.4; 4.8; 5.0; 5.8; 6.1; 7.7	-0.5; 1.4; 1.5; 3.1	-1.5; -2.1	-1.3; -2.1
M4	2.6	n.a.	n.a.	-1.2
M5	3.6	n.a.	n.a.	n.a.
M6	5.8	n.a.	n.a.	n.a.
M7	4.0; 4.5; 4.6; 8.2; 8.4; 8.5	1.4; 1.5; 3.7; 3.7	-3.1; -3.4; -3.6; -4.2	-2.7; -2.7; -2.9; -3.0

# Chapter 5

## Advances in construction materials for sewer systems affected by microbial induced concrete corrosion: A review

Cyrill Grengg<sup>1</sup>, Florian Mittermayr<sup>2</sup>, Neven Ukrainczyk<sup>3</sup>, Günther Koraimann<sup>4</sup>, Sabine Kienesberger<sup>4,5</sup> & Martin Dietzel<sup>1</sup>

<sup>1</sup> *Institute of Applied Geosciences, Graz University of Technology, Rechbauerstraße 12, 8010 Graz, Austria*

<sup>2</sup> *Institute of Technology and Testing of Construction Materials, Graz University of Technology, Inffeldgasse 24, 8010 Graz, Austria*

<sup>3</sup> *Institute of Construction and Building Materials, Technische Universität Darmstadt, Franziska-Braun-Straße 3, 64287 Darmstadt, Germany*

<sup>4</sup> *Institute of Molecular Biosciences, University of Graz, Humboldtstraße 50, 8010, Graz, Austria*

<sup>5</sup> *BioTechMed-Graz, Mozartgasse 12/II, 8010, Graz, Austria*

Keywords: sustainable construction, microbiological corrosion, concrete - microorganism interactions, geopolymer, antimicrobial agents

### 5.1. Abstract

Microbial induced concrete corrosion (MICC) is recognized as one of the main degradation mechanisms of subsurface infrastructure worldwide, raising the demand for sustainable construction materials in corrosive environments. This review aims to summarize the key research progress acquired during the last decade regarding the understanding of MICC reaction mechanisms and the development of durable materials from an interdisciplinary perspective. Special focus was laid on aspects governing concrete - microorganism interaction since being the central process steering biogenic acid corrosion. The insufficient knowledge regarding the latter is proposed as a central reason for insufficient progress in tailored material development for aggressive wastewater systems. To date no cement-based material exists, suitable to withstand the aggressive conditions related to MICC over its entire service life. Research is in particular needed on the impact of physiochemical material parameters on microbial community structure, growth characteristics and limitations within individual concrete speciation. Herein an interdisciplinary approach is presented by combining results from material sciences, microbiology, mineralogy and hydrochemistry to stimulate the development of novel and sustainable materials and mitigation strategies for MICC. For instance, the application of

antibacteriostatic agents is introduced as an effective instrument to limit microbial growth on concrete surfaces in aggressive sewer environments. Additionally, geopolymer concretes are introduced as highly resistant in acid environments, thus representing a possible green alternative to conventional cement-based construction materials.

## 5.2. Introduction

The efficient, safe and cost-effective collection and transport of wastewater is a key criteria maintaining expected sanitary standards of modern society (Hvitved-Jacobsen et al., 2013). Especially in developing countries insufficient operating or lacking wastewater networks can lead to the spread of infectious diseases and the contamination of drinking water (Hvitved-Jacobsen et al., 2002). Microbial induced concrete corrosion (MICC) has been recognized as one of the main processes for degradation of concrete based wastewater networks worldwide, increasingly triggering high economic expenses, as well as severe health and environmental concerns (Herisson et al., 2017; Islander et al., 1991; Jiang et al., 2016; Li et al., 2017; O'Connell et al., 2010; Peyre Lavigne et al., 2016). Typical damages of concrete elements from different sewer systems caused by MICC are shown in Figure 1.



Figure 1: Examples of typical deterioration symptoms within systems affected by microbial induced concrete corrosion. Pictures A, B and D were taken in concrete manholes following a power main, while pictures C and E display damages within wastewater catchment basins. For details regarding system and concrete.

Annual rehabilitation costs were estimated to reach over €450 million in Germany (Berger et al., 2016, 2011) and £85 million in the UK, while the USA needs to spend around \$390 billion within the next 20 years, in order to keep the existing wastewater infrastructure operational (Gutiérrez-Padilla et al., 2010). Additionally, hazardous gas production of mainly hydrogen sulfide ( $H_2S$ ) and carbon dioxide ( $CO_2$ ), but also methane ( $CH_4$ ), ammonia ( $NH_3$ ) and other volatile organic compounds (VOCs) associated

with MICC, represent a severe health risk for community workers and wastewater system operators (Gutierrez et al., 2014, 2008; World Health Organization, 2000). MICC is a complex process. To efficiently study MICC, an interdisciplinary approach that brings together the fields of civil and chemical engineering (material scientists), microbiology, mineralogy, hydro-geochemistry as well as environmental sciences is desired. A general description of biofilm characteristics together with the central physiochemical aspects of concrete are described in Figure 2.

Biofilm characteristics	Concrete - definition and chemical properties
<p>Biofilms are composed of communities containing microbial cells that are embedded in a self-produced matrix of extracellular polymeric substances (EPS) and are adherent to each other and/or to a surface (Flemming et al., 2016). They represent a strongly spatially and chronological heterogeneous ecosystem controlled by internal processes and environmental conditions (Donlan, 2002). Mixed culture biofilms, such as environmental biofilms, can be composed from a wide range of microorganisms including autotrophic and heterotrophic bacteria, fungi and archaea. Life essential compounds such as nutrients are provided by either gaseous diffusion or throughout interstitial voids lancing the biofilm.</p> <p><u>Autotroph bacteria:</u> Organisms that produces complex organic compounds gaining energy either by photosynthesis (photoautotrophic) or due to inorganic chemical reactions (chemoautotrophic).</p> <p><u>Heterotroph bacteria:</u> Organisms using organic carbon as an energy source and for synthesis of life essential modules.</p>	<p>Concrete is a multiphase, porous and strongly basic composite material (Alexander et al., 2013). The main components are cement (e.g. Portland cement based binder), aggregates (rock, sand, gravel) and water (for detail see Figure 5). Its structural properties are reached by a series of hydration chemical reactions during which a stable matrix that binds all components together into a stone-like material is established. To date there exist a wide range of concretes with Portland cement based concretes being the most common one. In order to achieve different physiochemical properties a wide range of chemical admixtures such as plasticizers and superplasticizers (e.g. polycarboxylate ether), and/or supplementary cementitious materials (SCM's), such as silica fume, fly ash and blast furnace slag can be added to the admixtures.</p>

Figure 2: A framework to understand the main characteristics of biofilms (left side) and physiochemical concrete parameters (right side).

Intensive research within segregate research areas has produced a wide spectrum of data and hypothesis. To further promote the emergence of innovations for sustainable building material design in wastewater infrastructure efficient cooperation between scientist from the before mentioned areas is required. While the fundamental corrosion processes have been intensely investigated (Islander et al., 1991; Jiang et al., 2014a; Ling et al., 2015), to date no sustainable product is available, which meets the long term requirements in such extremely aggressive and corrosive sewer environments. Extensive laboratory research and in-situ testing have shown that significant durability variations exist between different types of concrete subjected to MICC. Nevertheless, none of the so far tested materials can entirely resist this biogenic acid attack. All materials failed to reach their projected operating life time (Alexander et al., 2013; De Belie et al., 2004; Girardi et al., 2010; Goyns and Alexander, 2014; Herisson et al., 2013). Reasons for this failure may originate from insufficient knowledge on the initial processes leading to microbial colonization of construction materials in heterogeneous wastewater

environments. While Li et al. (2017) have recently summarized the existing knowledge on microbial community structures of acidophilic bacteria associated with MICC, little is known about initial microbial colonization of concrete structures in sewer systems. Moreover, it is largely unknown how biofilms develop, which organisms typically compose these communities, how dynamic they are over time, and how they interact with the applied concretes. Vice versa, the role of specific physical and chemical concrete properties on microbial growth, subsequent corrosion initiation, and propagation still needs further research.

To gain a better overview on the multifaceted phenomenon of MICC, this review aims to compile the key research findings in the field of MICC during the last decade from an interdisciplinary perspective, intertwining advances in concrete materials with microbiological and hydro(geo)chemical related aspects. This contribution emphasizes the central role of specific physical and chemical concrete properties on MICC initiation and propagation, allowing adhesion of microbial cells, microbial growth and subsequent biofilm development. These properties are likely key factors for MICC and are central for further research advances and the development of durable materials. Moreover, we summarize potential additives, such as antimicrobial agents applicable in MICC environments. In addition, possible advantages of geopolymer concretes, being cement free alternatives, compared to conventional cement based building materials, such as Portland cement (OPC) and calcium aluminate cement (CAC) based concretes, are discussed. Due to their acid resistance (Pacheco-Torgal et al., 2014), innovative geopolymer technology could represent a significant step towards the development of sustainable materials for MICC endangered environments.

### **5.3. Characteristics of wastewater environments inducing MICC**

MICC can be described as a sequence of biogenic controlled sulfate reduction and re-oxidation. Initial sulfide production occurs within the sludge and sediment layers, deposited along the inner surfaces of the piping system, favoring corners and turns, areas with long retention times of the wastewater and low abrasive forces. With decreasing oxygen and nitrate concentrations due to ongoing fermentation processes, dissimilatory sulfate respiration is initiated by different strains of sulfate reducing bacteria (SRB), e.g. *Desulfovibrio* and *Desulfomaculum* (Barton and Fauque, 2009) (Figure 3).

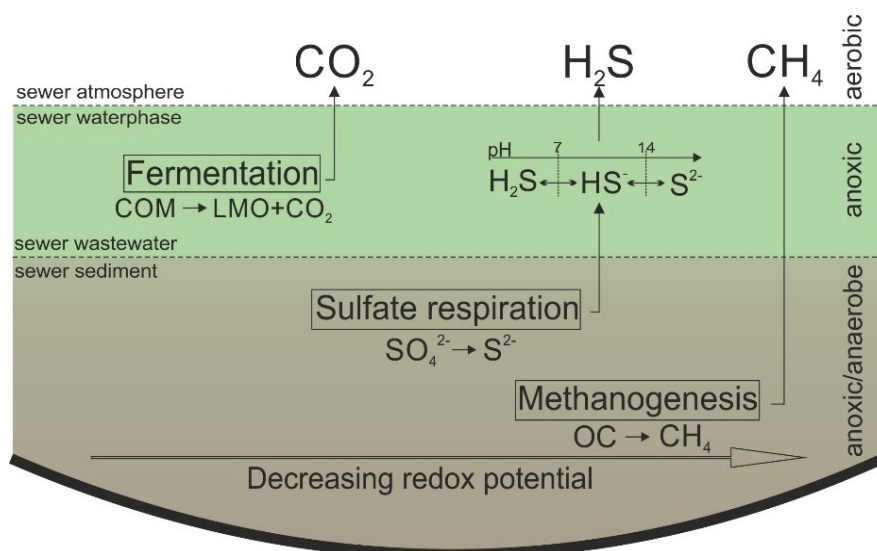


Figure 3: Schematic description of the microbial processes occurring within sludge and sediment layers of sewer pipes with decreasing redox potential. Initial fermentation processes are causing the transformation of complex organic molecules (COM) into low molecule organics (LMO) accompanied by CO<sub>2</sub> production. LMO are thereupon consumed during the sulfate respiration of sulfate-reducing bacteria, as well as during the methanogenesis of methane-producing bacteria under strongly anaerobic conditions, resulting in the production of sulfide species (H<sub>2</sub>S, HS<sup>-</sup> and S<sup>2-</sup>), methane (CH<sub>4</sub>) and CO<sub>2</sub>. Please notice the pH dependency of the sulfide speciation.

Accordingly, sulfides are formed as a side product of anaerobic oxidation of organic carbon, whereas sulfate is used as an external electron acceptor in the absence of oxygen and nitrate (Jensen, 2009; Jensen et al., 2011). The concentration and chemical speciation of the produced sulfides is controlled by: (i) temperature; (ii) pH of the wastewater; (iii) concentration of oxidized sulfur compounds in the wastewater; (iv) the biodegradability and composition of the organic matter present (e.g. complex or small organic molecules); and, (v) the multiphase (i.e. gas, liquid and solid) flow characteristics and retention times of the wastewater (Hvitved-Jacobsen et al., 2013, 2002). Gaseous hydrogen sulfide (H<sub>2</sub>S) is formed together with carbon dioxide (CO<sub>2</sub>), methane (CH<sub>4</sub>) and other VOCs and is partly degassing into the atmosphere of the wastewater piping system, wastewater treatment plants and/or pumping stations. The liberation of those volatile components is governed by changes in the surrounding gas pressure, pH, temperature and wastewater turbulences. Intensified gas liberation is favored by transition chutes after power mains and gravity wastewater system sections with turns and hydraulic drops (Grengg et al., 2016, 2015; Hvitved-Jacobsen et al., 2013; Hvitved-Jacobsen and Vollertsen, 2005). Via gaseous diffusion, H<sub>2</sub>S and CO<sub>2</sub> dissolve and accumulate in the moist pore space of the concrete (Yuan et al., 2015). Islander et al. (1991) first summarized the fundamental processes within the aerobic sequence of MICC, proposing a 3-step corrosion model (Figure 4).

Since concrete is an initially strongly alkaline, porous and multiphase material, with an initial pore solution of around pH 13 (Alexander et al., 2013; Vollpracht et al., 2015), the first stage of corrosion is dominated by abiotic acid-base reactions. Thereby, the pH reduction of concrete occurs due to carbonation and simultaneous attack of thiosulfuric and polythionic acids produced by chemical



oxidation of H<sub>2</sub>S (Roberts et al., 2002). Described pH reduction is potentially controlled by physiochemical material properties steering abiotic oxidation of reduced sulfur species and associated precipitation of the latter. Oxidation products formed, such as elemental sulfur (S<sup>0</sup>) or thiosulfate (S<sub>2</sub>O<sub>3</sub>), provide the energy source for successive biotic acid production within the latter stages of corrosion (Grandclerc et al., 2017; Sun et al., 2013).

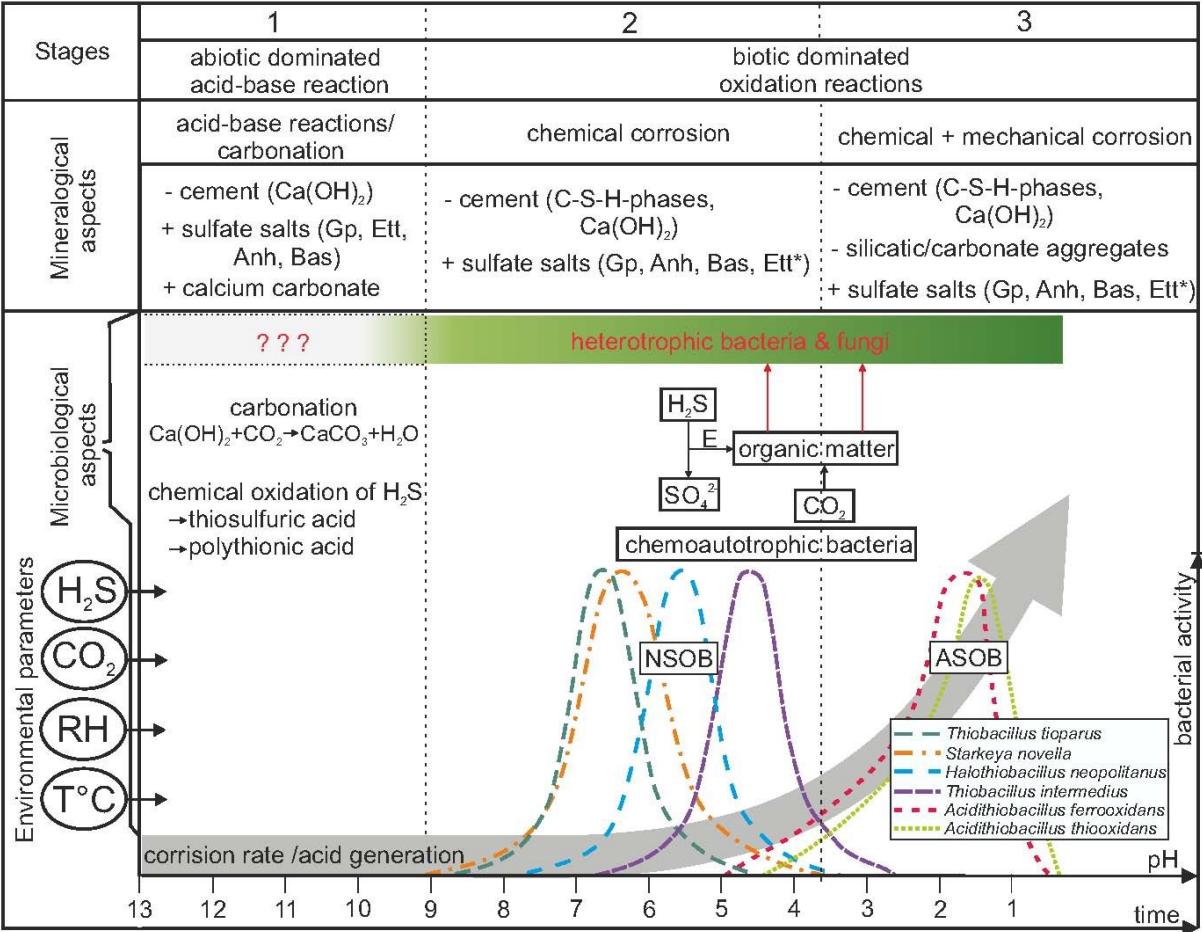


Figure 4: Describes the main mineralogical and microbiological aspects of the aerobic part of MICC sequence, based on an adapted corrosion model of Islander et al. (1991). The initial stage of corrosion is dominated by abiotic acid-base reaction resulting in carbonation and the formation of weak acids (thiosulfuric and polythionic acid). Within the biotic dominated part of MICC, a succession of neutrophil sulfur oxidizing bacteria (NSOB) dominate the pore spaces of the concrete, producing sulfuric acid due to oxidation of reduced sulfur species under humid conditions. Acidophil sulfur oxidizing bacteria (ASOB) dominate within the last stage of corrosion characterized by low pH and high corrosion rates (Ling et al., 2015; Okabe et al., 2007). \*Ettringite formation is limited to high pH areas (>10.7) such as the transition zone between non-corroded and strongly affected concrete layers where alkaline conditions still dominate but sulfate rich pore fluids are already present. Uncertainties within the model, such as the impact of bacteria within the initial pH reduction, the role of heterotrophs and fungi are highlighted in red.

To what extend microbial activity contributes towards the initial pH neutralization of concrete is still under debate. Commonly, it is considered that due to strongly alkaline conditions present in concrete, the microbial occurrence within this stage is limited (Joseph et al., 2012). Nevertheless, Okabe et al. (2007) reported four times higher pH declining rates on the surface of concrete specimen than calculated considering purely chemical neutralization reactions. Such a strong pH reduction was

consequently related to diverse bacterial species (mainly heterotrophic halotolerant and neutrophilic) found on the concrete surface. Generally, no loss of material occurs during this first stage, but similar to conventional sulfate attack, the diffusion of sulfate rich pore fluids is triggering initial leaching of calcium rich hydroxides and isochronal precipitation of expansive sulfate salts such as gypsum (Gp), or ettringite (Ett), especially within the cement rich interfacial transition zones close to the aggregates. Associated increase in pore pressure results in structural destabilization and crack formation (Grenng et al., 2015; Jiang et al., 2014b; Mittermayr et al., 2015; Scrivener et al., 2004).

The transition to the second stage of corrosion is marked by the colonization of various strains of neutrophilic sulfur oxidizing bacteria (NSOB) which adopt the moist concrete surface and pore structure at pH around 9 to 9.5 (Islander et al., 1991; Joseph et al., 2012; Satoh et al., 2009; Vincke et al., 2000). A succession of at least 4 phylotypes of NSOB with decreasing pH is reported (Figure 4). NSOB possess the ability to utilize different sulfur compounds to form sulfuric acid ( $H_2SO_4$ ) under moist conditions (Gomez-Alvarez et al., 2012; Okabe et al., 2007). Continued bacterial activity, associated with biogenic  $H_2SO_4$  production and corresponding acidification is causing dissolution of the cementitious matrix and, if present, carbonate aggregates, together with neo-formation of sulfate salts and consequent mass loss of material. The newly formed mineral phases, precipitating from strongly oversaturated interstitial concrete pore solutions, are dominated by expansive gypsum, bassanite (Bas) and anhydrite (Anh) (Grenng et al., 2015; Jiang et al., 2014b). The formation of secondary ettringite and associated internal cracking, as reported in conventional sulfate attack on concrete, is unlikely within the surface near, low pH areas due to its instability below pH 10.7 (Gabrisova et al., 1991; Mittermayr et al., 2015). Additionally, concrete standard regulations (e.g. EN-206-1) stipulate tri-calcium aluminate ( $C_3A$ ) free (OPC) cement for concretes used in such aggressive environments, thereby limiting the aluminum source central for ettringite formation. Nevertheless, ettringite appearance is reported in various studies (Jiang et al., 2015; Peyre Lavigne et al., 2016, 2015). Presumably, secondary ettringite could form within the transition zone between non-corroded and strongly affected concrete layers where alkaline conditions still dominate but sulfate rich pore fluids are already present. There, ettringite formation could trigger initial crack formation, thereby actively enhancing concrete degradation. Depending on the concrete chemistry, the formation of iron oxyhydroxides, e.g. lepidocrocite ( $\gamma\text{-FeO(OH)}$ ) and goethite ( $\alpha\text{-FeO(OH)}$ ), and iron hydrosulfates, such as parabutlerite ( $Fe(SO_4)(OH)\cdot 2H_2O$ ) within the deterioration layers are possible (Grenng et al., 2017; Jiang et al., 2014b). The third corrosion stage begins once a pH of  $\sim 4$  is reached, as acidophil bacteria are starting to dominate the biofilm, with *Acidithiobacillus thiooxidans* being the most common one (Jiang et al., 2016; Li et al., 2017; Okabe et al., 2007; Satoh et al., 2009). While the central role of *A. thiooxidans* is well described, little information exists regarding the contribution of other bacterial



species. Especially the impact of *Acidithiobacillus ferrooxidans*, a chemoautotrophic ASOB well known from acid mine drainage environments (Osorio et al., 2013; Sugio et al., 1992; Valdés et al., 2008), on corrosion, which is often found within strongly deteriorated systems is under debate (Maeda et al., 1999; Yamanaka et al., 2002). While Okabe et al. (2007) reported low abundances of the latter ones and consequently low impact on corrosion processes within their sampling campaign, other studies emphasized their possible impact under suitable conditions (Grenng et al., 2017, 2015; Jiang et al., 2016). This last stage of MICC is associated with massive loss of material, as reported by corrosion rates of  $> 10 \text{ mm yr}^{-1}$  (Grenng et al., 2015; Mori et al., 1992) (Figure 4). During the biotic cycle of MICC, the appearance and dominance of single SOB (both NSOB and ASOB) is controlled by pH, trophic properties and the ability to utilize different sulfur compounds, e.g.  $\text{H}_2\text{S}$ ,  $\text{S}^0$ ,  $\text{S}_2\text{O}_3$  (Islander et al., 1991; Li et al., 2017). Besides SOB, heterotrophic bacteria and fungi have been found in biofilms observed in various deteriorated wastewater systems (Cho and Mori, 1995; Davis et al., 1998; Peyre Lavigne et al., 2015; Nica et al., 2000; Okabe et al., 2007). The importance of fungi, algae, and lichens in colonization of stone and concrete buildings especially under extreme environmental conditions is well documented and they are important in biofilm formation and stabilization (Flemming et al., 2016). If and how heterotrophs contribute to the corrosion process in wastewater systems still remains uncertain. However, Peyre Lavigne et al. (2015) outlined the impact of heterotrophs on  $\text{O}_2$  mass transfer and their capability to produce  $\text{CO}_2$  locally. Alternatively, they could limit the self-inhibition of growth of autotrophic bacteria by consumption of organic cell material of the latter. Both processes would stimulate autotrophic metabolic activities and associated acid production, thus representing important aspects regarding the microbial cycle during MICC progress. Scrutinizing of metabolic processes as well as characterization of microbial communities contributing to biofilm structure is required to better understand the biotic stages of MICC. Therefore, it is essential to quantify functional capabilities of heterotroph bacteria and fungi, especially since the contribution of the latter is still under debate (Valix and Shanmugarajah, 2015). Detailed knowledge on the metabolic interaction of these microorganisms is crucial to decipher reactions between such biofilms and cementitious materials. Associated gaps in knowledge have to be bridged by complementary research activities in order to develop sustainable materials and efficient mitigation strategies for MICC environments (Gomez-Alvarz et al., 2012; Okabe et al., 2007; Satoh et al., 2009).

#### **5.4. Effect of concrete characteristics on MICC**

To date no concrete product exists withstanding the aggressive MICC environments over its entire service life but also there is no standard regulation for concrete, which recognizes the processes responsible for this specific type of sulfate attack. Contrarily to the conventional form of sulfate attack,

where concrete degradation proceeds due to the interaction between sulfate rich fluids and the concrete, MICC is controlled via the emission and transport of hazardous gases. Therefore, conventional exposition classes defined by critical sulfate/acid concentrations within the interacting fluids cannot address the requirements. On the other hand, researchers have described temperature, relative humidity (RH), H<sub>2</sub>S and CO<sub>2</sub> concentrations as the key environmental parameters in MICC (Jensen, 2009; Jiang et al., 2015; Nielsen et al., 2006; Okabe et al., 2007; Satoh et al., 2009; Vollertsen et al., 2008), however variations in single parameters show relatively small effect on durability of investigated concretes. Jiang et al. (2014) for example observed a corrosion difference of only 10 months for an individually fixed corrosion level to be reached between specimens exposed to 50 and 5 ppm H<sub>2</sub>S (Jiang et al., 2014a). The expected service life for concrete based wastewater systems is up to 100 years, thus 10 months in durability variation appears insignificantly small. In contrast, large durability variations are known to exist between different types of concretes subjected to MICC (Alexander et al., 2013; De Belie et al., 2004; Girardi et al., 2010; Goyns and Alexander, 2014; Lors et al., 2017; Herisson et al., 2013). For instance calcium aluminate cements (CAC) with carbonate aggregates have shown to perform up to 6 times more effective than ordinary portlandite cement (OPC) based concretes within the same aggressive environments (Goyns and Alexander, 2014; Kiliswa, 2016). Hence, it can be concluded that the specific interaction of microorganism with certain materials, rather than different levels of other environmental parameters are steering the degradation rates of concrete-based construction materials in wastewater applications. Accordingly, the prevention of the catalytic microbial growth within concrete is crucial for MICC mitigation. In depth knowledge of the physiochemical concrete parameters and their impact regarding biofilm adhesion, biofilm development and microstructure form the basis for future development of suitable concrete technology for sustainable wastewater systems. An overview of chemical and physical concrete parameters controlling MICC is summarized in Figure 5. To date no systematic study exists focusing on the latter subject matter.

The impact of certain physicochemical concrete parameters on MICC initiation and propagation have been recognized from a material sciences perspective (De Belie et al., 2004; Girardi et al., 2010; Goyns and Alexander, 2014; Herisson et al., 2014a, 2014b). Cement/concrete chemistry, water/binder (w/b) ratio or pore size and distribution could be attributed to process relevant aspects, such as diffusion rates of H<sub>2</sub>S and CO<sub>2</sub>, water saturation and acid neutralization capacity, and were subsequently assigned to corrosion rates and material sustainability (Figure 5). Especially the pore size distribution and connectivity is central within all types of diffusion based transport processes. Accordingly, new concrete formulations were designed which account for those parameters, thereby achieving significant durability improvements (Herisson et al., 2017; Peyre Lavigne et al., 2015).

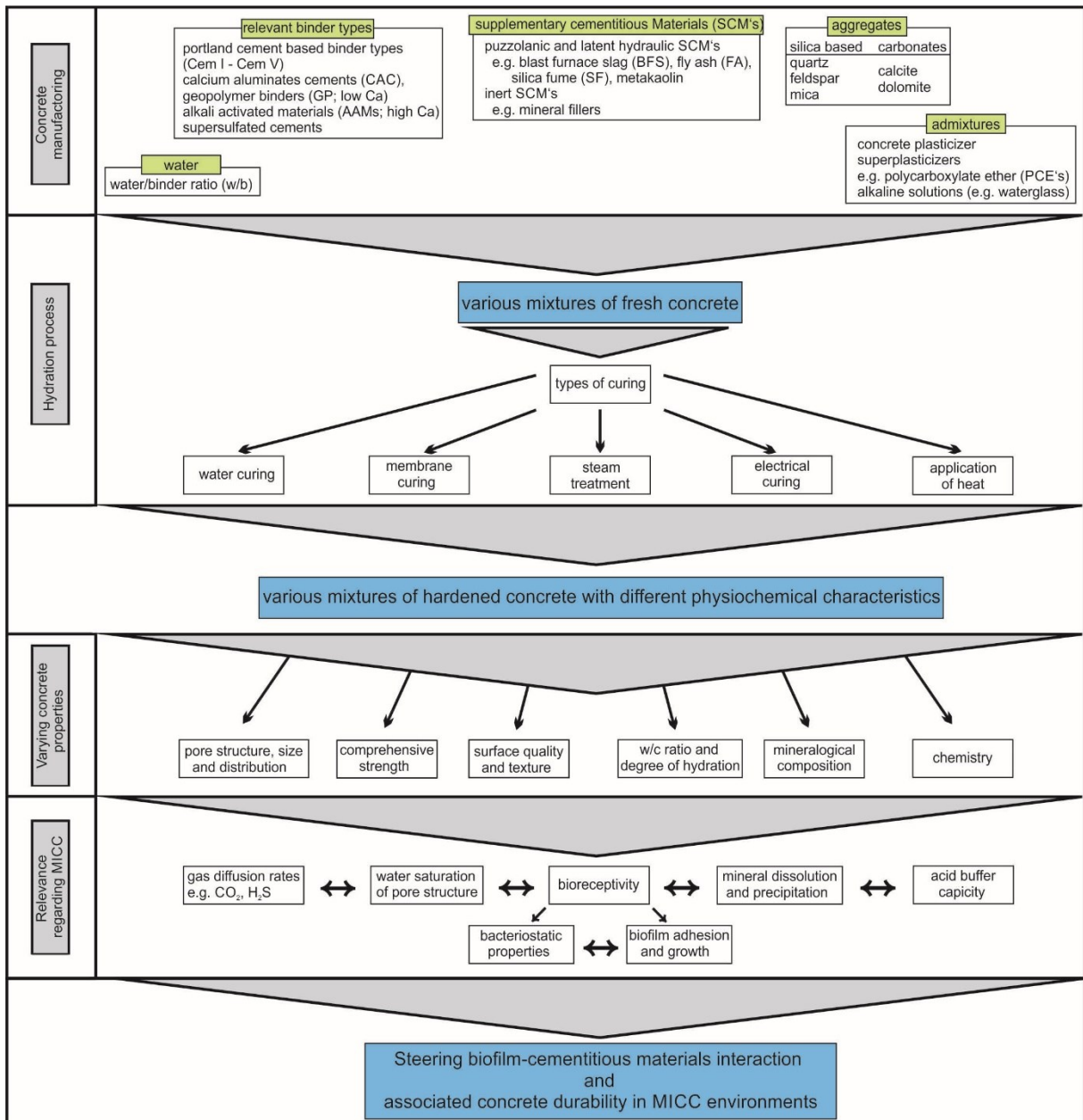


Figure 5: Displays an overview of differences in chemical and physical concrete parameters steering microorganism - cementitious material interactions. Different bioreceptivity of concrete materials was attributed to chemical variations of the different mixing designs during concrete manufacturing and corresponding differences in chemical and physical material properties.

Especially the application of CAC cements has provided significant advantages compared to conventional OPC based concretes according to standard regulations (e.g. EN 206-1). This is attributed to i) CACs higher acid neutralization capacity (Kiliswa, 2016); ii) the formation of an aluminum hydroxide gel under acid attack, which is stable above pH 4 and decreases porosity and associated ingress of aggressive species; and iii) possibly antibacteriostatic characteristics due to higher Al content (Herisson et al., 2017, 2014a; Valix et al., 2014). Nevertheless, to date a complete inhibition of corrosion could not be achieved. One reason for this is that hardly any concrete parameter has been considered for its characteristics regarding biofilm adhesion, composition and development. For

example, the impact of total porosity and pore size distribution on diffusion of aggressive species and water saturation capacity has been extensively studied in various applications (Page and Page, 2007). At the same time, in order to characterize its effect on biofilm development extended research is needed. Also, little is known about the impact of cement chemistry on microbial growth characteristics. In this context, especially the role of Ca for the metabolic cycle of SOB must be content of further research. Kierek and Watnick (2003), showed the  $\text{Ca}^{2+}$  dependency of biofilm development in seawater containing mainly gram negative proteobacteria (Kierek and Watnick, 2003). Accordingly, Ca could also occupy a key position regarding the metabolism of phylogenetically similar SOB. Additionally, the influence of surface conditions like surface roughness and texture, controlled by chemical composition of mortar admixtures as well as the type of curing applied, on bio-adhesion should be investigated in more details in future studies. The application of possible surface treatments and sealing methods with focus on applicability in MICC environments should be substance of further research.

To date a variety of organic polymer based sealers are applied to prevent the access of aggressive substances in wastewater networks (Valix and Shanmugarajah, 2015). For instance, the "patch repair no-dig method" is widely used for rehabilitation of the concrete pipes where organic polymer binders allow for rapid repair without pipe excavation or shrinkage problems. According to EN 1504-2 (Products and systems for protection and repair of concrete structures – Definitions, requirements, quality control and evaluation of conformity – Part 2: Surface protection systems for concrete) the latter surface protecting methods can be classified into two distinct groups: hydrophobic impregnation (e.g. silanes and siloxanes) and impregnation (styrene-butadiene rubbers (SBR)). The most widely used water repellent is silane and its derivatives, e.g. silane-siloxane. While the use of such polymer-modified mortars and linings could potentially improve the durability of concrete sewer pipes in the latter aggressive environments (Beeldens et al., 2001), its impact and interaction on and with microorganisms and on associated transformation of harmful gaseous species is unknown. Presumably, the application of sealing methods described, would potentially contribute towards increased accumulations of toxic and odorous substances, e.g.  $\text{H}_2\text{S}$  and VOCs, in the pipe atmospheres, eventually representing a potential harmful source for continuing operations of wastewater networks.

## **5.5. Geopolymer technology for wastewater applications**

Geopolymer concretes (GPC) have a great potential as a new multi-functional material for the wastewater infrastructure (Pacheco-Torgal et al., 2014). Due to their geopolymer characteristics, they combine positive properties of vitreous ceramic pipes (acid, permeability and abrasion resistance) with advanced performance of concrete pipes (low temperature molding, no dig repair, any pipe diameter possible), while overcoming their individual specific limitations at the same time (Ceramic: brittle,

small diameters, dig renewal, higher cost; Concrete: low durability). Compared to existing concepts for concrete durability based on neutralization by an inevitable dissolution of a sacrificial layer thickness, of about 3-10 mm/year (Kiliswa, 2016), GPC exhibit high acid resistance (Davidovits, 2015; Pacheco-Torgal et al., 2014; Provis et al., 2015) (Figure 6).

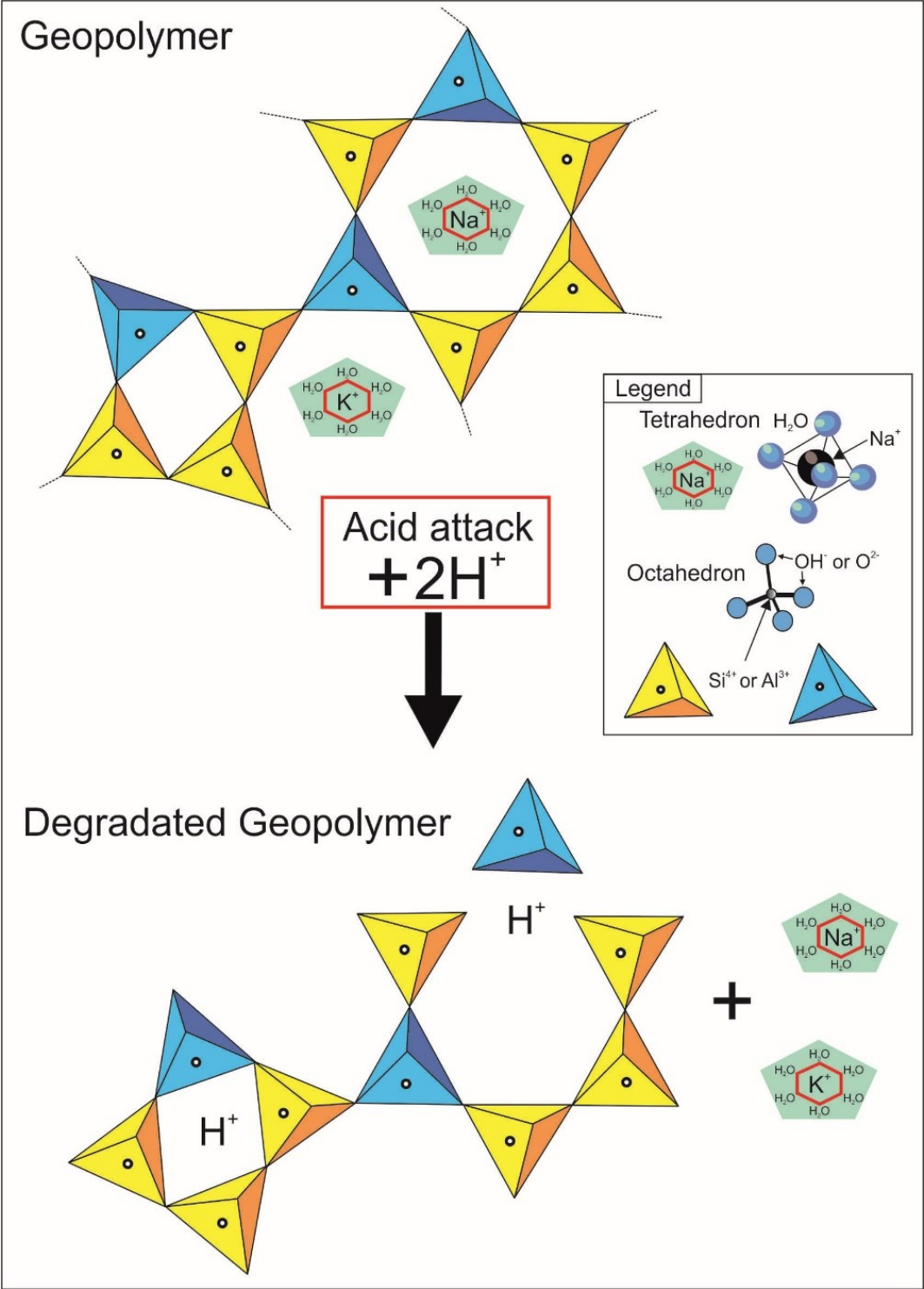


Figure 6: Schematic structural description of geopolymer structure, together with the potential degradation of the GP framework due to acid ingress, including ion exchange reactions between H<sup>+</sup> and charge compensating cations (Na<sup>+</sup>, K<sup>+</sup>) and the dissolution of tetrahedral Al from aluminosilicate framework (breaking of Si-O-Al bonds).

Especially in combination with potential antimicrobial properties, they may provide a much longer (stable) barrier against MICC, while acting as an implicit pipe protection. Traditional, OPC cement-based materials are formed via the cement hydration reactions to form mainly calcium hydroxide (portlandite) and calcium silicate hydrates (C-S-H phases), whereas GPC is produced by polycondensation of alumino-silicates. Thereby, alumina silicate materials (calcined clays, volcanic rocks, blast furnace slag (BFS), fly ash (FA)) are mixed with an alkaline reagent solutions, e.g. sodium or potassium soluble silicates, water and stone aggregates to form a hardened concrete-like texture with similar strength properties (Davidovits, 2013). GPC technology avoids the formation of Ca-rich acid-dissolvable hydration products, as so far present in all cement-based materials, as well as in alkali activated Ca-rich binders, thereby exhibiting high acid resistant properties (Provis and van Deventer, 2009). Geopolymer binders (GPB) build a three-dimensional network of  $[\text{SiO}_4]^{4-}$  and  $[\text{AlO}_4]^{5-}$  tetrahedrons linked randomly by sharing oxygen atoms (Figure 6). Thereby, the negative charge of the  $[\text{AlO}_4]^{5-}$  tetrahedron is balanced by additional framework cations ( $\text{Na}^+$ ,  $\text{K}^+$  etc.). Possible chemical and mineralogical reactions of GPBs compared to different cement-based materials in aggressive biotic controlled acidic environments are summarized in Table 1. While the chemical resistance of cement-based concretes is based on their acid buffer capacity of its constituents and associated dissolution of the cementitious matrix and carbonate aggregates, GPB resistance is governed by ion exchange reactions (absorption, leaching, de-alumination and zeolite crystallization) and permeability (Table 1). GPBs are considered as analogues of zeolites, due to their nano-structural similarity, but packed in an amorphous microstructure (Pacheco-Torgal et al., 2014), which enables them to have analogous applications. Some examples include embodiment of antimicrobial cation additives to sharply reduce bacterial colonization (Hashimoto et al., 2015), as well as for toxic waste immobilization (Andrejkovicova et al., 2016; Pacheco-Torgal et al., 2014). Research so far covered only empirical GPC tests on acid resistance (Gao et al., 2013; Pacheco-Torgal et al., 2014). In this context, acid degradation of GPC depends on the concentration of the acid and can be described as follows (Figure 6; Table 1):

- 1) ion exchange reaction between the penetrating acid protons ( $\text{H}^+$ ) and the charge compensating cations ( $\text{Na}^+$  or  $\text{K}^+$ ) of the geopolymer framework (Škvára et al., 2012; Ukrainczyk et al., 2016), along with
- 2) dissolution of tetrahedral Al from the aluminosilicate framework by breaking of Si–O–Al bonds and formation of water as a by-product, resulting in an increase in solution pH (neutralization capacity), as well as
- 3) crystallization of zeolites causing some additional strength loss.

Table 1: Compares the change in mineralogical composition, including chemical dissolution and precipitation reactions, of different construction materials, including ordinary Portland cements (OPC), calcium aluminate cements (CAC), low Ca geopolymers (GP) and Ca rich alkali activated materials (AAM) within the different stages (1-3) of MICC. \*Ettringite formation is limited to high pH areas (>10.7), such as the transition zone between non-corroded and strongly affected concrete layers where alkaline conditions still dominate but sulfate rich pore fluids are already present.

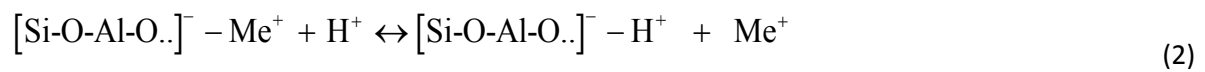
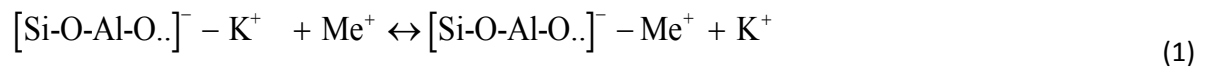
Stages	1	2	3
mineralogical aspects	acid base reactions/carbonation	chemical corrosion	chemical + mechanical corrosion
mechanism	abiotic dominated acid-base reactions	biotic dominated oxidation reactions	
OPC	- cement - Ca(OH) <sub>2</sub> , Ca from C-S-H (incongruent decalcification) + CaCO <sub>3</sub>	- cement - Ca(OH) <sub>2</sub> , C-S-H, Fe-phases, CaCO <sub>3</sub> + Sulfate salts (Gp, Anh, Bas, Ett*)	- cement - Ca(OH) <sub>2</sub> , C-S-H, Fe-phases, CaCO <sub>3</sub> + Sulfate salts (Gp, Anh, Bas, Ett*) - silicate/carbonate aggregates
CAC	- CAH <sub>10</sub> , C <sub>2</sub> AH <sub>8</sub> , C <sub>3</sub> AH <sub>6</sub> + AH <sub>3</sub> , CaCO <sub>3</sub>	- C <sub>3</sub> AH <sub>6</sub> , Fe-phases + AH <sub>3</sub> , CaCO <sub>3</sub> , sulfate salts	- AH <sub>3</sub> + sulfate salts
low Ca GPBs (based on MK, FA)	- unreacted precursors - Na <sup>+</sup> /K <sup>+</sup> (ion exchange) + carbonate salts (Na(K)CO <sub>3</sub> )	- unreacted precursors - Na <sup>+</sup> /K <sup>+</sup> , Al (dealumination of GP gel) + sulfate salts, carbonates	- Al, Si, Na <sup>+</sup> /K <sup>+</sup> (from GP gel) + zeolites, sulfates
Ca-rich AAM (based on slag, FA, ...)	- unreacted precursors - CASH (incongruent decalcification) - anionic clays (Mg-LDH) - Na <sup>+</sup> /K <sup>+</sup> (ion exchange) + carbonate salts (Na(K)CO <sub>3</sub> )	- unreacted precursors - Ca, Al from CASH (incongruent diss.), Fe-phases - anionic clays (Mg-LDH) - Na <sup>+</sup> /K <sup>+</sup> , Al + sulfate salts, carbonates	- CASH + zeolites, sulfates

The framework vacancies formed by Al dissolution are mostly re-occupied by Si resulting in the formation of an imperfect (amorphous) highly siliceous framework that is relatively hard but brittle. Such an undissolved corroded layer could effectively inhibit the process of corrosion by acting as a barrier to the transport of acid protons as well as dissolved constituents if the shrinkage cracks due to the leaching of soluble constituents can be minimized. Thus, compared to the neutralization capacity, achieved by dissolution of hydration products, the permeability of the acidified GPC layers governs the rate of further ingress of acids. While conventional concrete exhibits dissolution rates of 3 to 10 mm y<sup>-1</sup> within MICC environments, accelerated acid tests on (non-optimized) GPC have shown that



dissolution rates for the latter are at least an order of magnitude lower (Kwasny et al., 2016; Pacheco-Torgal et al., 2014). In this context, in depth knowledge of GPB solubility is central to evaluate the permeability and acid resistance of GPB based materials. However, predicting the extent of dissolution reactions of zeolites, and even more so of GPB, has so far been impeded by insufficient thermodynamic data which could not entirely consider the large variations in Si/Al proportions, and H<sub>2</sub>O and cation contents. Another aspect controlling the chemical resistance of GPCs in aggressive environments is the intrinsic ordering present within aluminosilicate gel (Gao et al., 2013; Pacheco-Torgal et al., 2014). Accordingly, additional aluminum in metakaolin-based geopolymer cements might favor their resistance against acid attack (cross-linking gel property) as well as presumably the biological de-activity.

The nano-structural similarity of GPB with zeolites enables GPB to have analogous applications as a carrier of antimicrobial cations (see in detail section 5.6), particularly due to their cation-exchange properties. The potential mechanism of metal ions (Me<sup>+</sup>) interaction with GPB is proposed in the following equations:



The incorporation of Me<sup>+</sup> within the GP network, according to cation-exchange reaction (Equation 1), can be performed in two ways (Hashimoto et al., 2015; Pacheco-Torgal et al., 2014):

- 1) During GP synthesis by addition of metal salts during mixing in a fresh state; and/or
- 2) impregnation of hardened GP with a solution of metal cations.

Upon acid attack, the Me<sup>+</sup> will be gradually released according to the cation-exchange reaction (Equation 2), keeping them enclosed (minimizing leaching and therefore environmental problems), but allowing the interaction with microorganisms. Another mechanism for metal incorporation in GP structures considers the amphoteric behavior of metals, which in alkaline environments creates hydroxide aqua-complexes (e.g. [Zn(OH)<sub>4</sub>]<sup>2-</sup>) that are potentially strongly (covalently) incorporated in the geopolymer structure.

Additionally, GPC can add to the pressing need for innovative green construction materials, which contributes towards a reduction of the CO<sub>2</sub> footprint associated with cement production. GPB raw material production (Metakaolin (MK) and water-glass) cradle to gate CO<sub>2</sub> embodiment is about 70% (Davidovits, 2015) of OPC-based binders and 82% of raw material extraction (Kwasny et al., 2016).

Moreover, the MK production requires much less capital investment in plant and equipment, than cement production. CO<sub>2</sub> emissions for MK production depend on clay purity and crystallinity, calcination and transport to the production site. Recent developments include optimized K-based waterglass for improved workability and efflorescence over Na-based ones, MK substitutions, and alternative cost-effective waterglass production from reuse of SF (Silica fume) and RHA (Rice Husk Ash) (Tchakouté et al., 2016). Partial replacement of MK by reuse of waste materials (e.g. fly ash (FA), waste FCC catalyst; MK from paper sludge waste ash, kaolin sludge waste), may enable further decrease of GPC CO<sub>2</sub> embodiment and cost reduction, as well as improvement in workability and thus reduction in waterglass requirement, while maintaining optimal mechanical properties and durability. Moreover, expected increased durability of GP based products for MICC-resistant infrastructure, or durable repair mortars, will lower maintenance cost and result in decreasing overall CO<sub>2</sub> embodiment for the concrete structure.

Described properties clearly demonstrate the general applicability potential of GPC for wastewater applications. Additionally, the incorporation of antimicrobial agents into the GPC structure could contribute towards further increase in its MICC resistance (Hashimoto et al., 2015). Nevertheless, more research, especially regarding GPC-biofilm interaction is needed in order to verify GPC long-term performance, to characterize possible limitations and to validate suitable antimicrobial additives.

## **5.6. Antimicrobial agents**

The successful use of antimicrobial agents has been documented in various applications, ranging from environmental studies investigating the tolerance of (heavy) metals on Fe(III)-reducing microbial communities in soils (Burkhardt et al., 2011), to the antimicrobial function of copper coatings in the public sectors (Wei et al., 2014). Within recent years, antimicrobial additives have also been increasingly used in conventional concretes. For instance, Alum et al. (2008) studied different antimicrobial formulations containing FA, silica fume (SF), ZnO, Cu-slag, ammonium and bromide (Alum et al., 2008). They demonstrated by field and laboratory tests that concrete mixtures containing 10% ZnO had comparable antimicrobial properties similar to commercial biocides. Accordingly, bacteriostatic characteristics of (heavy) metal ions could provide novel, sustainable and economic answers to many aspects of biodeterioration, but especially for MICC environments (Gu et al., 2011). A summary of the relevant studies on the effects of potential antimicrobial agents in MICC relevant settings is presented in Table 2.

Table 2: Summary of relevant studies describing the effects of Me<sup>+</sup>, utilized as antimicrobial agents in various applications, with special focus on relevant bacterial species such as SOB.

Setup	Material	Metal addition	Conclusion/Effect	Reference
in situ experiments	OPC	Ni	Significant inhibitory effects on different strains of neutrophil bacteria	(Negishi et al., 2005)
in situ experiments	OPC	CaWO <sub>4</sub> , Ni	Complete inhibition of growth of 5 different strains of <i>Acidithiobacillus spp.</i> from concentrations >50 μM	(Negishi et al., 2005)
laboratory testing	OPC	Ni, W, ZnSiF <sub>6</sub>	Suppressed growth of diverse SOBs	(Kim et al., 2009)
field and laboratory testing	OPC	ZnO, Cu-slag, Br, NH <sub>4</sub>	Mixtures containing 10% ZnO had similar bacteriostatic properties as commercial biocides.	(Alum et al., 2008)
laboratory testing	GP	Ag	99% mortality for gram positive/negative bacteria	(Adak et al., 2015)
laboratory testing	Zeolites	Ag, Zn, Cu	Binary Cu/Zn same bacteriostatic efficiency as Ag	(Kaali et al., 2011)
laboratory testing	PPC	Cu	95% mortality of <i>E. coli</i> after 4h contact	(Delgado et al., 2011)
laboratory testing	MK GP	Cu	Suppressed growth of oyster mushrooms	(Hashimoto et al., 2015)

GP...geopolymer; MK GP... geopolymer; OPC...ordinary Portland cement; PPC...polypropylene composites

The toxic effect of (heavy) metal ions (Me<sup>+</sup>) on bacteria is based on Me<sup>+</sup> reactions with the negatively charged cell walls of bacteria and associated formation of complex compounds within the bacterial membrane. This reactions is suggested to inhibit life essential activity of sensitive enzymes, as well as to disturb the osmotic stability of the cell, resulting in the leakage of intracellular constituents (Nies, 1999). The inhibitory efficiency and applicability of Me<sup>+</sup> on microbial growth in MICC environments is based on their solubility (and/or ion exchange) function under acid attack conditions, their affinity to sulfur, their interaction with microbiological populations, as well as on their geochemical abundances (Nies, 1999). Therefore, the range of Me<sup>+</sup>, possibly eligible as antimicrobial agents for wastewater networks can be limited to Al, Fe, Mo, Mn, Zn, Ni, Cu, V, Co, W and Cr. Since Fe and Mn are always present in significant concentrations within concrete admixtures, they are not seen as decisive for achieving the desired bacteriostatic effects. Contrarily, higher Fe concentration could be positively correlated to bacterial activity of *A. ferrooxidans* and associated acid production (Grenng et al., 2017,

2015; Maeda et al., 1999). Diverse studies have already demonstrated the bacteriostatic effects of different (heavy) metal ions described on the growth of relevant SOB in various environments (Ezaka and Anyanwu, 2011; Navarro et al., 2013; Orell et al., 2013) (Table 2). For instance, Navarro et al., (2013) determined the minimum inhibitory concentration of Cu, As, Zn, Cd and Ni for different strains of acidophilic bacteria associated with a certain relevance regarding biomining, including two strains of *A. caldus* and *A. ferrooxidans*. At the same time, Orell et al., (2013) investigated the tolerance of thermoacidophilic *crenarchaeon*, used in high-temperature bioleaching processes, regarding Cd and Cu concentrations. Negishi et al. (2005) were able to inhibit the growth of five strains of SOB, including *A. thiooxidans*, completely by the addition of 50  $\mu\text{M}$  of sodium tungstate to the nutrient solution (Negishi et al., 2005). In the process, tungsten was bound to the cell structure, thereby inhibiting the activity of the sulfur oxidase of the bacteria and co-depending cell growth. In a further step 0.075 wt. % calcium tungstate was added to Portland cement bars and outsourced to a wastewater system with mean  $\text{H}_2\text{S}$  concentrations of 28 ppm. Significant decrease in weight loss for the calcium tungstate bearing mortars could be observed, demonstrating the inhibitory effect of W on the growth of SOB present. At the same time a bacteriostatic impact of Al on microbial growth is proposed as one of the reasons for higher durability of CAC-based materials observed in MICC environments (Herisson et al., 2017, 2013). Alternatively, the application of zeolites exchanged with  $\text{Me}^+$  could provide a promising substitute for concretes suitable for aggressive wastewater systems (Inoue et al., 2002; Kaali et al., 2011; Zhang et al., 2009). Kaali et al., (2011) investigated the influence of  $\text{Ag}^+$ ,  $\text{Zn}^{2+}$  and  $\text{Cu}^{2+}$  exchanged zeolite on antimicrobial and long term in vitro stability of medical grade polyether polyurethane, finding that the binary Cu/Zn system had the same bacteriostatic efficiency as the single silver systems. The synergetic effect was explained by different toxic mechanisms within the cell initiated by the individual metal cation. Accordingly, they concluded that zeolites exchanged with metal cations exhibit a high potential technology to enhance antimicrobial properties of materials. Alternatively, Hashimoto et al (2015) have shown that the antimicrobial activity of metakaolin GP's against fungi hyphae could be significantly increased by the incorporation of copper ions into the GP structure, due to immersing the latter in a 0.1 molar copper chloride solution for 24h (Hashimoto et al., 2015). In both contexts, the antimicrobial mechanism of metal cation loaded zeolites is based on cation exchange reactions, during which the inorganic molecular sieves trap the antibacterial metals, keeping them enclosed and thus minimizing leaching and associated environmental problems, but allowing the interaction with microorganisms (as explained in detail within the section on Geopolymers).

The above-mentioned studies indicate the enormous potential of (heavy) metal ions as anti-microbial agents in materials suited for aggressive wastewater environments. However, since the  $\text{Me}^+$  resistance of acidophilic bacteria is generally magnitudes higher than those of neutrophilic bacteria, the most

promising approach should focus on the inhibition of NSOB (Dopson et al., 2003). Since the NSOB are mainly responsible for the pH reduction from 9.5 to around 4 during MICC propagation, a discontinuity of the succession of NSOB must inevitably constrain the growth of ASOB. In this regard, additional research has to focus on advanced knowledge on the dynamically changing microbial community structure in MICC environments in order to quantify the possible impact of antimicrobial agents during different corrosion stages. Additionally, the potential impact of  $Me^+$  addition on structural and mechanical concrete properties, together with their environmental compatibility, has to be considered.

## 5.7. Conclusions and Outlook

Microbial induced concrete corrosion represents one of the main degradation mechanisms of subsurface infrastructure, thereby raising high economic expenses as well as severe health related concerns. While the overall process mechanisms and environmental parameters responsible for MICC are fairly well understood, to date, no commercially available concrete can entirely withstand the adverse conditions in such aggressive environments over its projected operating life. A reason for present inability to design durable materials lies in the gap of knowledge that combine the reaction mechanisms and kinetics between microbial metabolism and degradation of concrete material. As long as concrete surface conditions support microbial growth, biogenic acid production is initiated, which is accompanied by subsequent autocatalytic intensification and degradation of cement-based construction materials. Accordingly, further research should focus on how to constrain concrete - microorganism interactions. On one hand, physical and chemical concrete parameters have to be characterized in details regarding their impact on microbial growth. On the other hand, a better understanding of the microbial ecology supporting MICC must be attained, including metabolic process reactions, a holistic characterization of the microbial communities involved, biofilm structure and distribution as well as the functional capabilities of heterotrophs and fungi involved. New knowledge on those topics represents a fruitful new avenue towards the development of sustainable materials for MICC environments.

In this context, geopolymer technology could represent promising construction materials, suitable for MICC environments, due to properties such as low permeability caused by its fine pore structure, cation exchange properties and chemical stability at low pH due to a lack of highly soluble Ca-hydration products, as so far present in all cement-based materials.

The application of (heavy) metals as anti-microbial additives for concretes should be considered in further research since their bacteriostatic effects are widely approved and tested in various

applications. Their incorporation could contribute positively towards durability of concrete-based sewer systems, impartially of the construction material applied.

## 5.8. Acknowledgment

The authors gratefully thank the Graz University of Technology (Austria) scientific grant program for financial support. Financial support was greatly appreciated by Peter Rappold and the Department of Water Resources Management, Styria, as well as to Heinz Lackner and the Department of Energy, Residential Constructions and Technology, Styria.

## 5.9. Bibliography

- Alexander, M., Bertron, A., De Belie, N., 2013. Performance of Cement-Based Materials in Aggressive Aqueous Environments, 1st ed. Springer, Ghent. doi:10.1007/978-94-007-5413-3
- Alexander, M., Goyns, A., Fourie, C., 2008. Experiences with a full-scale experimental sewer made with CAC and other cementitious binders in Virginia, South Africa., in: Proceedings of the Centenary Conference on Calcium Aluminate Cements. IHS, Avignon, pp. 279–292.
- Alum, A., Rashid, A., Mobasher, B., Abbaszadegan, M., 2008. Cement-based biocide coatings for controlling algal growth in water distribution canals. *Cem. Concr. Compos.* 30, 839–847. doi:10.1016/j.cemconcomp.2008.06.012
- Andrejkovicova, S., Sudagar, A., Rocha, J., Patinha, C., Hajjaji, W., Da Silva, E.F., Velosa, A., Rocha, F., 2016. The effect of natural zeolite on microstructure, mechanical and heavy metals adsorption properties of metakaolin based geopolymers. *Appl. Clay Sci.* 126, 141–152. doi:10.1016/j.clay.2016.03.009
- Barton, L.L., Fauque, G.D., 2009. Biochemistry, physiology and biotechnology of sulfate-reducing bacteria., in: *Advances in Applied Microbiology*. Elsevier Inc., pp. 42–98. doi:10.1016/S0065-2164(09)01202-7
- Beeldens, A., Monteny, J., Vincke, E., Belie, N. De, Gemert, D. Van, Taerwe, L., 2001. Resistance to biogenic sulphuric acid corrosion of polymer-modified mortars. *Cem. Concr. Compos.* 23, 47–56.
- Berger, C., Falk, C., Hetzel, F., Innekamp, J., Roder, S., Ruppelt, J., 2016. Zustand der Kanalisation in Deutschland: Ergebnisse der DWA-Umfrage 2015. Sonderdruck Korrespondenz Abwasser, Abfall. doi:10.3242/kae2011/01.001
- Burkhardt, E.M., Bischoff, S., Akob, D.M., Büchel, G., Küsel, K., 2011. Heavy metal tolerance of Fe(III)-reducing microbial communities in contaminated creek bank soils. *Appl. Environ. Microbiol.* 77, 3132–3136. doi:10.1128/AEM.02085-10
- Cho, K.-S., Mori, T., 1995. A newly isolated fungus participates in the corrosion of concrete sewer pipes. *Water Sci. Technol.* 31, 263–271. doi:10.1016/0273-1223(95)00343-L
- Davidovits, J., 2015. Environmental implications of Geopolymers. *materialstoday*.
- Davidovits, J., 2013. Geopolymer Cement, a review. *Geopolymer Inst. Libr.* 1–11.
- Davis, J.L., Nica, D., Shields, K., Roberts, D.J., 1998. Analysis of concrete from corroded sewer pipe. *Int. Biodeterior. Biodegrad.* 42, 75–84. doi:10.1016/S0964-8305(98)00049-3

- De Belie, N., Monteny, J., Beeldens, a., Vincke, E., Van Gemert, D., Verstraete, W., 2004. Experimental research and prediction of the effect of chemical and biogenic sulfuric acid on different types of commercially produced concrete sewer pipes. *Cem. Concr. Res.* 34, 2223–2236. doi:10.1016/j.cemconres.2004.02.015
- Dopson, M., Baker-Austin, C., Koppineedi, P.R., Bond, P.L., 2003. Growth in sulfidic mineral environments: Metal resistance mechanisms in acidophilic micro-organisms. *Microbiology* 149, 1959–1970. doi:10.1099/mic.0.26296-0
- Ezaka, E., Anyanwu, C.U., 2011. Chromium ( VI ) tolerance of bacterial strains isolated from sewage oxidation ditch. *Int. J. Enviromental Sci.* 1, 1725–1734.
- Flemming, H., Wingender, J., Szewzyk, U., Steinberg, P., Rice, S.A., 2016. TH RE Biofilms : an emergent form of bacterial life. *Nat. Publ. Gr.* 14, 563–575. doi:10.1038/nrmicro.2016.94
- Gabrisova, A., Havlica, J., Sahu, S., 1991. Stability of calcium sulphoaluminates hydrates in water solutions with various pH values. *Cem. Concr. Res.* 21, 1023–1027. doi:10.1016/0008-8846(91)90062-M
- Gao, X.X., Michaud, P., Joussein, E., Rossignol, S., 2013. Behavior of metakaolin-based potassium geopolymers in acidic solutions. *J. Non. Cryst. Solids* 380, 95–102. doi:10.1016/j.jnoncrysol.2013.09.002
- Girardi, F., Vaona, W., Di Maggio, R., 2010. Resistance of different types of concretes to cyclic sulfuric acid and sodium sulfate attack. *Cem. Concr. Compos.* 32, 595–602. doi:10.1016/j.cemconcomp.2010.07.002
- Gomez-Alvarez, V., Revetta, R.P., Domingo, J.W., 2012. Metagenome analyses of corroded concrete wastewater pipe biofilms reveal a complex microbial system. *BMC Microbiol.* 12, 122. doi:10.1186/1471-2180-12-122
- Goyns, A.M., Alexander, M., 2014. Performance of various concretes in the Virginia experimental sewer over 20 years. *Calcium Aluminates.* Balkema.
- Grandclerc, A., Minerbe-Guéguen, M., Nour, I., Dangla, P., Chaussadent, T., 2017. Impact of cement composition on the adsorption of hydrogen sulphide and its subsequent oxidation onto ... *Constr. Build. Mater.* 152, 576–586. doi:10.1016/j.conbuildmat.2017.07.003
- Grengg, C., Kiliswa, M., Mittermayr, F., Alexander, M., 2016. Microbially-induced Concrete Corrosion- A worldwide problem, in: *Microorganisms-Cementitious Materials Interactions.* pp. 1–19, Delft.
- Grengg, C., Mittermayr, F., Baldermann, A., Böttcher, M, E., Leis, A., Koraimann, G., Grunert, P., Dietzel, M., 2015. Microbiologically induced concrete corrosion: A case study from a combined sewer network. *Cem. Concr. Res.* 77, 16–25.
- Grengg, C., Mittermayr, F., Koraimann, G., Szabo, M., Demeny, A., Dietzel, M., 2017. The decisive role of acidophilic bacteria in concrete sewer networks: A new model for advanced microbial concrete corrosion. *Cem. Concr. Res.* (in Press), doi.org/10.1016/j.cemconres.2017.08.020
- Gu, J.D., Ford, T.E., Mitchellm, R., 2011. Microbiological corrosion of concrete, in: *Uhlig's Corrosion Handbook.* John Wiley & Sons, pp. 451–460.
- Gutiérrez-Padilla, M.G.D., Bielefeldt, A., Ovtchinnikov, S., Hernandez, M., Silverstein, J., 2010. Biogenic sulfuric acid attack on different types of commercially produced concrete sewer pipes. *Cem. Concr. Res.* 40, 293–301. doi:10.1016/j.cemconres.2009.10.002
- Gutierrez, O., Mohanakrishnan, J., Sharma, K.R., Meyer, R.L., Keller, J., Yuan, Z., 2008. Evaluation of oxygen injection as a means of controlling sulfide production in a sewer system. *Water Res.* 42, 4549–61. doi:10.1016/j.watres.2008.07.042



- Gutierrez, O., Sudarjanto, G., Ren, G., Ganigué, R., Jiang, G., Yuan, Z., 2014. Assessment of pH shock as a method for controlling sulfide and methane formation in pressure main sewer systems. *Water Res.* 48, 569–78. doi:10.1016/j.watres.2013.10.021
- Hashimoto, S., MacHino, T., Takeda, H., Daiko, Y., Honda, S., Iwamoto, Y., 2015. Antimicrobial activity of geopolymers ion-exchanged with copper ions. *Ceram. Int.* 41, 13788–13792. doi:10.1016/j.ceramint.2015.08.061
- Herisson, J., Gueguen-Minerbe, M., Van Hullebusch, E.D., Chaussadent, T., 2014a. Biogenic corrosion mechanism: Study of parameters explaining calcium aluminate cement durability., in: *Calcium Aluminates*. Balkema, pp. 645–58.
- Herisson, J., Guéguen-Minerbe, M., van Hullebusch, E.D., Chaussadent, T., 2017. Influence of the binder on the behaviour of mortars exposed to H<sub>2</sub>S in sewer networks: a long-term durability study. *Mater. Struct.* 50, 8. doi:10.1617/s11527-016-0919-0
- Herisson, J., Guéguen-Minerbe, M., van Hullebusch, E.D., Chaussadent, T., 2014b. Behaviour of different cementitious material formulations in sewer networks. *Water Sci. Technol.* 69, 1502–8. doi:10.2166/wst.2014.009
- Herisson, J., van Hullebusch, E.D., Moletta-Denat, M., Taquet, P., Chaussadent, T., 2013. Toward an accelerated biodeterioration test to understand the behavior of Portland and calcium aluminate cementitious materials in sewer networks. *Int. Biodeterior. Biodegradation* 84, 236–243. doi:10.1016/j.ibiod.2012.03.007
- Hvitved-Jacobsen, T., Vollertsen, J., 2005. Odor from sewer networks - processes and prediction, in: *Odor from Sewer Networks - Processes and Prediction*. Stockholm.
- Hvitved-Jacobsen, T., Vollertsen, J., Nielsen, A.H., 2013. *Sewer Processes - Microbial and Chemical Process Engineering of Sewer Networks*, 2nd ed. CRC Press, London.
- Hvitved-Jacobsen, T., Vollertsen, J., Yongsiri, C., Nielsen, A.H., 2002. Sewer microbial processes, emissions and impacts, in: *Sewer Processes and Networks*. Paris, p. 13.
- Inoue, Y., Hoshino, M., Takahashi, H., Noguchi, T., Murata, T., Kanzaki, Y., Hamashima, H., Sasatsu, M., 2002. Bactericidal activity of Ag-zeolite mediated by reactive oxygen species under aerated conditions. *J. Inorg. Biochem.* 92, 37–42. doi:10.1016/S0162-0134(02)00489-0
- Islander, B.R.L., Devanny, J.S., Member, A., Mansfeld, F., Postyn, A., Shih, H., 1991. Microbial ecology of crown corrosion in sewers. *J. Environ. Eng.* 117, 751–770.
- Jensen, H.S., 2009. PhD thesis; Hydrogen sulfide induced concrete corrosion of sewer networks. Aalborg University.
- Jensen, H.S., Lens, P.N.L., Nielsen, J.L., Bester, K., Nielsen, A.H., Hvitved-Jacobsen, T., Vollertsen, J., 2011. Growth kinetics of hydrogen sulfide oxidizing bacteria in corroded concrete from sewers. *J. Hazard. Mater.* 189, 685–91. doi:10.1016/j.jhazmat.2011.03.005
- Jiang, G., Keller, J., Bond, P.L., 2014a. Determining the long-term effects of H<sub>2</sub>S concentration, relative humidity and air temperature on concrete sewer corrosion. *Water Res.* 65, 157–69. doi:10.1016/j.watres.2014.07.026
- Jiang, G., Sun, X., Keller, J., Bond, P.L., 2015. Identification of controlling factors for the initiation of corrosion of fresh concrete sewers. *Water Res.* doi:10.1016/j.watres.2015.04.015
- Jiang, G., Wightman, E., Donose, B.C., Yuan, Z., Bond, P.L., Keller, J., 2014b. The role of iron in sulfide induced corrosion of sewer concrete. *Water Res.* 49, 166–74. doi:10.1016/j.watres.2013.11.007
- Jiang, G., Zhou, M., Chiu, T.H., Sun, X., Keller, J., Bond, P.L., 2016. Wastewater-Enhanced Microbial Corrosion of Concrete Sewers. *Environ. Sci. Technol.* 50, 8084–8092. doi:10.1021/acs.est.6b02093

- Joseph, A.P., Keller, J., Bustamante, H., Bond, P.L., 2012. Surface neutralization and H<sub>2</sub>S oxidation at early stages of sewer corrosion: influence of temperature, relative humidity and H<sub>2</sub>S concentration. *Water Res.* 46, 4235–45. doi:10.1016/j.watres.2012.05.011
- Kaali, P., Pérez-Madrigal, M.M., Strömberg, E., Aune, R.E., Czél, G.Y., Karlsson, S., 2011. The influence of Ag<sup>+</sup>, Zn<sup>2+</sup> and Cu<sup>2+</sup> exchanged zeolite on antimicrobial and long term in vitro stability of medical grade polyether polyurethane. *Express Polym. Lett.* 5, 1028–1040. doi:10.3144/expresspolymlett.2011.101
- Kierck, K., Watnick, P.I., 2003. The *Vibrio cholerae* O139 O-antigen polysaccharide is essential for Ca - dependent biofilm development in sea water. *Proc. Natl. Acad. Sci.* 100, 14357–14362.
- Kiliswa, M., 2016. Composition and microstructure of concrete mixtures subjected to biogenic acid corrosion and their role in corrosion prediction of concrete outfall sewers. University of Cape Town.
- Kwasny, J., Soutsos, M.N., McIntosh, J.A., Cleland, D.J., 2016. banahCEM - comparison of properties of a laterite-based geopolymer with conventional concrete. *Proc. 9th Int. Concr. Conf. 2016 Environ. Effic. Econ. Challenges Concr.* 383–394.
- Li, X., Jiang, G., Kappler, U., Bond, P., 2017. The ecology of acidophilic microorganisms in the corroding concrete sewer environment. *Front. Microbiol.* 8, 683. doi:10.3389/FMICB.2017.00683
- Ling, A.L., Robertson, C.E., Harris, J.K., Frank, D.N., Kotter, C. V, Stevens, M.J., Pace, N.R., Hernandez, M.T., 2015. High-resolution microbial community succession of microbially induced concrete corrosion in working sanitary manholes. *PLoS One* 10. doi:10.1371/journal.pone.0116400
- Lors, C., Dorelle, E., Miokono, H., Damidot, D., 2017. International Biodeterioration & Biodegradation Interactions between *Halothiobacillus neapolitanus* and mortars: Comparison of the biodeterioration between Portland cement and calcium aluminate cement. *Int. Biodeterior. Biodegradation* 121, 19–25. doi:10.1016/j.ibiod.2017.03.010
- Maeda, T., Negishi, A., Komot, H., Oshima, Y., Kamimura, K., Sugi, T., 1999. Isolation of Iron-Oxidizing Bacteria from Corroded Concretes of Sewage Treatment Plants. *Biosci. Bioeng.* 4, 300–305.
- Mittermayr, F., Rezvani, M., Baldermann, A., Hainer, S., Breitenbücher, P., Juhart, J., Graubner, C.-A., Proske, T., 2015. Sulfate resistance of cement-reduced eco-friendly concretes. *Cem. Concr. Compos.* 55, 364–373. doi:10.1016/j.cemconcomp.2014.09.020
- Mori, T., Nonaka, T., Tazaki, K., Koga, M., Hikosaka, Y., Noda, S., 1992. Interactions of nutrients, moisture and pH on microbial corrosion of concrete sewer pipes. *Water Res.* 26, 29–37. doi:0043-1354'92 \$5,00 + 0.00
- Navarro, C.A., von Bernath, D., Jerez, C.A., 2013. Heavy metal resistance strategies of acidophilic bacteria and their acquisition: Importance for biomining and bioremediation. *Biol. Res.* 46, 363–371. doi:10.4067/S0716-97602013000400008
- Negishi, A., Muraoka, T., Maeda, T., Takeuchi, F., Kanao, T., Kamimura, K., Sugio, T., 2005. Growth Inhibition by Tungsten in the Sulfur-Oxidizing Bacterium *Acidithiobacillus thiooxidans*. *Biosci. Biotechnol. Biochem.* 69, 2073–2080. doi:10.1271/bbb.69.2073
- Nica, D., Davis, J.K., Kirby, L., Zuo, G., Roberts, D.J., 2000. Isolation and characterization of microorganisms involved in the biodeterioration of concrete in sewers. *Int. Biodeterior. Biodegradation* 46, 61–68. doi:10.1016/S0964-8305(00)00064-0
- Nielsen, A.H., Vollertsen, J., Jensen, H.S., Madsen, H.I., Hvitved-Jacobsen, T., 2006. Aerobic and Anaerobic Transformations of Sulfide in a Sewer System – Field Study and Model Simulations. *Proc. Water Environ. Fed.* 2006, 3654–3670. doi:10.2175/193864706783751447

- Nies, D.H., 1999. Microbial heavy-metal resistance. *Appl. Microbiol. Biotechnol.* 51, 730–750. doi:10.1007/s002530051457
- O’Connell, M., McNally, C., Richardson, M.G., 2010. Biochemical attack on concrete in wastewater applications: A state of the art review. *Cem. Concr. Compos.* 32, 479–485. doi:10.1016/j.cemconcomp.2010.05.001
- Okabe, S., Odagiri, M., Ito, T., Satoh, H., 2007. Succession of sulfur-oxidizing bacteria in the microbial community on corroding concrete in sewer systems. *Appl. Environ. Microbiol.* 73, 971–980. doi:10.1128/AEM.02054-06
- Orell, A., Remonsellez, F., Arancibia, R., Jerez, C.A., 2013. Molecular characterization of copper and cadmium resistance determinants in the biomining thermoacidophilic archaeon *Sulfolobus metallicus*. *Archaea* 2013. doi:10.1155/2013/289236
- Osorio, H., Mangold, S., Denis, Y., Ancuqueo, I., Esparza, M., Johnson, D.B., Bonnefoy, V., Dopson, M., Holmesa, D.S., 2013. Anaerobic sulfur metabolism coupled to dissimilatory iron reduction in the extremophile *Acidithiobacillus ferrooxidans*. *Appl. Environ. Microbiol.* 79, 2172–2181. doi:10.1128/AEM.03057-12
- Pacheco-Torgal, F., Labrincha, J., Leonelli, C., Palomo, A., Chindaprasit, P., 2014. *Handbook of Alkali-Activated Cements, Mortars and Concretes*, 1st Editio. ed. Woodhead Publishing.
- Page, C.L., Page, M.M., 2007. *Durability of concrete and cement composites*. CRC Press.
- Peyre Lavigne, M., Bertron, A., Auer, L., Hernandez-Raquet, G., Foussard, J.-N., Escadeillas, G., Cockx, A., Paul, E., 2015. An innovative approach to reproduce the biodeterioration of industrial cementitious products in a sewer environment. Part I: Test design. *Cem. Concr. Res.* 73, 246–256. doi:10.1016/j.cemconres.2014.10.025
- Peyre Lavigne, M., Bertron, A., Botanch, C., Auer, L., Hernandez-Raquet, G., Cockx, A., Foussard, J.-N., Escadeillas, G., Paul, E., 2015. Innovative approach to simulating the biodeterioration of industrial cementitious products in sewer environment. Part II: Validation on CAC and BFSC linings. *Cem. Concr. Res.* doi:10.1016/j.cemconres.2015.10.002
- Peyre Lavigne, M., Lors, C., Valix, M., Herrison, J., Paul, E., Bertron, A., 2016. Microbial induced concrete deterioration in sewers environment: Mechanisms and microbial populations, in: *Microorganisms-Cementitious Materials Interactions*. pp. 1–17.
- Provis, J.L., Palomo, A., Shi, C., 2015. Advances in understanding alkali activated materials. *Cem. Concr. Compos.* 78, 110–125.
- Provis, J.L., van Deventer, J.S.J., 2009. *Geopolymers. Structures, Processing, Properties and Industrial Applications*, CRC Press, Woodhead Publishing, Great Abington, Cambridge, UK. doi:10.1533/9781845696382
- Roberts, D.J., Nica, D., Zuo, G., Davis, J., 2002. Quantifying microbially induced deterioration of concrete: initial studies. *Int. Biodeterior. Biodegradation* 49, 227–234. doi:10.1016/S0964-8305(02)00049-5
- Satoh, H., Odagiri, M., Ito, T., Okabe, S., 2009. Microbial community structures and in situ sulfate-reducing and sulfur-oxidizing activities in biofilms developed on mortar specimens in a corroded sewer system. *Water Res.* 43, 4729–39. doi:10.1016/j.watres.2009.07.035
- Scrivener, K.L., Crumbie, A.K., Laugesen, P., 2004. The Interfacial Transition Zone (ITZ) Between Cement Paste and Aggregate in Concrete. *Interface Sci.* 12, 411–421.
- Škvára, F., Šmilauer, V., Hlaváček, P., Kopecký, L., Cílová, Z., 2012. A weak alkali bond in (N, K)-A-S-H gels: Evidence from leaching and modeling. *Ceram. - Silikaty* 56, 374–382.

- Sugio, T., White, K.J., Shute, E., Choate, D., Blake, R.C., 1992. Existence of a hydrogen sulfide ferric ion oxidoreductase in iron-oxidizing bacteria. *Appl. Environ. Microbiol.* 58, 431–433.
- Sun, X., Jiang, G., Bond, P.L., Keller, J., 2013. Impact of fluctuations in gaseous H<sub>2</sub>S concentrations on sulfide uptake by sewer concrete: The effect of high H<sub>2</sub>S loads. *Water Res.* 81, 84–91. doi:10.1016/j.watres.2015.05.044
- Tchakouté, H.K., Rüscher, C.H., Kong, S., Kamseu, E., Leonelli, C., 2016. Geopolymer binders from metakaolin using sodium waterglass from waste glass and rice husk ash as alternative activators: A comparative study. *Constr. Build. Mater.* 114, 276–289. doi:10.1016/j.conbuildmat.2016.03.184
- Ukrainczyk, N., Vogt, O., Koenders, E.A.B., 2016. Reactive Transport Numerical Model for Durability of Geopolymer Materials. *Adv. Chem. Eng. Sci.* 6, 355–363. doi:10.4236/aces.2016.64036
- Valdes, J., Pedroso, I., Quatrini, R., Dodson, R.J., Tettelin, H., Blake, R., Eisen, J.A., Holmes, D.S., 2008. *Acidithiobacillus ferrooxidans* metabolism: from genome sequence to industrial applications. *BMC Genomics* 9, 597. doi:10.1186/1471-2164-9-597
- Valix, M., Cheung, A.W.H., Sunarho, J., Bustamante, H., 2014. The impact of calcium aluminate cement and aggregates on conversion and on field performance in sewers, in: *Calcium Aluminates*. IHS, p. 663.
- Valix, M., Shanmugarajah, K., 2015. Biogenic acids produced on epoxy linings installed in sewer crown and tidal zones. *Water Res.* 80, 217–26. doi:10.1016/j.watres.2015.05.027
- Vincke, E., Verstichel, S., Monteny, J., Verstraete, W., 2000. A new test procedure for biogenic sulfuric acid corrosion of concrete 421–428.
- Vollertsen, J., Nielsen, A.H., Jensen, H.S., Wium-Andersen, T., Hvitved-Jacobsen, T., 2008. Corrosion of concrete sewers—the kinetics of hydrogen sulfide oxidation. *Sci. Total Environ.* 394, 162–70. doi:10.1016/j.scitotenv.2008.01.028
- Vollpracht, A., Lothenbach, B., Snellings, R., Haufe, J., 2015. The pore solution of blended cements : a review. *Mater. Struct.* doi:10.1617/s11527-015-0724-1
- Wei, X., Yang, Z., Wang, Y., Tay, S., Gao, W., 2014. Polymer antimicrobial coatings with embedded fine Cu and Cu salt particles. *Appl. Microbiol. Biotechnol.* 98, 6265–74. doi:10.1007/s00253-014-5670-2
- World Health Organisation, 2000. Hydrogen Sulfide, in: *Air Quality Guidelines for Europe*. Copenhagen, p. 7.
- Yamanaka, T., Aso, I., Togashi, S., Tanigawa, M., 2002. Corrosion by bacteria of concrete in sewerage systems and inhibitory effects of formates on their growth. *Water Res.* 36, 2636–2642.
- Yuan, H., Dangla, P., Chatellier, P., Chaussadent, T., 2015. Degradation modeling of concrete submitted to biogenic acid attack. *Cem. Concr. Res.* 70, 29–38. doi:10.1016/j.cemconres.2015.01.002
- Zhang, Y., Zhong, S., Zhang, M., Lin, Y., 2009. Antibacterial activity of silver-loaded zeolite A prepared by a fast microwave-loading method. *J. Mater. Sci.* 44, 457–462. doi:10.1007/s10853-008-3129-5

# Chapter 6

## Outlook and Afterword

### 6.1. Outlook

Field studies and material investigations conducted have highlighted the inadequateness and limitations of the current state of the art on cementitious materials for aggressive sewer environments and the associated need for sustainable construction materials for the latter. Gained in depth knowledge of the physicochemical construction material characteristics and their impact regarding biofilm adhesion, development and structure form the basis for continuative development of suitable materials. Accordingly, in cooperation with different scientific partners, last year an extensive field testing campaign over the period of several years has been established. The aim of this campaign is to test particularly designed geopolymer concretes regarding their behavior in MICC environments. Outsourced GPCs are and will be tested regarding their microstructural behavior, microbial accessibility and hydro-chemical alterations over time and compared to commercially produced cement based products, including OPC and CAC concretes. Additionally, the system specific environmental parameters, such as relevant gas concentrations ( $\text{H}_2\text{S}$ ,  $\text{CO}_2$ ,  $\text{CH}_4$ ), relative humidity and temperature are constantly monitored. Preliminary results on different, non-optimized, geopolymer concretes (GPC) showed already considerably better durability compared to conventional cement based materials after an exposure period of 12 months. While no structural damage could be observed on the GPC specimen, strong deterioration was seen on the surfaces of cement-based reference materials. Based on the results obtained within the first year a second, optimized set of GPCs was developed which will be outsourced shortly. Following this concept of tailored GPC optimization, we hope to develop a sustainable construction material to withstand the harsh conditions of aggressive sewer environments over its entire service life.

### 6.2. Curriculum Vitae

Cyrill Grengg was born on August 31<sup>st</sup> 1988 in Graz, Austria. He attended high school at the BG/BRG Oeversee from which he graduated 2006. After completing a seven-month language course in Sydney, Australia he enrolled for studying Earth Sciences at University of Graz and TU Graz. After finishing his bachelor degree in 2011 he received a one-year scholarship at the Western Washington University, USA. After returning he enrolled in the Master Program of TU Graz specializing in Hydrology and Hydro-geochemistry, which he finished with his diploma thesis entitled “Bacteriogenically induced

sulfuric acid corrosion in an Austrian sewer system” in 2014. In the same year he started working at the Institute of Applied Geosciences at TU Graz as project assistant within a project called “Microbial induced concrete corrosion”, a program partly funded by the Styrian Government, as a part of the Doctoral School of Geosciences. Since 2015 he is actively involved within the RILEM Technical-Committee: Microorganisms – Cementitious Materials Interaction (TC-MCI-253).

### 6.3. References

Reviewed journal and conference papers

#### 6.3.1. Related to MICC

- Grengg, C.,** Mittermayr, F., Baldermann, A., Böttcher, M.E., Leis, A., Koraimann, G., Grunert, P., Dietzel, M., 2015. Microbiologically induced concrete corrosion: A case study from a combined sewer network. *Cem. Concr. Res.* 77, 16–25. doi:10.1016/j.cemconres.2015.06.011
- Grengg, C.,** Mittermayr, F., Baldermann, A., Böttcher, M.E., Leis A., Dietzel, M., Concrete corrosion in an Austrian sewer system, in: *Proceedings of the 4th International Conference on Concrete Repair, Rehabilitation and Retrofitting, ICCRRR 2015*, pp. 5.
- Grengg, C.,** Kiliswa, M., Mittermayr, F., Alexander, M., 2016. Microbially-induced Concrete Corrosion- A worldwide problem, in: *Microorganisms-Cementitious Materials Interactions*. pp. 1–19, Delft, Netherlands.
- Grengg, C.,** Mittermayr, F., Baldermann, A., Böttcher, M.E., Leis, A., Koraimann, G., Dietzel, M., 2015a. Stable Isotope Signatures within Microbial Induced Concrete Corrosion: A Field Study. *Procedia Earth Planet. Sci.* 13, 68–71. doi:10.1016/j.proeps.2015.07.016
- Grengg, C.,** Mittermayr, F., Koraimann, G., Konrad, F., Szabó, M., Demeny, A., Dietzel, M., 2017. The decisive role of acidophilic bacteria in concrete sewer networks: A new model for fast progressing microbial concrete corrosion. *Cem. Concr. Res.* doi:10.1016/j.cemconres.2017.08.020
- Grengg, C.,** Mittermayr, F., Koraimann, G., Szabo, M., Demeny, A., Dietzel, M., 2017. A new model approach describing the decisive role of acidophilic bacteria on concrete corrosion in sewers. 14<sup>th</sup> International Conference on Durability of Building Materials and Components, Ghent, Belgium.
- Grengg, C.,** Mittermayr, F., Koraimann, G., Szabo, M., Demeny, A., Dietzel, M., 2017. The decisive role of acidophilic bacteria on microbial induced concrete corrosion in sewers. 1<sup>st</sup> International Conference on Construction Materials for Sustainable Future, Zadar, Croatia.
- Grengg, C.,** Mittermayr, F., Ukrainczyk, N., Koraimann, G., Kienesberger, S., Dietzel, M., 2017. Advances in construction materials for sewer systems affected by microbial induced concrete corrosion: A review. Under Review.
- Grengg, C.,** 2017. H<sub>2</sub>S-Korrosion: Der Aggressivste chemische Angriff auf Abwasseranlagen. –in: *Der Laubfrosch: Aktuelles aus der Umwelttechnik*, VTA Austria GmbH
- Grengg, C.,** Mittermayr, F., Dietzel, M., 2017. Biogen induzierter Schwefelsäureangriff in Abwasseranlagen: Ursachen – Prozessmechanismen – Reduzierungsstrategien. *DWA BW Landesverbandstagung, Fellbach*, P. 36-42.

### 6.3.2. Related to topics in Applied Mineralogy and Environmental Sciences

Mavromatis V., Goetschl K.E., **Grengg C.**, Konrad F., Purgstaller B., Dietzel M., 2017. Ba partitioning in calcite and aragonite as a function of growth rate at 25 oC. *Geochimica et Cosmochimica Acta*, under Review.

Baldermann A., Rezvani, M., Proske, T., **Grengg C.**, Emmerich F., Stauffacher A., Sarkopanig M., Steindl F., Baldermann C., Galan I., Graubner C., Mittermayr F., 2017. Effect of very high limestone content and quality on the sulfate resistance of low-clinker cement blends. *Cem. Concr. Res.*, under Review.

Stammeier J. A., Hippler D., Nebel O., Leis A., **Grengg C.**, Mittermayr F., Kasemann S. A., Dietzel M., 2017. Radiogenic (Sr) and stable (C and O) isotope distribution 1 across the Precambrian - Cambrian transition in phosphorites and carbonates (Malyi Karatau, Kazakhstan) - Implications for paleo-environmental conditions. *Chemical Geology*, under Review.